



NTNU – Trondheim
Norwegian University of
Science and Technology

Investigation on an Open Cycle Water Chiller based on Desiccant Dehumidification

Sindre Pettersen

Master of Energy and Environmental Engineering

Submission date: August 2012

Supervisor: Arne Mathias Bredesen, EPT

Co-supervisor: Yong Li, SJTU
Trygve M. Eikevik, EPT

Norwegian University of Science and Technology
Department of Energy and Process Engineering

EPT-M-2012-73

MASTER THESIS

for

student Sindre Pettersen

Spring 2012

Research on an open cycle water chiller based on desiccant dehumidification.

Undersøkelser av et åpent system for vannkjøling basert på en adsorberende avfukting

Background and objective

Desiccant cooling system is an effective cooling system which can be used in humid area and solar energy can be used as heat source. In SJTU, a novel open cycle water chiller driven by solar air collector and based on two stage desiccant dehumidification has been developed and an experimental set-up has been built. The objective of this research is to conduct experiments in Spring season (which is humid in Shanghai) and in early summer (which is hot and humid in Shanghai). The performance of the system as well as important components will be tested and evaluated. The suggestions on improving such system will be provided.

The following tasks are to be considered:

1. Literature review on desiccant cooling system, solar air heating and testing methods.
2. Add more temperature and humidity sensors into the test system. Test the system performance in humid weather conditions when solar energy is available. Provide processed air to the room to test practical effects.
3. Evaluate the performance solar air collector. Study the efficiency the first stage desiccant wheel and the heat exchanger in front of it which is newly installed.
4. Test the system performance in humid weather conditions when solar energy is available.
5. Make a draft paper of the results from the project
6. Make proposal for further work

-- " --

Within 14 days of receiving the written text on the master thesis, the candidate shall submit a research plan for his project to the department.

When the thesis is evaluated, emphasis is put on processing of the results, and that they are presented in tabular and/or graphic form in a clear manner, and that they are analyzed carefully.

The thesis should be formulated as a research report with summary both in English and Norwegian, conclusion, literature references, table of contents etc. During the preparation of the text, the candidate should make an effort to produce a well-structured and easily readable report. In order to ease the evaluation of the thesis, it is important that the cross-references are correct. In the making of the report, strong emphasis should be placed on both a thorough discussion of the results and an orderly presentation.

The candidate is requested to initiate and keep close contact with his/her academic supervisor(s) throughout the working period. The candidate must follow the rules and regulations of NTNU as well as passive directions given by the Department of Energy and Process Engineering.

Risk assessment of the candidate's work shall be carried out according to the department's procedures. The risk assessment must be documented and included as part of the final report. Events related to the candidate's work adversely affecting the health, safety or security, must be documented and included as part of the final report.

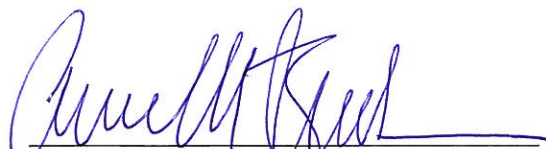
Pursuant to "Regulations concerning the supplementary provisions to the technology study program/Master of Science" at NTNU §20, the Department reserves the permission to utilize all the results and data for teaching and research purposes as well as in future publications.

The final report is to be submitted digitally in DAIM (<http://daim.idi.ntnu.no/>). An executive summary of the thesis including title, student's name, supervisor's name, year, department name, and NTNU's logo and name, shall be submitted to the department as a separate pdf file. The final report, with summary and all other material and documents have to be given to the supervisor in digital format on a CD.

Department of Energy and Process Engineering, 16. February 2012



Prof. Olav Bolland
Department Head



Prof. Arne M. Bredesen
Academic Supervisor
e-mail: trygve.m.eikevik@ntnu.no

Co-supervicer:

Prof. Yong Li, Shanghai Jiao Tong University, e-mail: liyo@sjtu.edu.cn

Prof. Trygve M. Eikevik, NTNU, e-mail: trygve.m.eikevik@ntnu.no

Preface

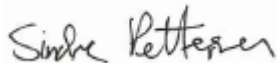
This report is the written work of my Master thesis at the Norwegian University of Science and Technology, Department of Energy and Process Engineering, TEP4920. The subject of the thesis was decided in cooperation with Shanghai Jiao Tong University and was performed and written at SJTU in the spring of 2012.

During my work with this thesis my knowledge has been tested thoroughly by different challenges, both theoretical and practical. I have gained new knowledge of the principles behind desiccant cooling systems, and my experimental work has given me an understanding on how real systems functions and operates.

I would like to thank my Norwegian supervisors, Professor Arne Bredesen and Professor Trygve Eikevik, for good advising, and I am especially grateful for them giving me the exiting opportunity of traveling to Shanghai to write my thesis abroad. I would also like to thank my Chinese supervisor, Professor Young Li, for an interesting problem statement and for thorough supervision and advising throughout my work.

Special thanks go to my co-student, Haibin He, whom I have spent countless hours with working on the system setup for the experimental work. He has not only helped me in the work of my thesis but also in private matters making my stay in Shanghai that much easier, and for that I am very grateful.

Finally, I would like to thank my fellow Norwegian travel companion and co-student, Candice Yu, for contributing to a professional and good working environment and providing moral support.



Sindre Pettersen

Shanghai, August 2012

Summary

In this thesis, a novel open cycle desiccant dehumidification system is experimentally studied. The system is installed and operated at Shanghai Jiao Tong University (SJTU) as part of the Green Energy Laboratory (GEL) initiative. The system uses two-stage desiccant dehumidification as well as regenerative evaporative cooling for chilled water production. The purpose of the thesis is to evaluate the system performance during different ambient and operational conditions. The investigated system has great potential regarding the environmental aspect of HVAC system solutions. The system is more energy efficient compared to conventional air conditioning systems and uses solar thermal power provided by evacuated tube solar air collectors as the main source of energy. Therefore, this type of system can contribute in reducing the use of non-renewable energy sources.

A lot of experiments have been performed from June to July 2012 during varying ambient conditions. As a first step, the necessary regeneration temperature level is established. The results show that this temperature should be in the range of 70-75°C or higher to be able to achieve desired dehumidification effect. Then, experiments regarding the overall system performance during different ambient temperature and humidity conditions are performed and analyzed. The results show that the system excels good performance during periods of high ambient humidity and is capable of achieving average COP_{th} and COP_{el} around 0.8 and 5.7 respectively. The total dehumidification efficiency is approximately 58% and is proven to vary with respect to the regeneration temperature, where increasing regeneration temperature results in higher amount of moisture removed from the processed air. The solar collectors providing heat to the regeneration air has an efficiency of 47-60% depending on the available level of solar radiation intensity. During periods of low intensity it is proven that the heating system needs assistance from an auxiliary device to be able to generate a sufficient temperature level. The evaporative cooler producing chilled water is capable of providing water at a temperature below 21°C during periods of high ambient temperature, and temperatures below 16°C if the ambient temperature decreases. The achieved dehumidification and cooling capacity of the desiccant system makes it possible to provide qualified supply air with temperature in the range of 20-26°C and absolute humidity below 12 g/kg. Also, an experiment with the purpose of investigating the newly installed second desiccant wheel is carried out. The system is operated with only the second wheel running and the results show that the dehumidification performance is very good when the second wheel provides the first stage dehumidification. Lastly, experiments investigating the impact of the pre-cooling heat exchanger is performed and analyzed.

Sammendrag

Denne oppgaven omhandler eksperimentelle undersøkelser gjennomført på et åpent system basert på adsorberende avfukting. Systemet er installert og driftet ved Shanghai Jiao Tong University (SJTU) og er en del av det pågående "Green Energy Laboratory" (GEL) initiativet. Systemet utnytter totrinns avfukting samt en regenererende fordampningskjøler for produksjon av nedkjølt vann. Foremålet med oppgaven er å evaluere systemets ytelse under ulike omgivelsesforhold og driftsbetingelser. Det undersøkte systemet har et stort potensial med tanke på miljøaspektet for systemløsninger innefor HVAC. Sammenlignet med konvensjonelle ventilasjonsanlegg er dette systemet mer energieffektivt, hvor det i tillegg bruker varmeenergi produsert av vakuumsolfangere for luft som hovedenergikilde. Dette gjør at denne typen system kan bidra til å redusere bruken av ikke-fornybare energikilder.

Gjennom juni og juli 2012 har en mengde forsøk blitt gjennomført under varierende omgivelsesforhold. Det første som er gjort er å fastsette den nødvendige temperaturen for regenerering av avfuktingsenhetene. Resultatene viser at denne temperaturen burde være i størrelsesordenen 70-75°C eller høyere for å oppnå ønsket avfukningseffekt. Deretter blir det utført eksperimenter for å analysere den samlede systemytelsen under forskjellige omgivelsestemperaturer og luftfuktigheter. Resultatene viser at systemet presterer bra i perioder med høye luftfuktigheter og er i stand til å oppnå verdier i området 0,8 og 5,7 for henholdsvis COP_{th} og COP_{el} . Den totale avfukningseffektiviteten er rundt 58 % og viser seg å variere med hensyn til temperaturen for regenerering, hvor økende regenereringstemperatur gir større mengde fukt fjernet fra ventilasjonslufta. Solfangerne som leverer varme til lufta brukt for regenerering har en effektivitet i området 47-60 % avhengig av tilgjengelige strålingsintensitet fra sola. I perioder med lav intensitet viser det seg at varmesystemet har behov for assistanse fra en tilleggsenhet for å kunne generere et tilstrekkelig temperaturnivå. Fordampningskjøleren brukt for vannkjøling er i stand til å produsere vann med en temperatur lavere enn 21°C under perioder med høy omgivelsestemperatur, og temperaturer under 16°C hvis omgivelsestemperaturen synker. Luftavfuktingen og vannkjølingen oppnådd av systemet gjør det mulig å levere ventilasjonsluft med temperaturer i området 20-26°C med en absolutt luftfuktighet under 12 g/kg. Det er også gjennomført eksperiment der det nylig installerte andretrinns avfukningshjulet blir spesielt undersøkt. Systemet blir da driftet med bare dette hjulet kjørende og resultatet viser at avfukningsytelsen er svært god når dette hjulet får fungerer som førstetrinns avfukter. Til slutt er det også gjennomført eksperimenter der effekten av å bruke en forkjølede varmeveksler er undersøkt og analysert.

Nomenclature

Abbreviations

ARI	Air-conditioning and Refrigeration Institute
COP	Coefficient of Performance
GEL	Green Energy Laboratory
HVAC	Heating, Ventilation and Air-conditioning
HX	Heat Exchanger
OTSDC	One-rotor Two-stage Desiccant Cooling
RH	Relative Humidity
SJTU	Shanghai Jiao Tong University
TTSDC	Two-rotor Two-stage Desiccant Cooling

Symbols

Q	Heat	[W]
W	Work	[W]
ε	Efficiency	[%]
η	Efficiency	[%]
T	Temperature	[°C]
m	Mass flow	[kg/s]
h	Specific enthalpy	[kJ/kg]
d	Humidity ratio	[kg/kg]
C_p	Specific heat	[kJ/kg K]
H	Head	[m]
ΔP	Pressure difference	[Pa]
g	Gravity of earth	[m/s ²]
z	Fan constant	[-]
I	Solar radiant intensity	[W/m ²]
A	Area	[m ²]
R	Resistance	[ohm]

Subscripts

pro	Process air
reg	Regeneration air
a	Air
w	Water
cs	Cooling system
el	Electrical
k	Kinetic

<i>me</i>	Mechanical
<i>th</i>	Thermal
<i>sc</i>	Solar collector
<i>rad</i>	Radiation
<i>in</i>	Inlet
<i>out</i>	Outlet
<i>cf</i>	Cross-flow heat exchanger
<i>ev</i>	Evaporative cooler
<i>wb</i>	Wet bulb
<i>cw</i>	Chilled water
<i>1-13</i>	State points

Table of Contents

1	Literature Review	1
1.1	Background.....	1
1.2	Principles of Adsorption	6
1.3	Desiccant Material.....	8
1.4	Desiccant Cooling System.....	10
1.4.1	Desiccant Dehumidifier	11
1.4.2	Cooling Unit	12
1.4.3	Regeneration Heat Source.....	13
1.5	Solar Air Heating.....	14
2	The Novel Open Cycle Two-stage Desiccant Cooling System.....	19
2.1	Location and Design of the System	19
2.2	System Components.....	21
2.2.1	Two-stage Desiccant Wheels.....	21
2.2.2	Air to Water Heat Exchangers	23
2.2.3	Regenerative Evaporative Cooler	23
2.2.4	Evacuated Tube Solar Air Collector	25
2.2.5	Auxiliary Heater	27
2.2.6	Cooling Tower.....	28
2.2.7	Other Components	29
2.3	Explanation of the System Process.....	30
2.4	Psychrometric Representation of the System Process	33
3	Testing and Experimental Work	35
3.1	Renovation of the System	35
3.2	Testing Equipment.....	36
3.2.1	Temperature Measurement.....	36
3.2.2	Temperature and Humidity Measurement	37
3.2.3	Solar Radiation Measurement.....	38
3.2.4	Flow-rate Measurement.....	39
3.3	Performance Indexes.....	40

3.4	The Test Program	44
3.5	Ambient conditions	46
4	Results and Discussion	48
4.1	Performance during Different Regeneration Temperatures.....	48
4.2	Performance during Typical Working Conditions.....	50
4.2.1	ARI Summer Conditions.....	51
4.2.2	ARI Humid Conditions.....	56
4.2.3	Shanghai Summer Conditions	61
4.2.4	Evaluation of the Performance during Different Conditions	66
4.3	Performance without the Pre-cooling Heat Exchanger.....	67
4.4	Performance with only the Second Desiccant Wheel Running.....	70
4.5	Performance of the Evacuated Tube Solar Air Collector.....	72
4.5.1	during High Solar Radiation Intensity.....	72
4.5.2	during Moderate Solar Radiation Intensity.....	74
4.6	Performance of the Regenerative Evaporative Cooler	76
4.6.1	during Moderate Ambient Temperature	76
4.6.2	during High Ambient Temperature	78
5	Conclusion	80
6	Further work.....	82
	References.....	83
	List of Figures.....	86
	List of Tables.....	89
	List of Equations	90
	Appendix A: Detailed Characteristics of Test Components.....	91
	Appendix B: The Data Recording Software	93
	Appendix C: Theoretical Estimation of Supply Air Temperature	95
	Appendix D: Draft of Scientific Paper	97

1 Literature Review

1.1 Background

Increase of the energy consumption around the world, as well as the desire to prevent further increased global warming, has set a major focus on developing energy efficient and environmentally friendly system solutions. In the summer season especially, air conditioning systems represents a growing market in commercial and residential buildings. Two of the main reasons are that the demands for acceptable living standards are increasing as well as the comfort demands of the occupants. The air-conditioning unit covers both temperature and humidity control, which leads to conventional vapor compression cooling systems consuming large amounts of electrical energy as well as exhausting a lot of usable waste heat. In the USA, two-thirds of the energy used in buildings and industrial facilities are for heating needs. In China, the national annual energy consumption for heating is about 130 million ton standard coal, which makes up 10% of the total energy consumption [1].

HVAC systems are a significant contributor to the energy use in buildings. The total load of air-conditioning systems includes two different heat loads called sensible and latent heat load. Sensible heat load is the heat exchanged by the system, while latent heat load is the heat that is occurring during a phase change. Traditional vapor compression air-conditioning systems usually cools the air down to below dew point temperature to be able to deal with both loads. This results in a problem concerning large energy consumption when the system is used to satisfy the temperature and humidity requirements of a conventional building. Other problems with conventional refrigerated cooling units are that they often make the processed ventilation air dry while using refrigerants which may harm the environment. Because of this, it has been showed a growing interest in alternative heat-powered refrigeration and air-conditioning systems. Utilization of innovative and clean energy sources has lead technology research in new directions. One of the most important clean energy sources is solar power. Solar-assisted air-conditioning systems are therefore an interesting field of research, which still is in the early stages of development. In an overview presented by [2] in 2006 it is mentioned that about 70 solar-assisted systems are installed in Europe. As showed in Figure 1, most of these systems are located either in Germany or Spain. The systems installed are mainly using absorption or adsorption system solutions. It is stated that 59% of the systems uses absorption chillers while 11% uses adsorption chillers. Systems where a desiccant

material is used as the adsorption material is also represented where 23% of the installations use a solid desiccant wheel and 6% uses liquid desiccant technology.

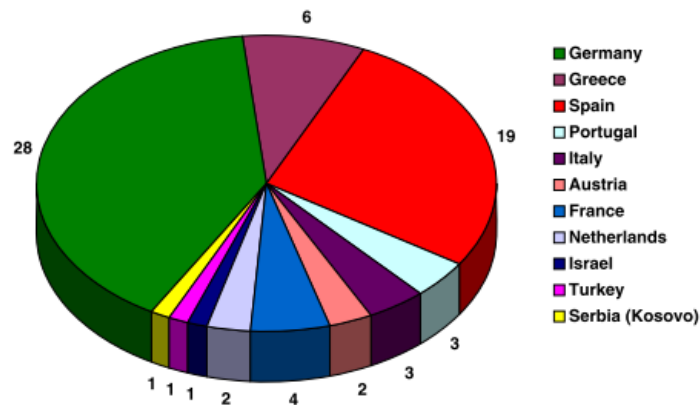


Figure 1: Overview of solar assisted systems installed in Europe [2]

Vapor compression refrigeration is the most common type of cooling and dehumidification system used followed by absorption cooling as the second most common system [3]. An interesting alternative to these systems are adsorption cooling systems using desiccant materials as the adsorber. These systems are usually referred to as desiccant cooling systems where the desiccant material controls the humidity, and a cooling unit, for instance an evaporative cooler, controls the temperature. Desiccant cooling systems are energy efficient and are considered to be an important technology with respect to manufacturing environmental friendly temperature and humidity control systems in the future. Figure 2 illustrates a basic open-cycle desiccant cooling system with 100% fresh air, which is one of the most common desiccant cooling systems. The desiccant system needs thermal energy from a heat source to be able to work continually over a long time period. Solar thermal systems, or systems that utilize other low-grade energy sources, have been considered to be a potential energy efficient technology. In this case, an air condition system that uses desiccant material for dehumidification connected with a solar thermal system for regeneration heat has now more frequently become a subject of research. The use of desiccant cooling systems started as early as in 1955 in the form of a simple open-cycle desiccant cooling system introduced by Pennington [3]. In this system, the desiccant dehumidifier was coupled with a heat source creating an adiabatic regenerative dehumidifier. Since then many different desiccant cooling systems has been introduced and investigated, especially systems with the focus of using solar thermal heat as the source of energy.

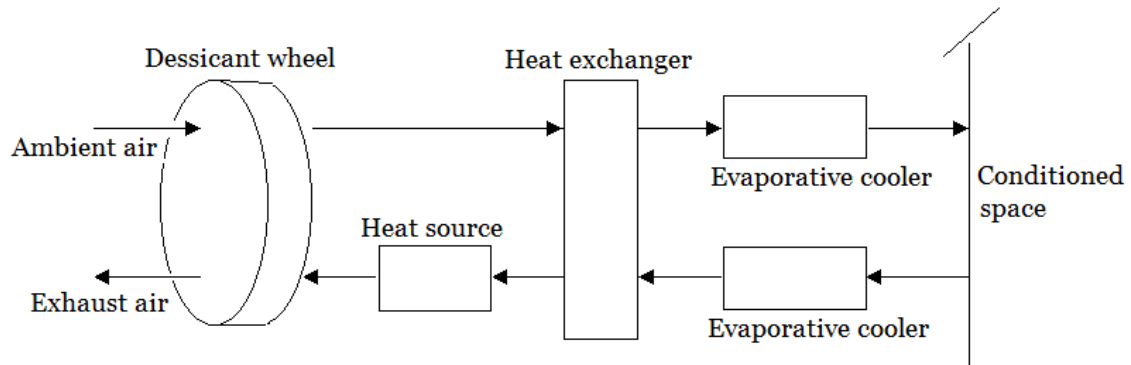


Figure 2: Basic open-cycle desiccant cooling system using 100% fresh air.

In Shanghai Jiao Tong University, two different desiccant cooling systems have been studied thoroughly; two-rotor two-stage desiccant cooling system and one-rotor two-stage desiccant cooling system. The reason behind the two-stage process is to approach close-to isothermal dehumidification conditions [4]. When the air is dehumidified by the desiccant, the temperature of the air will increase as the humidity decreases. The reason behind this will be explained in the following sections. As the humidity of the air decreases, the moisture content of the desiccant wheel increases. This means that the humidity difference between the dehumidified air and the desiccant material will decrease as well as the further dehumidification ability. For a one-stage desiccant system, the dehumidification load of the desiccant wheel is higher than for a multi-stage system. This means that the regeneration temperature needs to be higher in order to achieve desired dehumidification of the process air. As a result, the process air outlet temperature will be high. By applying a multistage desiccant system with intercoolers between each stage, the regeneration temperature needed for each stage will be lower. This is because the dehumidification loads of the desiccant wheels are lower, meaning that the system regeneration temperature is not required to be at the same level as for one-stage systems. The outlet temperature of the process air after the dehumidification stages will then be lower. The theoretical difference in performance between a multistage and a one-stage desiccant system is given in Figure 3.

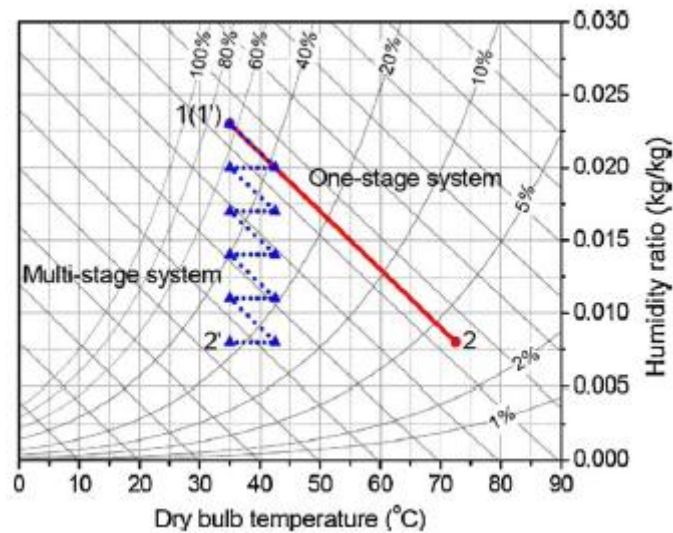


Figure 3: Psychrometric comparison between one-stage and multistage systems [4]

One of the main differences between two-rotor two-stage desiccant cooling systems and one rotor two-stage desiccant cooling systems are the division of the cross-section area of the wheel [4]. The cross-section difference is because of the TTSDC using two desiccant wheels in the dehumidification process, while the OTSDC uses one desiccant wheel. For the OTSDC, this means that the same desiccant wheel will be used twice in one cycle to obtain sufficient dehumidification of the process air. One of the main advantages of using OTSDC compared to a conventional TTSDC is the size-reduction obtained by using one desiccant wheel instead of two. Since the TTSDC uses two wheels it is only necessary with one regeneration side and one process side. For the OTSDC however, the desiccant wheel needs to be divided in four regions where two regions cover the regeneration air and two regions cover the process air because the process and regeneration air each passes the wheel twice during the process cycle. The schematic of the difference between the two designs are illustrated in Figure 4.

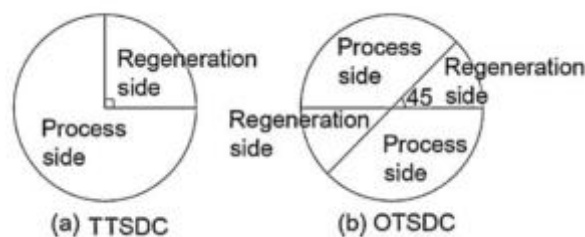


Figure 4: Cross section area of (a) TTSDC and (b) OTSDC [4]

The TTSDC has been evaluated in an experimental study done by [5], where one of the conclusions are that the regeneration temperature requirements of this system is much lower compared with a

one-stage system. This means that low-grade energy sources like solar energy can be used effectively as regeneration heat source. The thermal coefficient of performance for this system is proven to be almost higher than one, meaning that the cooling provided by the system is almost the same as the heat added by the regeneration energy source.

Also, an experimental study of the OTSDC has been carried out at SJTU with the objective of evaluating the moisture removal, cooling capacity and thermal coefficient of performance [6]. From this study it is concluded that the OTSDC system in hot and humid summer conditions is capable of reaching a moisture removal of 8 to 9 g/kg and a thermal COP of 0.95.

These results indicate that both system designs have the ability to achieve good thermal performances. The setups of the two different desiccant systems are presented in Figure 5 and Figure 6.

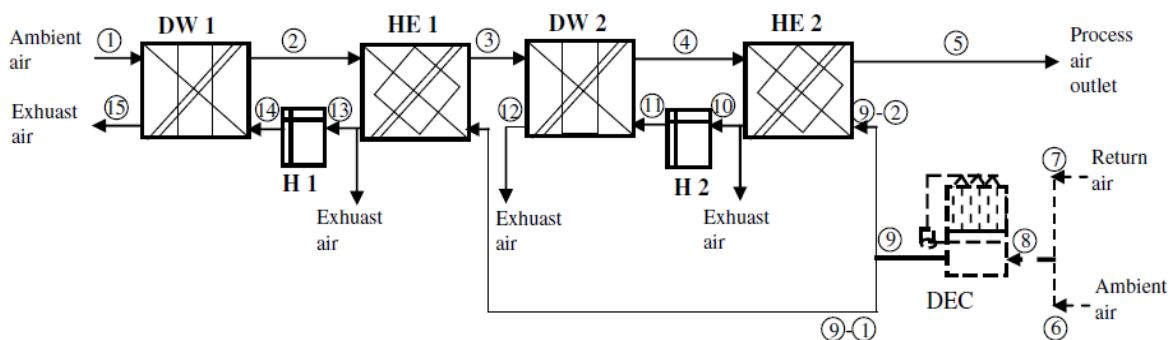


Figure 5: Schematic of a two-rotor two-stage desiccant cooling system [5]

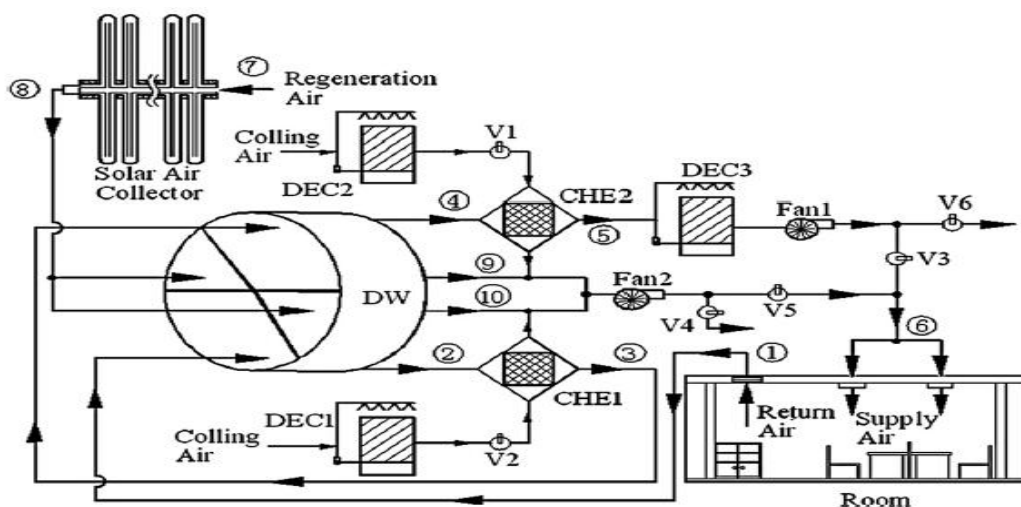


Figure 6: Schematic of a one-rotor two-stage desiccant cooling system [6]

In 2010, a new desiccant cooling system was installed at SJTU. This system uses two desiccant wheels for dehumidification as well as a regenerative evaporative cooler for chilled water production. In this thesis, it is this system that will be investigated and evaluated by performing experiments testing the performance of the system. The purpose of this investigation is based on the environmental aspect of HVAC system solutions. The desiccant cooling system uses solar thermal power as the main heat source and has therefore great potential in being an environmentally friendly alternative to conventional air conditioning systems with high energy consumption and in reducing the use of non-renewable energy sources.

1.2 Principles of Adsorption

The ability to adsorb and accumulate water is a feature that almost all materials possess, but some materials have a significantly larger capacity. This is the case for the commercial desiccants used in dehumidification processes. To understand how a desiccant material works, the principles of adsorption need to be explained. Adsorption is defined as selective binding of a substance by another solid substance [7]. The solid substance will in the case of the system described in this thesis be the desiccant wheel, where the desiccants act as the binding substance and are capable of adsorbing large amounts of water molecules into pores on the surface. The forces which primarily are responsible for the sorption processes arise from interactions of the electric field at the surface of the solid substance with the water molecules.

There are two different processes which together makes adsorption possible. The first process is chemical sorption, which arises due to the binding between water molecules and hydroxyl groups on the surface pores of the desiccant. This process is permanent in nature meaning that it cannot be reversed by heating [7]. Figure 7 illustrates the irregular active surface of the commercial desiccant silica gel where chemical sorption takes place and hydroxyl groups take part in binding of water molecules. The second process is physical adsorption, which is a reversible process. This process is a result of the intermolecular forces called Van Der Waal forces. The Van Der Waal forces attract and hold water molecules on the pore surface of the adsorbing substance. These forces are based on intermolecular electric polarities divided in two types: alternating polarities and stationary polarities [8]. The alternating polarities occur when molecules approach each other generating synchronously alternating polarities which may establish a binding bond. The reason for this reaction is the disturbance which the binding molecules create in the surrounding electron clouds, as illustrated in Figure 8. The stationary polarities are attraction forces where the molecules are binding to each

other by bedding dipole against dipole. Large dipole moment and polarization ability causes the molecules to produce heat of adsorption which for water can be in the range of 10.8 – 20 kcal/mole [3].

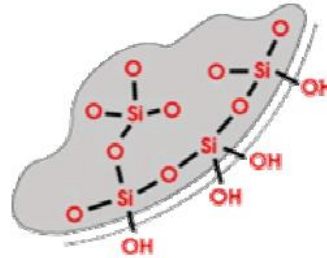


Figure 7: Hydroxyl groups on the surface of silica gel [7]

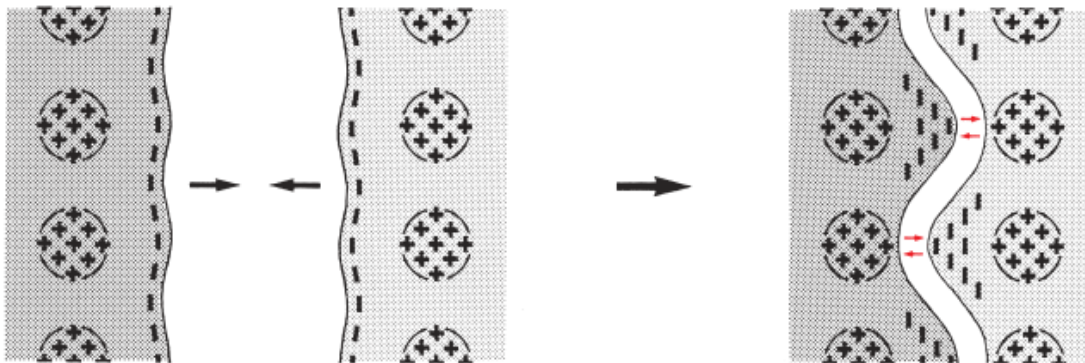


Figure 8: Synchronously alternating polarities establishing bonds between molecules [8]

Compared to the absorption process, where the water molecules penetrate the surface of the adsorbent, the adsorbed molecules do not diffuse into the volume of the adsorbent. The water molecules just attach to the surface of the substance making desorption a possibility. Desorption is the opposite of adsorption which means that the attached molecules breaks free from the bindings holding the molecules to the substance. This process takes place if a molecule has enough energy to overcome the activation energy for desorption [9]. It can be achieved by thermal desorption where the adsorbing substance is heated by a heat source. The ability of desorption makes physical adsorption a reversible process, which is a very important ability for temperature and humidity control systems where the dehumidification is performed by a desiccant material. This is because it allows the desiccant wheel to regenerate, making the wheel somewhat renewable meaning that the process can be done repeatedly over a period of time.

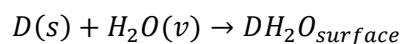
1.3 Desiccant Material

The adsorption process is a physical phenomenon which means that the desiccants used in the dehumidification process needs to possess the relevant properties and features which will maximize these effects. Commercially viable desiccants have a number of properties which separate them from other desiccant materials. The four most important properties are [10]:

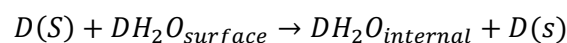
- Chemical and physical stability over many cycles
- Ability to hold large weight fractions of water
- Ability to separate water vapor from other constituents
- Ability to attract water vapor at desired partial pressure

That the desiccant remains stable during the sorption process is very important when used in a desiccant cooling system. To be able to operate in cycles, the system is depending on the desiccant material not changing during the sorption of the water vapor. The ability to hold large weight fractions of water are important with respect to the dehumidification capability of the desiccant system. When dehumidifying air, the desiccant is used to separate water vapor from other constituents. This selectivity of the desiccant is therefore an important ability. At vapor pressure close to the saturation pressure a lot of materials have the ability to attract water vapor. For some systems the dehumidification will take place at a vapor pressure which is much lower. Therefore, it is important that the desiccant material used can function under the desired partial pressure.

The desiccants used in dehumidification processes can either be natural or synthetic substances which are capable of adsorbing water vapor due to pressure difference between the surrounding air and the desiccant surface [3]. The following reaction schemes illustrate the desiccant materials sorption of water vapor:



Equation 1: Adsorption of water molecules



Equation 2: Satisfied total sorption

In these schemes, $D(S)$ represents a solid desiccant adsorption site and $H_2O(v)$ the water vapor. The first reaction that occurs is the adsorption of water vapor onto the surface represented by Equation 1. The second reaction occurring is when the total sorption is satisfied as the vapor permeates into the solid by several possible diffusion processes represented by Equation 2. To obtain desorption of

water vapor from the desiccant the sequence needs to be reversed, resulting in a dry desiccant ready to once again be used for adsorption. It is important to note that the molecular processes of sorbing water are in reality much more complex. The presented reaction schemes only illustrates that the sorption capacity is gained by at least two kinetic steps.

This water sorbing and accumulating ability has made desiccant materials widely used in many different industries. The desiccant material can be used in liquid or solid state depending on which advantages or shortcomings it is desirable that the system gains or avoids. The advantage of using liquid desiccants is that it has lower regeneration temperature and high flexibility in utilization, as well as lower pressure drop on the air side. Solid desiccants however, are more compact and less subject to corrosion and carryover. There are many different kind of desiccant materials used today. The most commonly used include lithium chloride, triethylene glycol, silica gels, aluminum silicates, aluminum oxides, lithium bromide solution and lithium chloride solution with water [11].

When selecting a desiccant to be used in a system it is important to choose a type that optimizes the system. There are mainly two key factors to consider while evaluating different desiccant materials [4]:

- The desiccant materials should possess large saturated adsorption amount and can easily be regenerated.
- The adsorption performance of the desiccant materials should approach the Type 1M material.

The saturated adsorption amount indicates how much water vapor the desiccant material is capable of accumulating, and is therefore a deciding factor regarding how well the desiccant dehumidifies the air. Regenerating the desiccant material means desorbing and preparing it for another adsorption cycle. The regeneration requires energy and this is usually provided by a thermal energy source. To make the system as energy efficient as possible it is important that the thermal energy demand needed to regenerate the desiccant material is low. A desiccant that easily desorbs has not a high requirement for the thermal energy and different energy sources can therefore be used in the regeneration process.

The Type 1M (moderate) material represents the optimum shape when the desiccant material is used in air conditioning application. Figure 9 shows the normalized loading fraction of different materials as a function of the relative humidity. Normalized loading fraction means the actual desiccant water content at corresponding relative humidity divided by maximum desiccant water

content at relative humidity equal 100%. It is clear that Type 1E (extreme) material has a higher normalized loading fraction than Type 1M. But because Type 1E has a nearly complete loading at a low relative humidity, it means that that this type of material will be more difficult to regenerate. The reason why desiccants with the Type 1M material adsorption performance is preferred in desiccant systems, is that the sorption characteristics of this material is best suited with respect to minimizing the costs of desiccant air conditioning systems in typical residential and commercial buildings [10].

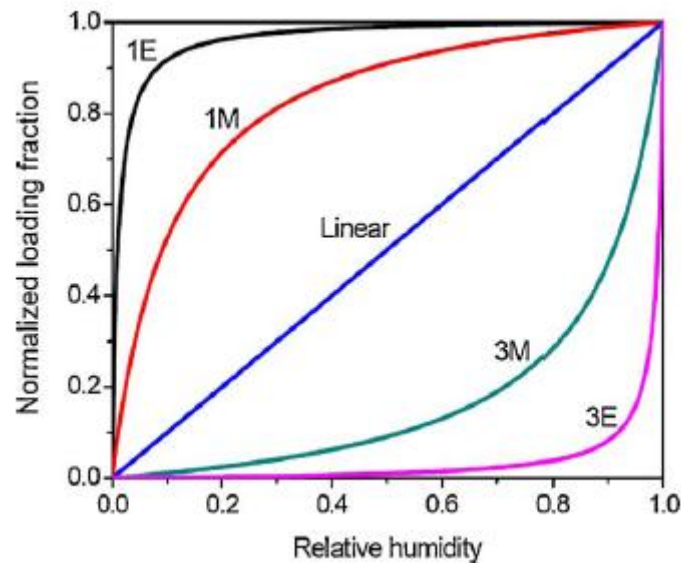


Figure 9: Adsorption isotherms of Type 1E, Type 1M, linear, Type 3M and Type 3E [4]

1.4 Desiccant Cooling System

Desiccant cooling is generally a process that consists of dehumidifying the incoming air stream by forcing it through a desiccant material, and cooling this air to a desired indoor temperature by using a cooling unit. The system is made continuously by driving out the adsorbed water vapor of the desiccant material using a thermal energy source. In other terms, the desiccant dehumidification stage is a physical process where water vapor is sorbed and desorbed by the desiccant material. Dividing the desiccant dehumidification in multiple stages will lower the requirement of the energy source. Therefore, applying a multistage desiccant system will enable the required heat to be applied by low-grade thermal energy sources such as solar energy, district heating, waste heat and bio-energy. Desorbing the desiccant material will regenerate the system and the material can again be used to adsorb water vapor in the next cycle of the system. The system can be operated as an open or a closed cycle. If the system is an open cycle the operating pressure would be close to the atmospheric pressure, but in the case of a closed cycle the operating pressure could be either lower or higher than the atmospheric pressure.

The desiccant cooling system usually consists of a combination between desiccant dehumidification and evaporative cooling. In the desiccant dehumidification process, the air passes through the adsorbing desiccant while releasing a large amount of the water vapor present in the air stream. In the evaporative cooling process following the desiccant dehumidification it is used cold water as a refrigerant to obtain desired indoor air temperature. This process is considered to be a close-to-zero cost technology meaning that a desiccant cooling system, not only is energy efficient and environmentally-friendly, but also cost-competitive compared to other cooling systems [4]. The desiccant cooling system can principally be divided into three different components, namely the dehumidifier, the cooling unit and the regenerative heat source. This is illustrated in Figure 10, which represents a simplified description of a basic desiccant cooling system. Figure 11 shows a psychrometric representation of the system, highlighting the different phases during a desiccant cooling system cycle.

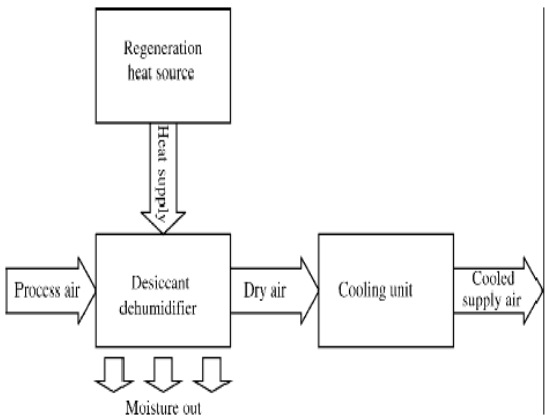


Figure 10: Principles of a desiccant cooling system [11]

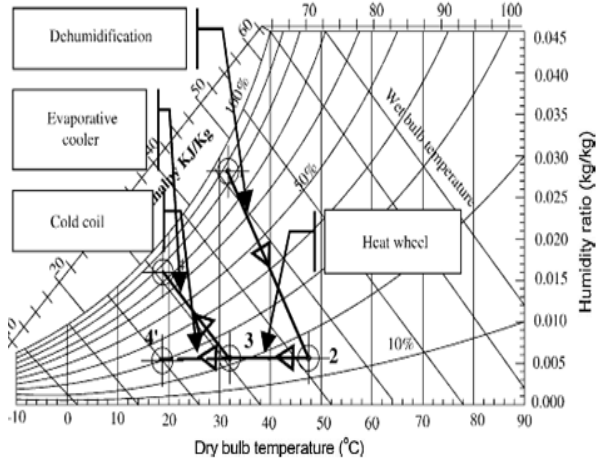


Figure 11: Psychrometric graph on desiccant cooling

[11]

1.4.1 Desiccant Dehumidifier

The desiccant material used in a desiccant dehumidifier can operate in solid or liquid state. In case of solid state, the dehumidifier is either operating in the form of a slowly rotating desiccant wheel or a periodically regenerated adsorbent bed. In case of liquid state, the dehumidifier is the equipment inside which the liquid desiccant is brought into contact with the process air stream [11]. Due to being advantageous in handling latent heat load, all these technologies have been used widely.

Rotating desiccant wheel is the technology which it will be focused on, since this is the relevant technology for the testing system. Desiccant wheels are air-to-air heat and mass exchangers which are commonly used as a way to adsorb water from the process air [12]. The reason behind this is that this system in addition to being able to run continuously are compact and less subject to corrosion

compared to other desiccant system solutions [4]. The desiccant wheel is rotating continuously and is in contact with both the process air and the regeneration air streams. While one part of the desiccant wheel is in contact with the process air, the other part of the wheel is in contact with the regeneration air. The rotor matrix of the desiccant wheel consists of a high number of channels with porous desiccant walls. The air flows through these channels leading to a set of physical phenomena occurring which include heat and mass convection on the gas side as well as heat and mass diffusion and water sorption in the desiccant [12]. Figure 12 represents a typical desiccant wheel where the porous structure of the matrix is visible, and Figure 13 illustrates a basic setup of a desiccant wheel.

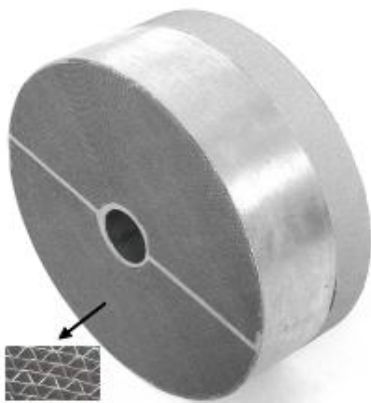


Figure 12: Desiccant wheel [12]

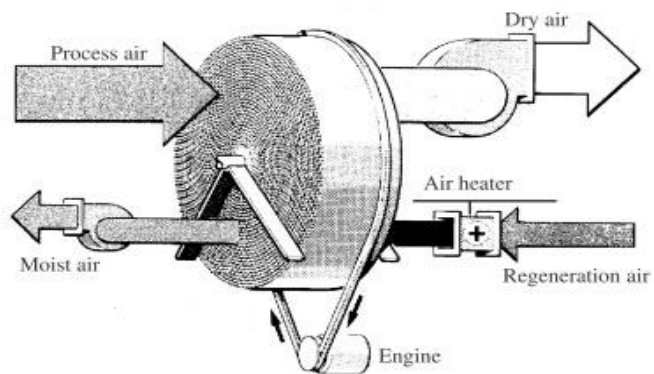


Figure 13: Schematic on the function of desiccant wheels [4]

The desiccant wheel adsorbs water from the process air onto its surface and releases the water to the regeneration air. It is the high temperature of the regeneration air which causes the desiccant wheel to desorb. This sensible heat from the regeneration side of the desiccant wheel, as well as the latent heat from the adsorption process, raises the temperature of the process air interacting with the wheel. After the regeneration air has gained the water molecules released from the desiccant, the now cooled and humidified regeneration air usually gets discharged to the surrounding environment.

1.4.2 Cooling Unit

The function of the cooling unit used in a desiccant cooling system is to make the system capable of dealing with the sensible and latent heat load occurring during the process. This can be done by different types of cooling units. The three most common types are [11]:

- Evaporative cooling unit
- Cooling coils
- Evaporator of a traditional air conditioner

The main target of the cooling unit is to ensure that the air entering the conditioned space has a comfortable temperature. Humans are more sensitive to variation of temperature than of relative humidity [13]. This makes the cooling unit one of the most crucial parts of the air conditioning system because the ability to keep the inlet air at a stable temperature is deciding with respect to achieving thermal comfort.

The cooling unit most relevant for the system investigated in this thesis is the evaporative cooler. In the evaporative cooler, process air is brought in direct contact with water causing the temperature to decrease. The air will absorb some of the water molecules which changes from liquid to vapor in the dry air. This evaporation process requires energy in the form of heat taken from both the interacting water and air, causing both to be cooled. This phenomenon makes the evaporative cooler capable of producing chilled water and chilled air in the same process. The humidity level of the process air is the deciding factor in the amount of cooling which can be accomplished. This means that the dryer the process air, the greater the potential for the evaporative cooler. However, the water and air cannot be cooled to a temperature lower than the wet bulb temperature of the air. The evaporative cooler can sometimes, in addition to cooling the air and water, also be used to ensure that the humidity of the air entering the conditioned space is at a comfortable level. This is an ability that can be used for systems operated during winter when the dryness of the air can create a comfort problem, and is possible because of the humidity increase of the interacting process air.

To improve the total dehumidification of the system, and maintain a relatively low temperature of the air entering the evaporative cooler, generally additional heat exchangers are used to assist in the heat removal. If the dehumidification process is consisting of more than one desiccant process, heat exchangers removing the heat gained from the process can be placed between the desiccant units. A heat exchanger can also be placed in front of the first desiccant material to pre-cool the air before entering the dehumidifying process.

1.4.3 Regeneration Heat Source

If the system is going to run continuity it is as mentioned necessary that the water which has been adsorbed by the desiccant material is being removed by desorption. The desorption process is driven by heated regeneration air flowing through the desiccant material. The heat of the regeneration air is obtained by thermal energy from a heat source. It is possible to utilize a variety of different energy sources to provide the heat for the regeneration air. The regeneration heat is generally introduced to a small separated section of the desiccant material, desorbing this section as the rest of the desiccant area dehumidifies the process air.

1.5 Solar Air Heating

Solar energy is available all over the earth, and it is relatively evenly distributed between countries. In this perspective, solar energy has the potential to be one of the most important renewable energy sources in the future. The availability of the solar energy is a result of the solar radiation hitting the surface of the earth. The solar radiation can in principle be divided in three different components: direct solar radiation, diffuse solar radiation and reflected solar radiation. Direct solar radiation is the radiation that moves in a straight line from the sun down to the surface of the earth. Diffuse radiation is the radiation that has been scattered by the atmosphere hitting the surface of the earth at multiple locations. The reflected solar radiation is the radiation that has been reflected from a surface. There are different ways of utilizing and transforming solar radiation. For heating and cooling purposes, the utilization of solar energy can be divided in three groups [14]:

- Passive solar energy
- Solar cells
- Active solar energy

Passive solar heating takes place when heat is added to a space due to radiation through windows and other transparent parts of the building. In solar cell technology the cells convert the energy from the sun directly into electricity. This electricity is then used to power different electrical heating or cooling systems. In active solar heating the principle of using energy from the sun is the same as for solar cells. The difference is that instead of producing electricity the solar collectors transfer and utilizes the solar energy to heat up air, water or other working fluids.

In a desiccant cooling system, active solar air heating done by solar collectors is the preferred method used. This is because during the summer season the regeneration air can directly be heated by solar collectors without using additional heat exchangers, thereby limiting the total heat losses. During the winter season hot air from the solar air collector can be directly directed for space heating if the system setup allows for this.

Different air collector types can be very varied with respect to efficiency, even though the collector composition is not varying that much. This can be a result from difference in nature and characteristic components, place of air channels in the collector or the collector shape [15]. One of the most important elements defining the quality of the solar collector is the absorber, which allows for transformation from solar radiation into heat. The absorber should be in a dark color, as well as have a high solar absorptance and a low emittance so that the collector can intercept the whole spectrum of the radiation.

The main advantages of solar air collectors compared to solar water collectors are the lower costs, the simple structure and their reliability. Low specific heat and the energy consumption by the fan are the main disadvantages [16]. Another difference is the effect that potential leakage of the working fluid has on the collector. Air leakage in a solar air collector, besides from leading to increased heat loss, also leads to increased power consumption of the fan when matching the desired air flow. The heat transfer in a solar air collector is relatively low compared to a solar water collector which means that the performance of an air collector becomes closely related to the collector design. Therefore, when considering solar air collectors, finding the optimal design is important when installing an energy efficient temperature and humidity control system.

Evacuated tube solar collector and flat-plate solar collector are two different designs of solar collectors that are commonly used. Between the two designs, flat-plate solar collectors are the older technology. This collector design has largely phased out in most European and Asian markets but can still occur frequently in lagging markets including the U.S. market. The flat-plate solar collector experiences large heat losses due to conduction and convection. During the winter season when the weather is cold and windy, more than half of the produced heat can be lost from the collector surface area. The evacuated tube solar collectors are the newer and rapidly improving technology. This collector design is already dominant in the most European and Asian markets. In the evacuated tube solar collector, the heat absorber is sealed within a vacuum glass tube [17]. This makes the glass evacuated tube capable of providing both the effects of a selective surface coating and vacuum insulation of the absorbing element, minimizing convection, conduction and radiation heat losses, resulting in high heat extraction efficiency. This is one of the reasons that evacuated tube collectors are becoming more and more popular in solar thermal utilization. Evacuated tube collectors also allows collection of solar energy at lower solar radiation levels compared to flat-plate collectors, which means that the collector can provide heating earlier in the morning and later in the evening. The evacuated tube collector exhibit better performance in particular for high temperature operation. Evacuated tube solar air collectors are the collector design which is relevant for the system which will be tested, and is therefore the design which is focused on [18] [19].

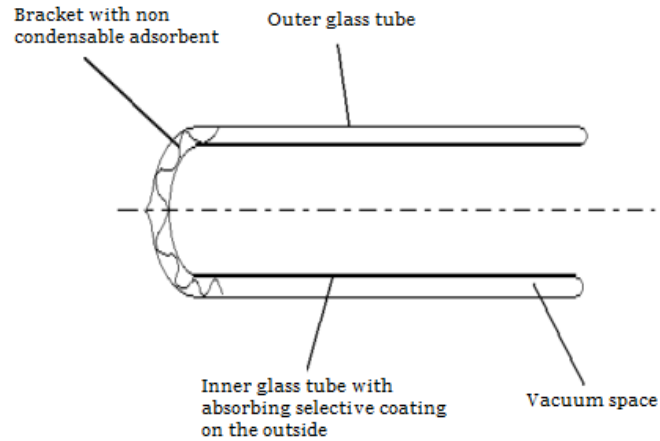


Figure 14: Setup of an evacuated tube solar collector [20]

Evacuated tube solar air collectors are usually consisting of a header pipe with several rows of glass tubes connected together. Figure 15 shows the setup of the pipes in a basic evacuated tube solar collector array. The header pipe distributes the air to the glass tubes where the air is heated by the solar radiation. The air returns to the header pipe and is directed towards the system where the hot air is utilized.

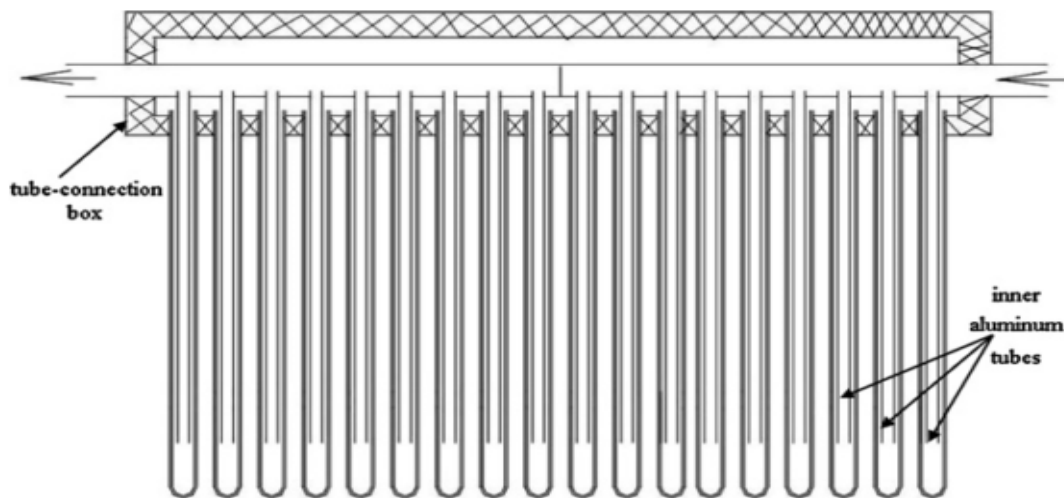


Figure 15: Schematic of a basic evacuated tube solar collector array [21]

In an evacuated tube solar collector an entry tube is often inserted into the collector, making the fluid firstly flow through the entry tube and secondly flow back between the tube and the glass tube of the collector. Figure 16 illustrates this concept. Recently there have been performed studies related to which entry pipe design and material gives the best results. In a study done by [16], two different configurations of solar air collectors were tested. The different configurations were

collectors inserted with 25 mm alumina tubes and collectors inserted with 19 mm stainless steel tubes. The result was that the thermodynamic and economic properties of 25 mm alumina make this configuration the superior choice compared to 19 mm stainless steel.

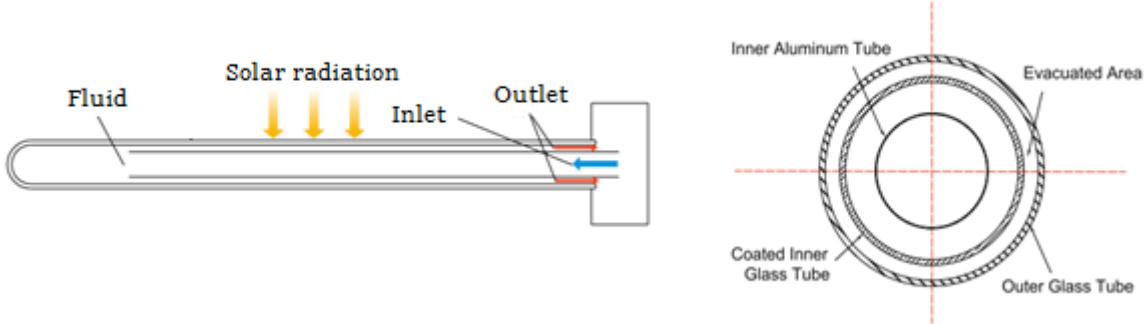


Figure 16: Schematic of an evacuated solar air collector tube [16]

There are different ways to realize a system configuration where solar thermal heat is used as the regeneration source in a desiccant system. Two relative simple systems are; system which uses the return air as regeneration air and system which uses ambient air as regeneration air [22]. As Figure 17 illustrates, both of these systems are working without an auxiliary heater installed. If it is necessary, this can be included in the system by installing the auxiliary heater at the point after the air has passed the solar collectors to insure that the regeneration temperature is at the desired level. Collectors which use the return air in the regeneration process needs to have a tubing system that connects the air with the solar collector. This can in some situations be impractical.

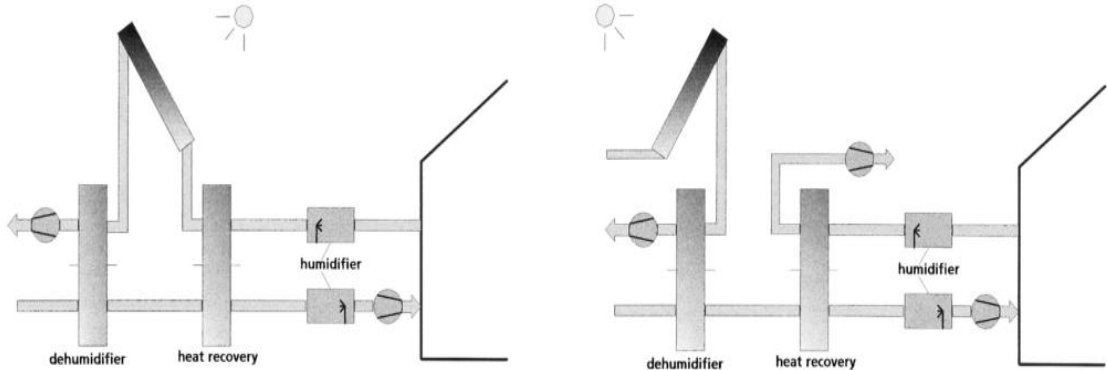


Figure 17: Two different desiccant cooling system using solar air collectors as heat source [22]

The heating performance of a solar collector is decided by many different factors. Among these factors are the collector tilt angle and the orientation of the collector two of the most important. The optimal tilt angle of the solar collector is decided by the latitude of the location, where an angle close to equal the latitude would give the highest effect of the incoming radiation. To be able to achieve maximum energy production the orientation of the collector is also important. The orientation should ideally be in the direction that allows the most solar radiation hitting the solar collector and is depending on the geographical location of the collector. However, the collector orientation is often decided by the orientation of the roof of the building where the collectors usually are installed [23].

2 The Novel Open Cycle Two-stage Desiccant Cooling System

2.1 Location and Design of the System

The novel open cycle two-stage desiccant cooling system incorporating close-to isothermal dehumidification and regenerative water chilling is located in the GEL-building at SJTU which is showed in Figure 18. GEL stands for Green Energy Laboratory and is a study and test platform where experiments and analysis of building based energy systems and energy saving devices are performed. In addition to function as a test platform, the GEL-building also functions as an office building and exhibition center. The desiccant cooling system is installed on the roof of the building and is located under the solar thermal air collectors which are used as the main source of thermal energy. The roof of the GEL-building, as well as an overview of the desiccant system is showed in Figure 19.



Figure 18: The GEL-building located in Shanghai Jiao Tong University

There are a number of different components working together to create chilling water and processed ventilation air. The ventilation air is meant supplied to an apartment in the second floor of the building. A schematic of this apartment is provided in Figure 20. The location of the apartment is directly underneath the desiccant cooling system so that the processed air easily can be directed towards this space, but to be able to provide the apartment with processed air it is necessary to have a duct leading the processed air into the building. This was not installed during the testing which means that during the experiments, the process air is just released to the environment after flowing through the system. The generated chilling water which normally would be used to cool the

ventilation air is instead directed through a pipe system exchanging heat with the ambient surroundings.

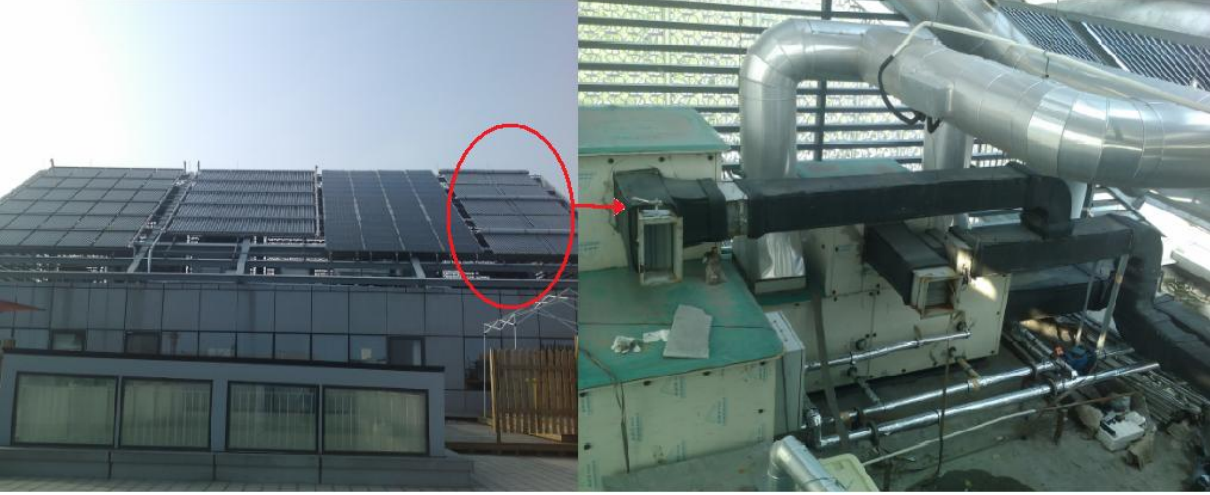


Figure 19: The roof of the GEL-building and the desiccant cooling system

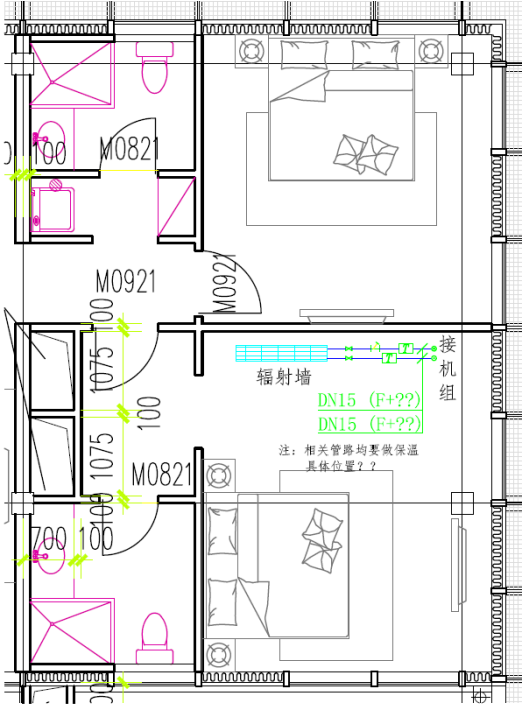


Figure 20: Schematic of the conditioned space

2.2 System Components

Various parts of the system are housed inside unit boxes, and the process and regeneration air flows inside cabinets making sure that they do not interfere with each other. The main components that take part in the system are:

- Two desiccant wheels
- Regenerative evaporative cooler
- Three air-water heat exchangers
- Two auxiliary heaters
- Cooling tower
- Evacuated tube solar air collectors

To run the system there are in total three different electrical control lockers needed to be operated. Figure 21 shows the main control locker used to control the electrical powered fans, pumps and motors of the system. In addition there are a similar locker for operating the auxiliary heaters and the cooling tower.



Figure 21: Electrical control locker

2.2.1 Two-stage Desiccant Wheels

The main components of the desiccant wheel are the desiccant material, the dividing clapboard, the wheel casing, the transfer core and the electrical engine. The desiccant material which is used in the two-stage desiccant wheel dehumidification process has a lithium chloride and silica gel based composition. This composition adsorbs the water molecules from the process air, and regenerates by desorbing these molecules when in contact with the hot regeneration air. The dehumidification performance of the desiccant wheels will vary depending on the temperature of the regeneration air.

If the temperature of the regeneration air is not high enough, this will result in a lower desorption amount and a poorer dehumidification performance. The two-stage process is consisting of two wheels running simultaneously in different stages of the system. The purpose of this setup is to dehumidify the process air effectively while requiring as low-grade regeneration heat as possible. Dividing the dehumidifying desiccant wheel process into two stages also makes it possible to implement interstage heat exchangers to deal with the adsorption and regeneration heat. The process air firstly enters the first desiccant wheel, then enters an interstage heat exchanger and then enters the second desiccant wheel. The wheels are divided into two regions by the clapboard, one region is for the process air and the other region is for the regeneration air. The area of the process air region is larger than the regeneration air region; the ratio is approximately 3:1.

The desiccant wheel structure is produced in Japan and the desiccant material composition is produced and applied at SJTU. The desiccant matrix of the wheel has a porous structure creating a number of channels for the air to flow through. The desiccant composition is applied on the walls of these channels. It is in these channels that the dehumidification by adsorption takes place. The wheel structure is attached at the core to a shaft which holds the wheel at a fixed position. The core is consisting of a transfer ring which allows the wheel to rotate around its center. The rotation is applied by an electrical driven motor installed next to the wheel. The motor uses a belt connected around the outside of the desiccant wheel casing, forcing a slow rotary velocity of approximately 8r/h.

The desiccant wheels installed in the system has both the same shape and dimensions, with a thickness of 100mm and a diameter of 550mm. The transfer core and the casing have a thickness of 0.7mm and 0.8mm respectively. The second stage desiccant wheel is newly installed in the system and will therefore be focused on the most during the performance evaluation.



Figure 22: The two desiccant wheels

2.2.2 Air to Water Heat Exchangers

The purpose of the air to water heat exchangers is to lower the temperature of the process air flowing in the dehumidification part of the system. There are three of these heat exchanger units installed at different stages of the system. The first unit is installed at the inlet of the system and is used to pre-cool the ambient air entering the process air cycle. The second unit is installed after the first desiccant wheel and is removing the regeneration and adsorption heat gained by the process air. The third unit is installed after the second desiccant wheel for the same reason. The cooling water is provided by a cooling tower located close to the desiccant cooling system. Figure 23 shows the pipes where the cooling water enters and exits the heat exchanger, process air enters from the right. The inlets are at the lower pipes and the outlets are at the upper pipes.



Figure 23: The cooling water piping system

2.2.3 Regenerative Evaporative Cooler

The regenerative evaporative cooler is consisting of two different components:

- Cross-flow heat exchanger
- Direct evaporative cooler

The cross-flow heat exchanger is introduced to the system to improve the performance of the chilled water production by utilizing the cold process air exiting the evaporative cooler to lower the temperature of the process air entering the evaporative cooler. Figure 24 shows the cross-flow heat exchanger installed in the system. The plates inserted into the exchanger create channels where the two air streams can flow separately. The streams cross enter into every other channel, as illustrated in Figure 25, and heat exchanges with each other. Since the two air streams do not mix there is no moisture transfer between the two streams. The cross-flow heat exchanger uses high quality

seawater corrosion resistant hydrophilic aluminum plates that gives good heat transfer ability and ensures a long lifetime of the exchanger. The heat exchanger has no running components so the maintenance cost is minimal. The spacing between the exchanger plates is 3mm and the overall dimensions of the exchanger are a length of 300mm, a width of 300mm and a height of 700mm.

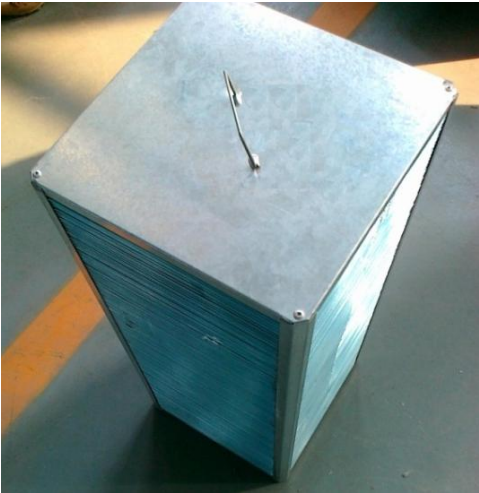


Figure 24: The cross-flow heat exchanger

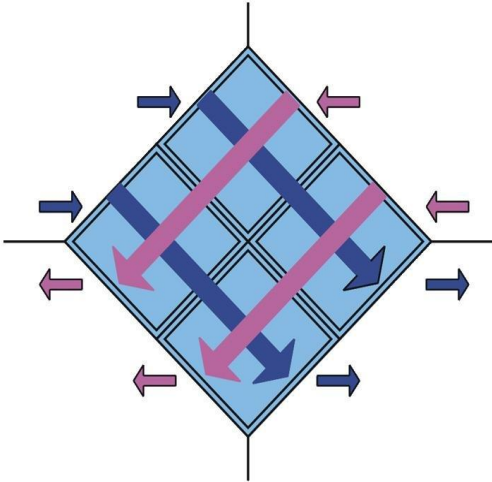


Figure 25: Principle of a cross-flow heat exchanger

The evaporative cooling unit used in this system is a cross-flow direct evaporative cooler mainly consisting of a water pump, a sprinkler and honeycomb paper. The water is sprayed at the top by the sprinkler to generate a falling film effect at the surface of the honeycomb wall. The honeycomb paper is porous and durable for repeatedly wetting and drying. The pattern of the paper forms channels where the air flows. The air entering the channels comes in contact with the falling film water. This generates a mass exchange where some of the water evaporates and mixes with the air. This evaporation requires energy in the form of heat which is provided by the water and the air. As a result, the temperature of both the air and water decreases. The chilled water at the outlet of the evaporative cooler is gathered in a chilled water tank and distributed in the chilled water cycle. The purpose of the generated chilled water is to provide cooling of the process air which will be supplied to the building. The unit that would have been used for heat exchange between this generated chilled water and the process air is not installed in the experimental system. Therefore, the heat exchange of the chilled water is between the chilled water pipe and the ambient air. After returning from the chilled water cycle, the water is again sprinkled at the top of the cross-flow direct evaporative cooler. The principle of the evaporative cooler is illustrated in Figure 27, where the water is gathered at the bottom of the cooler and distributed by the pump.

Figure 26 shows the evaporative cooler installed in the desiccant cooling system. The channels created by the honeycomb wall, as well as the chilled water tank at the bottom of the cooler are visible. The length, width and height of the evaporative cooler are 600mm, 500mm and 570mm respectively. Since the air is in direct contact with the water, the humidity of the air increases. This means that the amount of water present in the chilled water cycle slowly decreases. Therefore, the chilled water tank is connected to a supply pipe providing fresh water to the cycle, this inlet is visible at the bottom of Figure 26. The length, width and height of the chilled water tank are 1100mm, 700mm and 350mm respectively.



Figure 26: The cross-flow direct evaporative cooler

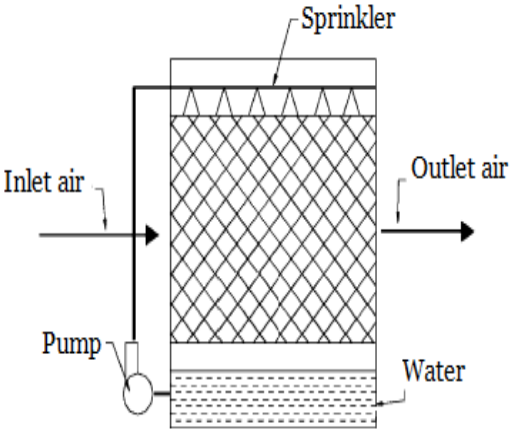


Figure 27: Principle of the evaporative cooling unit

2.2.4 Evacuated Tube Solar Air Collector

The main thermal energy source for the regeneration heat is the evacuated tube solar air collectors. Using solar radiation as the main energy source is perfect for this desiccant cooling system since this system is required to have the best performance during the summer when the ambient temperature and humidity ratio is at its highest. Solar thermal energy is also a clean energy source which makes the system become more environmentally friendly. The solar collectors are installed on the roof of the building, and have a tilt angle close to 45° in the south direction. The collector area is consisting of five groups of 55 evacuated tubes, all with a length and diameter of 1500 mm and 47 mm respectively. One of the evacuated tube groups were not connected to the system during the testing which means that the total potential of the solar heating system is not utilized. Four groups of evacuated tubes with the given length and diameter gives a total effective solar collector area of about 24 m². Figure 28 shows the area under the collectors where special designed pipes transfer the heated air form the solar collector into the regeneration side of the desiccant wheels. Before the inlet at the regeneration sides of the desiccant wheels, the heated air is divided evenly by splitting

the pipe in to different directions. This makes sure that the two desiccant wheels are supplied equally with heated regeneration air.



Figure 28: Pipes transferring heated air to the system

The air enters through the header pipes, showed in Figure 29, and is guided through the evacuated glass tubes. Figure 30 shows how the evacuated glass tubes are connected to the header pipes. There are in total three header pipes, two of them are connected to 110 evacuated glass tubes and the last one is connected to 55 evacuated glass tubes. The tubes heat the air by using the thermal energy provided by the incident solar radiation. Inside the tubes there is an absorber which has a dark blue color, allowing the tubes to intercept almost the entire solar radiation spectrum. Also, inside each of the glass tubes there are inserted a steel pipe which raises the efficiency of the collector by forcing the air to flow inside the metal pipe and back at the outside of the pipe. This allows more heat to be added to the regeneration air which lowers the requirements for an auxiliary heater.



Figure 29: Entering point of the regeneration air

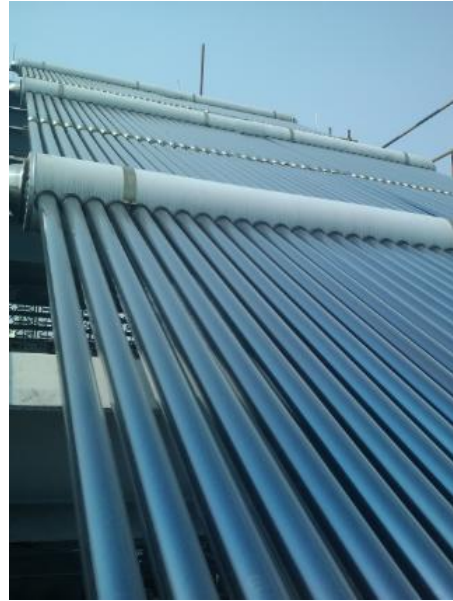


Figure 30: Evacuated tube solar air collector array

2.2.5 Auxiliary Heater

Using solar collectors as the regeneration heat source makes the system very dependent on the available sun radiation during the day. Sometimes, the solar collectors do not have the weather conditions to be able to generate the total amount of heat that is required to regenerate the desiccant wheels. It is therefore installed an auxiliary heating device after the air has passed the solar collectors. The auxiliary heater, showed in Figure 31, is consisting of two sets of electric heaters where one is designed with a 3kW heating wire and the other is designed with a 6kW heating wire. This guarantees that the heating system is capable of applying enough heat to the regeneration air. The auxiliary heater can be set to run if the weather conditions results in the solar collectors not being able to provide enough thermal heat to the regeneration air. The set point temperature of the auxiliary heaters is 65°C during the experiments. This means that if the auxiliary heater is turned on and the regeneration temperature is below this point the auxiliary heater will begin working. When the regeneration temperature reaches 65°C the auxiliary heater will be turned off.



Figure 31: The auxiliary heater of the system, 3 kW, 6 kW and 9 kW

2.2.6 Cooling Tower

Basically a cooling tower functions in the same way as the evaporative cooler unit, where the warm returning water gets sprayed from the top of the tower. Ambient air flows counter to the direction of the falling water droplets, causing some of the water to evaporate into the air stream. The energy required for the evaporation is mainly provided by the part of the water droplets not evaporating. The result is a temperature decrease of the water gathering at the bottom of the tower. The evaporated fraction of the water in the cycle needs to be replenished by new water. A cooling tower can operate by natural or forced convection, depending on the location and application of the system [24].

The cooling tower used in this system has one function; to remove heat from the cooling water returning from the air to water heat exchangers. The tower is located on the roof, approximately 15 meters from the desiccant system. The return water from the heat exchangers is pumped to the top of the cooling tower to a sprinkler which distributes the water as droplets falling down towards the bottom of the tower. The tower, showed in Figure 32, operates by forced convection meaning that a fan is running at the top of the tower forcing the air stream upwards in the opposite direction of the water droplets. When the water droplets reach the bottom of the tower, the temperature has decreased as a result of the energy required for evaporation when water is in contact with air. At the bottom of the tower, the cooling water is collected in a pool where it enters through a pipe leading to the inlet of the heat exchangers. Because evaporation of the water causes the water level to decrease, the pool is connected to a pipe replenishing water to the chilling cycle. The specifications of the cooling tower are presented in Table 1.



Figure 32: The cooling tower connected to the system

Table 1: Specifications of the cooling tower

Parameter	Value	Unit
Inlet pipe diameter	5	cm
Outlet pipe diameter	5	cm
Water flow	275	L/min
Power	2300	kJ/h
Stages/Voltage	6/386	P/V
Temperature	37-32-28	°C
Head	8	m

2.2.7 Other Components

In addition to the main components of the system it is also necessary with assisting components for providing mass flows and movement. All the assisting components installed in the desiccant cooling system are listed in Table 2. The process air, regeneration air, cooling water and chilling water cycle each have a component installed that ensures mass flow through the parts of the system. The air flows in the process and regeneration cycle are generated by fans, and the water flows in the cooling and chilling cycle are generated by pumps. Figure 34 shows the air fan that generates air-flow through the regeneration part of the system. The desiccant wheels needs to rotate for the system to be able to run continuously. Figure 33 shows the electric motor that provides the rotation of the second stage desiccant wheel. Also the first stage desiccant wheel has the same type of driving motor installed.

Table 2: Assisting components of the desiccant system

Component	Manufacturer	Model
Process air outlet fan	Kruger	BSB 225
Regeneration air outlet fan	Kruger	BSB 225
First desiccant wheel motor	SNOH	IP44
Second desiccant wheel motor	SNOH	IP44
Cooling water pump	Shanghai People Pump Factory	IRG
Chilling water pump	WILO	PUN-600E



Figure 33: Electrical powered motor



Figure 34: Regeneration air fan

2.3 Explanation of the System Process

The system investigated in this thesis is as mentioned a novel open cycle two-stage desiccant system driven by solar thermal air collectors which is used to produce chilled water and dehumidified air. To have the ability to perform both of these tasks, the system is divided in four processes where different fluids are active:

- Process air
- Regeneration air
- Chilling water cycle
- Cooling water cycle

Figure 35 represents a schematic of the system setup with the different working fluids. The process air part is starting at the entering point of the first heat exchanger, the regeneration air part is

starting at the entering point of the auxiliary heater and the chilling water cycle is the separate cycle involved with the evaporative cooler. The cooling water is not represented in the figure, but this is the cooling source used in the air to water heat exchangers located before, between and after the desiccant wheels. The system is divided in three different main parts marked with the letters A, B and C. Part A is the first desiccant wheel dehumidification process, part B is the second desiccant wheel dehumidification process and part C is the regenerative evaporative cooling process.

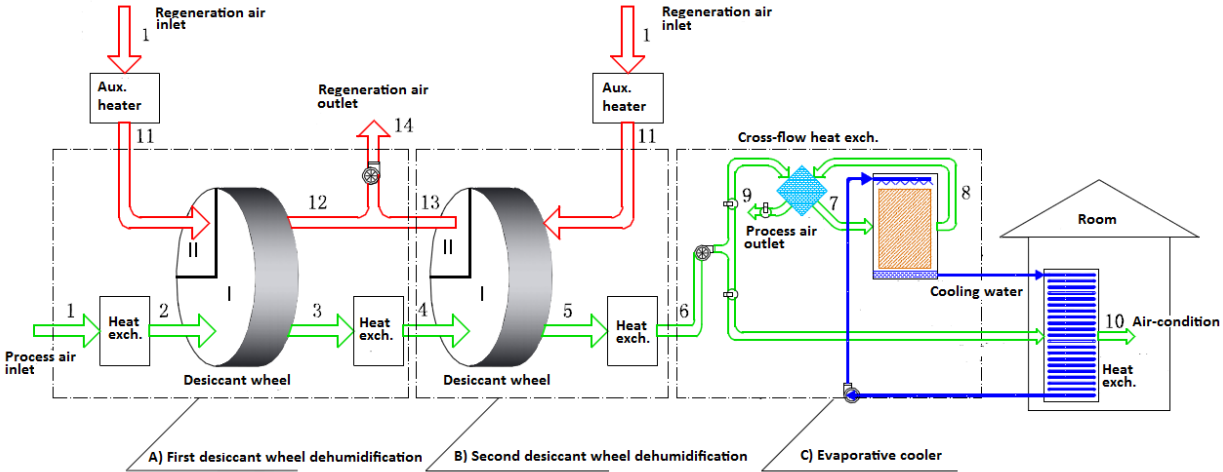


Figure 35: Schematic of the desiccant cooling system.

Part A starts with the process air entering the system through a duct. First, the air flow through a pre-cooling heat exchanger located in front of the first desiccant wheel. This heat exchanger is one of three heat exchangers that use cold water to cool the process air. The cold water is generated in the cooling tower, and the water is moved between the tower and the heat exchangers in a separate cycle. The heat exchanger is designed so that the air and the water are not in contact, ensuring that the humidity of the air is not increasing. After the process air has exchanged heat and the initial ambient temperature is lowered, it enters the first desiccant wheel. Also entering the desiccant wheel is the heated regeneration air. The process air and the regeneration air are entering in different channels while the desiccant wheel slowly rotates, ensuring that the entire area of the wheel is in contact with both air streams during one cycle. The desiccant wheel sorbs water from the process air and uses the warm regeneration air to desorb and be ready for a new dehumidifying cycle. When the process air is dehumidified, the temperature increases as a result of the adsorption of water and the heat coming from the hot area of the regeneration side of the desiccant wheel. Therefore, to ensure proper dehumidifying effect after the first desiccant wheel, the process air enters a second cooling heat exchanger. After this heat exchanger the now cooled process air enters part B of the system.

Part B starts with the process air entering the second desiccant wheel. Regeneration air is also here entering the wheel, and the following process is basically the same as for stage A. When the regeneration air has desorbed the wheel, it mixes with the regeneration air from stage A and gets transported back to the environment. After the dehumidification done by the second desiccant wheel, the process air is lead through the third cooling heat exchanger to again decrease the temperature before entering part C.

Part C is supposed to start with the process air being divided into two different air streams, one directed directly towards the room to be used for air-conditioning and one is directed towards the evaporative cooler to generate chilled water. As mentioned, the ability to add air to the building is not present meaning that all the air is directed towards the evaporative cooler. The process air meant for the evaporative cooler is first directed through a cross-flow heat exchanger. This is done to reduce the temperature of the air even more, making the process of creating chilled water more efficient. The cross-flow heat exchanger uses the process air after the evaporative cooler as the cold source. Before entering the evaporative cooler, the process air is cold and dry. In the evaporative cooler the process air is in direct contact with water. Some of the water evaporates and the dry air absorbs this water vapor. The heat required for the evaporation is taken from both the water and the air, causing both the water temperature and the air temperature to decrease. The cooling of the water used in the evaporative cooler makes it possible to use the system to generate chilled water and this chilled water can then be used for different cooling purposes. The chilled water cycle is a separate cycle where water is circulating between the evaporative cooler and a heat exchanger. Figure 36 represents the inlet and outlets of this cycle where also the circulation pump and supply water inlet are visible. After the evaporative cooler, the process air is lead trough the cross-flow heat exchanger to act as the cold-source for the process air entering the evaporative cooler. When this air exits the exchanger it is discharged to the environment. This is because, after passing through the evaporative cooler, the air is too humid to be used in the air-conditioning system. When adding air to the building becomes possible, a part of the process air before the evaporative cooler can be directed through a heat exchanger that uses the chilled water to decrease the temperature.

Table 3: Explanation of the stages occurring in the desiccant cooling system

<i>Process air</i>	
Stage	Explanation
1 → 2	Pre-cooling the ambient process air before entering the desiccant wheel in order to improve the dehumidifying effect of the wheel.
2 → 3	First desiccant dehumidification process where moisture is removed from the process air.
3 → 4	Second cooling process where sensible heat exchange occur.
4 → 5	Second desiccant dehumidification process where the second wheel ensures further drying of the process air, similar to stage 2 → 3.
5 → 6	Last surface cooler stage where sensible cooling of the process air reduces the temperature of the air, optimizing system performance.
6 → 7	The first part of the cross-flow heat exchanger process where the air gets cooled from stage 6 to 7.
7 → 8	Evaporative cooling process, humidity increases and temperature decreases.
8 → 9	The second part of the cross-flow heat exchange process where the process air from the evaporative cooling unit is redirected to the cross-flow heat exchanger to cool the air prior to the evaporative cooling unit.
6 → 10	Sensible cooling of the process air by exchanging heat with the produced chilled water, causing the temperature to drop to desired indoor temperature.
<i>Regeneration air</i>	
Stage	Explanation
1 → 11	Heating process where ambient regeneration air is heated by a heat source to a temperature suitable for renewing the desiccant wheel.
11 → 12	Desorption process where hot regeneration air is directed to the regeneration area of the first desiccant wheel.
12 → 13	Same principle as for stage 11 → 12 but this time it is a process involving the second desiccant wheel.

3 Testing and Experimental Work

3.1 Renovation of the System

The desiccant cooling system was installed in the summer of 2010. During the following winters and construction period towards finishing the building, the system has become worn down. Therefore, some renovation needed to be done prior to the testing of the system.

The chilled water system is using a centrifugal pump to circulate the water between the evaporative cooler and the ventilation air heat exchanger. This pump needed to be change because of some cracking which had occurred during the winter. During the first run of the system after changing the pump, the chilling water tank needed to be filled with water before the pump was turned on. This was done to ensure that sufficient chilling water was present in the system. Also, a leakage problem of the chilling water pipe needed to be fixed.



Figure 38: The broken chilling water pump



Figure 39: The new chilling water pump

All of the process water taking part in the system is transported in and out of the different components through pipes. The cooling tower uses pipes to transport the water from the tower to the pre- and interstate heat exchanger, and also the chilling water process uses separate pipes to transport the water. Large areas of these pipes are on the outside of the system and are therefore exposed to the sun. To prevent the sun radiation to influence the temperature of the fluid inside the pipes, reflecting insulation material is put around the outside of the pipes. During the winter the weather has worn most of the old insulation and there were a lot of fractures and bare spots. To protect the pipes and ensure that the sun is not influencing the test results, all of the old insulation needed to be replaced with new insulation.

Some of the temperature sensors also needed to be replaced, and some issues with the electricity supply cables needed to be adjusted. For the sensors the main issue was corrosion and loose connections between the sensor and the electricity cables. Also a new computer for recording the measurements needed to be installed and connected to the system.

3.2 Testing Equipment

When performing the experiments there is need of some different equipment for testing and gathering data from the system. The testing equipment used depends on which data are interesting to evaluate at the different stages of the system. Temperature, relative humidity, solar radiation intensity and fluid flow rate are all data which must be recorded. The relevant equipment for this system is listed in Table 4. In the following sections the application areas of the different testing equipment will be explained.

Table 4: The testing equipment

Instrument	Model	Range	Accuracy
Temperature sensor	PT100/PT1000	-200 - 500°C	+/- 0.2°C
Temperature and humidity sensor	THT-N263A	20 – 90%	+/- 3%
Solar radiation intensity	TBQ-2	0 - 2000W/m ²	+/- 2%
Flow rate	CF8585	0 - 50 m/s	+/- 3 %

The temperature and humidity sensors are connected to the recording computer which uses specific software to record and compare all the measured values. This software is called Keithley 2700, and a detailed description of this software can be found in appendix B. Regarding the adjustment of the air flow rate in the process and regeneration part of the system, a frequency converter is adopted.

3.2.1 Temperature Measurement

The temperature of the process air, the regeneration air and the water at specific points of the system is measured by ordinary temperature sensors. The sensors are winded together with the wires connected to the computer and protected with electrical insulation tape. At the test points the sensors are covered by a silicone substance, as shown in Figure 41, which protects the sensor from the ambient weather conditions and therefore helps in ensuring accurate measurements.

The temperature sensors used in the experiments are PT100 and PT1000 sensors which has a temperature measurement range from -200 to 600°C and an accuracy of +/- 0.2°C. Figure 40 and Figure 41 shows some of the PT1000 sensor used during the experiments. The sensors have high-accuracy wire wound, with class “A” platinum elements [25].

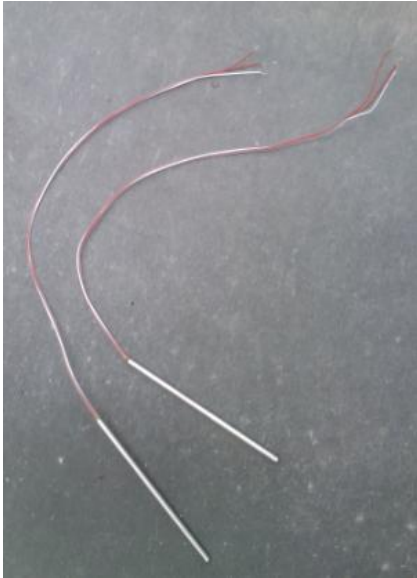


Figure 40: The PT1000 sensors



Figure 41: PT100 sensor covered by a silicon substance

3.2.2 Temperature and Humidity Measurement

At some test points it is necessary, when providing an accurate evaluation of the system performance, to measure both the temperature and the humidity ratio of the air. At these points, temperature and humidity sensors are used. The sensors are placed directly in the air stream and connected to the recording computer. The temperature and humidity sensors need to be powered by electricity and are therefore also connected to an electricity supply cable.

The temperature and humidity sensors are model THT-N263A sensors which is part of the THT-N series and has a temperature and relative humidity measurement range from 0 to 50°C and 20 to 90% respectively. This series is one of the best detectors for measurement of temperature and humidity, and is provided with a reliable macro-molecule humidity sensor [26]. Figure 42 and Figure 43 shows two of the temperature and humidity sensors used in the testing. Detailed characteristics of the THT-N263A sensors are provided in appendix A, Table 16.



Figure 42: The THT-N263A sensor



Figure 43: THT-N263A sensor measuring

3.2.3 Solar Radiation Measurement

The instrument which is used to test the available solar radiation is a TBQ-2 standard radiometer. The TBQ-2 radiometer sensor can be used to measure the spectral range from 300 to 3000nm of the irradiance to the surface of the earth. This sensor is widely used in meteorology, solar energy, agriculture and building material measurements [27]. Detailed characteristics of the component are provided in appendix A, Table 17.

Figure 44 shows the radiometer used to record the solar radiation. It is placed at the roof close to the solar collectors, with the same angle and direction as the collectors. The radiometer can therefore provide a realistic picture of the actual radiation hitting the collectors.



Figure 44: The solar radiometer

3.2.4 Flow-rate Measurement

The air velocity in the system is measured by an anemometer where multiple point-tests are carried out and an average velocity is calculated. The anemometer is placed directly into the air duct cross-sections of the system. Then this calculated average velocity is used together with the area of the cross-section and the density of the air to calculate the mass flow rate of air in the system using Equation 3 [28].

$$\dot{m} = \rho VA$$

Equation 3: Mass flow rate

Where ρ is the density, V is the velocity and A is the cross-section area of the air duct.

Figure 45 shows the equipment used for measuring the air velocity which is a CF8585-model TSI anemometer. This is a hand-held, battery powered, microprocessor based instrument capable of measuring air velocity in a range from 0 to 9999 ft/min or 0 to 50 m/s. The accuracy of the model is +/- 3 % or +/- 3 ft/min, depending on which of the values are highest [29]. Detailed characteristics of the anemometer are given in appendix A, Table 18.



Figure 45: The CF8585-model TSI anemometer

3.3 Performance Indexes

The two-stage desiccant cooling system uses heat and work to drive the cycle, and there are several indexes which can be used to indicate the total system performance. The following equations are used to calculate the relevant performance indexes. The point numbers of the equations are based on Figure 46.

The first parameter which is interesting to evaluate is the cooling capacity of the system given in Equation 4. The cooling capacity indicates the total achieved cooling of the process cycle.

$$Q_{cs} = m_{pro}(h_1 - h_6)$$

Equation 4: Cooling capacity

In this definition of the cooling capacity it is considered the change in enthalpy of the process air side, where h_1 is the inlet enthalpy value and h_9 is the outlet enthalpy value, and the mass-flow of the process air is represented by m_{pro} .

One of the main advantages of using solar air heating as source for the regeneration heat is the potential in electrical energy savings. Therefore it is interesting to calculate the electrical coefficient of performance of the system. The COP_{el} is based on all the electrical inputs to the desiccant system. This includes electrical energy from water pumps, air fans and desiccant wheel rotation motors used in the system. The total electrical energy demand is calculated using Equation 5.

$$W_{el} = W_{pump} + W_{fan} + W_{motor}$$

Equation 5: Total electrical demand

Here the work of the pump and the work of the fan are calculated using Equation 6 and Equation 7 respectively [30]. The parameter values used in the calculations are stated in Table 5.

$$W_{pump} = \frac{gm_w H}{\eta_{pump} \eta_k}$$

Equation 6: Electrical work of the pump

$$W_{fan} = \frac{m_a \Delta P z}{\rho_a \eta_{fan} \eta_{me}}$$

Equation 7: Electrical work of the fan

Table 5: Parameters used in Equation 6 and Equation 7

Parameter	Value	Unit
H	20	m
η_{pump}	60	%
η_k	85	%
ΔP_{pro}	1000	Pa
ΔP_{reg}	800	Pa
η_{fan}	85	%
η_{me}	100	%
z	1.3	-

The COP_{el} is calculated using Equation 8, which is the cooling capacity obtained by the system divided by the systems total electrical input.

$$COP_{el} = \frac{Q_{cs}}{W_{el}} = \frac{m_{pro}(h_1 - h_6)}{W_{pump} + W_{fan} + W_{motor}}$$

Equation 8: Electrical coefficient of performance

Another coefficient of performance which is calculated is the thermal coefficient of the system. This index indicates the ratio between the amounts of cooling the system is achieving and the amount of thermal energy the heating system is capable of providing. The later is given by two equations, where one is for the heating capacity of the solar air collector and one is for the heating capacity of the auxiliary heater. These two capacities are defined by Equation 9 and Equation 10 respectively. The COP_{th} is then calculated using Equation 11.

$$Q_{sc} = C_{p,a} m_{reg} (T_{11} - T_1)$$

Equation 9: Heating capacity of solar collector

$$Q_{aux} = C_{p,a} m_{reg} (T_{12} - T_{11})$$

Equation 10: Heating capacity of auxiliary heater

$$COP_{th} = \frac{Q_{cs}}{Q_{sc} + Q_{aux}} = \frac{m_{pro}(h_1 - h_6)}{C_{p,a} m_{reg} (T_{12} - T_1)}$$

Equation 11: Thermal coefficient of performance

Here the inlet temperature of the solar collector is represented by T_1 and the outlet temperature of the solar collector is represented by T_{11} , while the outlet temperature of the auxiliary heater is represented by T_{12} .

When evaluating the solar air collector it is necessary to look at the solar collector efficiency. To be able to calculate the efficiency of the solar collector, the total incident radiation needs to be determined. The total incident radiation heat, which is the radiation heat from the sun hitting the solar collector, is calculated by Equation 12.

$$Q_{rad} = I_{rad} A_{sc}$$

Equation 12: Total incident radiation heat

Here I_{rad} represents the solar radiant intensity, and A_{sc} represents the total solar collector area.

The efficiency of the solar air collectors indicates how much of the incident solar radiation the collectors are capable of transforming into thermal energy. This efficiency is calculated using Equation 13.

$$\varepsilon_{sc} = \frac{Q_{sc}}{Q_{rad}} = \frac{C_{p,a} m_{reg} (T_{11} - T_1)}{I_{rad} A_{sc}}$$

Equation 13: Efficiency of the solar collectors

The total moisture removal by the desiccant wheels and the wheels dehumidification efficiency is given by Equation 14 and Equation 15 respectively. These two indexes indicate how well the desiccant system is dealing with the humidity of the ambient air where d_{in} is the inlet humidity, d_{out} is the outlet humidity and $d_{out,ideal}$ is the ideal humidity ratio of the outlet process air [31]. By setting

$d_{out,ideal}$ equal zero the efficiency, when compared to a desiccant wheel with absolute moisture removal, is calculated.

$$\Delta d = d_{in} - d_{out}$$

Equation 14: Total moisture removal

$$\varepsilon_d = \frac{d_{in} - d_{out}}{d_{in} - d_{out,ideal}}$$

Equation 15: Dehumidification efficiency of desiccant wheel

In order to describe the performance of the cross-flow heat exchanger the efficiency is calculated using Equation 16. Here T_6 is the inlet of the air being cooled by the heat exchanger, T_7 is the outlet of the air being cooled by the heat exchanger and T_8 is the temperature of the cold inlet air. T_8 is the lowest achievable temperature of the cross-flow heat exchanger.

$$\varepsilon_{cf} = \frac{T_6 - T_7}{T_6 - T_8}$$

Equation 16: Efficiency of the cross-flow heat exchanger

The efficiency of the evaporative cooler producing chilled water is evaluated using Equation 17. Where T_{22} is the water inlet of the evaporative cooler, T_{21} is the outlet water of the evaporative cooler and $T_{7,wb}$ is the wet bulb temperature of the inlet process air [32]. The value of $T_{7,wb}$ is important because this shows the achievable temperature of the chilling water.

The evaporative cooler also produced chilled air which is used to pre-cool the process air streaming in to the evaporative cooler. The air cooling efficiency of the evaporative cooler is defined by Equation 18. Here T_7 is the inlet dry bulb air temperature, T_8 is the outlet dry bulb air temperature and $T_{7,wb}$ is the same temperature as in Equation 17 [33].

$$\varepsilon_{ev,w} = \frac{T_{22} - T_{21}}{T_{22} - T_{7,wb}}$$

Equation 17: Chilling water efficiency of the evaporative cooler

$$\varepsilon_{ev,a} = \frac{T_7 - T_8}{T_7 - T_{7,wb}}$$

Equation 18: Air cooling efficiency of the evaporative cooler

3.4 The Test Program

The open cycle desiccant cooling system has been operated during the summer of 2012. The goal of the test program is to test the different components involved in the desiccant cooling system and evaluate the overall performance of the system. Numerous experimental test runs have been performed and a lot of performance data has been registered. The first analysis is performed on the system under different regeneration temperatures. This is done to evaluate the grade of importance regarding the quality of the regeneration air entering the desiccant wheels. In order to investigate the effect of the pre cooling air to water heat exchange, the system is run with and without the first heat exchange, and the results from two different operation conditions are compared. Experiments are performed in July when ambient temperature and humidity are high. These results are then compared with experiments performed on days when the ambient temperature and humidity is not so high. The main performance index of the experiment is the chilling water temperature, the process air temperature and humidity, the COP_{th} and COP_{el} . To fully analyze the performance of the system, also the efficiency of the desiccant wheels, the regenerative evaporative cooler and the evacuated tube solar air collectors are evaluated. The system is also run without the first desiccant wheel. This is done to evaluate the dehumidification performance when only the second desiccant wheel, which is newly installed, is working.

As previously mentioned there are installed a number of measurement components at different stages of the test system. Figure 46 illustrates the desiccant cooling system and all the different points where measurements are performed.

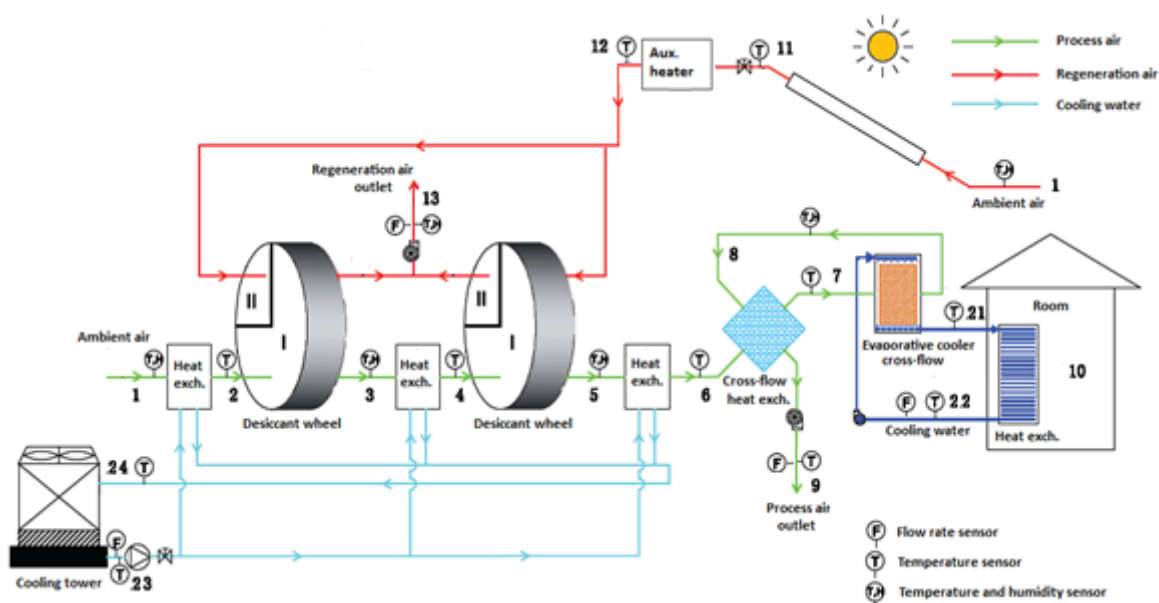


Figure 46: Schematic on the real two-stage desiccant cooling system

The process and regeneration air are measured and tested after every interaction with a system component. Different testing equipment is used depending on which performance data are relevant to investigate. The dry bulb temperature of the process and regeneration air is measured at every stage of the system because this is the easiest value to measure and one of the most important values when deciding other indexes. At the measurement points of the system that is after a component changing the absolute humidity ratio it is also necessary to measure the relative humidity of the air. Therefore, it is installed THT-N263A temperature and humidity sensors after the desiccant wheels and the evaporative cooler. Since measuring the relative humidity of the ambient air is important, a THT-N263A sensor is also placed at the process air inlet. The flow rates of the process and regeneration air are also values that are necessary to document. These flow rates can be measured at different points of the two cycles but it is most convenient to measure these parameters at the outlets of the system. Overviews of all the measurements done in the process and regeneration air cycle are provided in Table 6 and Table 7 respectively.

Table 6: Measurements done of the process air

Point	Type of measurement	Description
1	Temperature and humidity	Ambient air inlet
2	Temperature	After the pre-cooling heat exchanger
3	Temperature and humidity	After the first desiccant wheel
4	Temperature	After the interstage heat exchanger
5	Temperature and humidity	After the second desiccant wheel
6	Temperature	After the third cooling heat exchanger
7	Temperature	After the cross-flow heat exchanger
8	Temperature and humidity	After the evaporative cooler
9	Temperature and flow rate	At the outlet, after the regeneration part of the cross-flow heat exchanger

Table 7: Measurements done of the regeneration air

Point	Type of measurement	Description
1	Temperature and humidity	Ambient air inlet
11	Temperature and flow rate	After the solar collector
12	Temperature	After the auxiliary heater
13	Temperature, humidity and flow rate	At the outlet, after the desiccant wheels

The chilled water cycle and the cooling water cycle are also parts of the system which are important to measure, especially the chilled water cycle. Table 8 shows the measurements points of the chilled water cycle. The measurements from this cycle are very important because it gives the temperature

of the chilled water produced. This can be used to evaluate how well the system is capable of providing cooling to the process air meant for entering the conditioned space. The measuring of the chilled water cycle is consisting of two measurement points, and at each point there is installed a PT100/PT1000 temperature sensor. The first point is after the water exits the evaporative cooler and the second point is when the water returns from the cycle before entering the evaporative cooler. The flow rate of the chilling water at the inlet of the evaporative cooler is also measured.

The water from the cooling water cycle is used in the air to water heat exchangers in relation to the desiccant dehumidification part of the system. Monitoring the change in temperature before and after these exchangers helps control that the process air is cooled properly. Therefore, PT100/PT1000 temperature sensors are installed before and after the water are involved with the heat exchanger. In addition to the measurement data from these sensors providing information on how capable the heat exchangers are regarding cooling of the process air, it also indicates how well the cooling tower works. The flow rate of the cooling water is also data which are recorded. Table 9 shows the measurement points of the cooling water cycle.

Table 8: Measurements done in the chilled water cycle

Point	Type of measurement	Description
21	Temperature	Chilled water supply temperature
22	Temperature and flow rate	Chilled water return temperature

Table 9: Measurements done in the cooling water cycle

Point	Type of measurement	Description
23	Temperature and flow rate	Cooling water supply temperature
24	Temperature	Cooling water return temperature

In addition to the measurements mentioned, the incident solar radiation on the solar collectors is also measured. The solar radiation sensor is placed on the roof next to the solar collectors in the same angle as the collectors. This ensures accurate solar intensity recordings which can be used to decide the thermal energy available and the efficiency of the solar collector.

3.5 Ambient conditions

Since the desiccant cooling system uses thermal energy from evacuated tube solar air collectors as the main source of energy, the system is functioning best at days where the incident sun radiation intensity is high. Of course, the system can also be run when the radiation intensity is low because of

the auxiliary heaters. However, it is not desirable to perform experiments when it is raining. This is mainly because the main goal of the experiments is to evaluate the system performance during typical summer conditions with sunny weather, but also because of the risk of the measurement equipment being damaged. The test experiments are therefore planned and performed with respect to the weather forecast. The main part of the test program is taking place on sunny days so that the system performance under optimal weather conditions is documented. To compare the system performance at optimal weather conditions to the performance when the weather is not optimal, a small part of the test program is performed at not optimal weather conditions.

The weather conditions during the test period is varying and is therefore classified under standard conditions called Air-conditioning and Refrigeration Institute conditions and typical Shanghai summer conditions [34]. These standard conditions are divided into three different ranges called:

- ARI summer
- ARI humid
- Shanghai summer

The reason behind this classification is to separate and explain some of the difference in the results, and to investigate when the desiccant cooling system has the most optimal performance. The values of the three condition ranges are presented in Table 10.

Table 10: ARI and typical Shanghai summer conditions [34]

Condition	Ambient air conditions	
	Dry bulb temperature (°C)	Relative humidity (%)
ARI summer	35	40
ARI humid	30	60
Shanghai summer	34	65

4 Results and Discussion

4.1 Performance during Different Regeneration Temperatures

One of the most important factors deciding the system performance is the temperature of the regeneration air. This is because the regeneration temperature has a great influence on the moisture removed from the desiccant wheel by desorption. Therefore, the impact of regeneration temperature in the range of 60-100°C is investigated using results from an experiment performed June 21st 2012. Figure 47 shows the ambient conditions for this experiment. The average ambient temperature and relative humidity was 27°C and 61% respectively, which are values close to ARI humid conditions. The system operation conditions during the experiment are showed in Table 11.

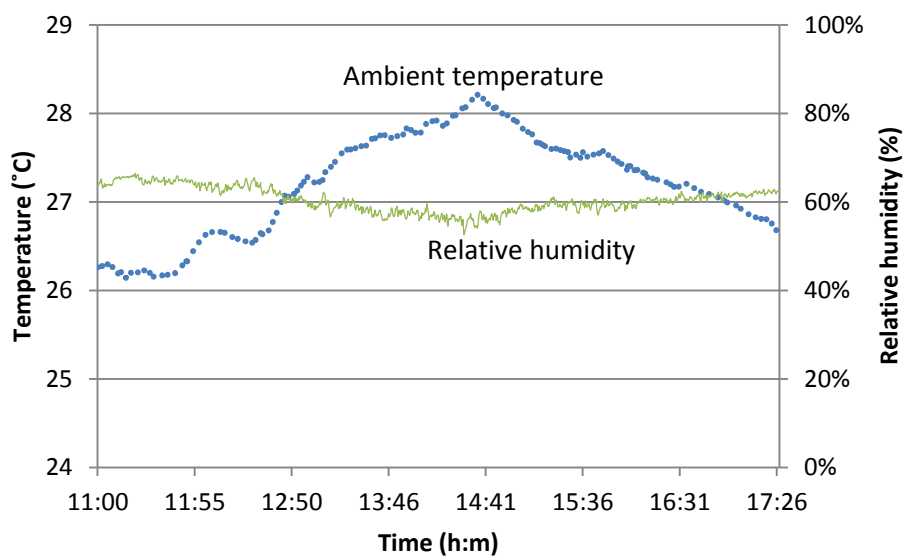


Figure 47: Ambient conditions, June 21st 2012

Table 11: System operation conditions, June 21st 2012

Parameter	Value
Flow rate of process air	900 m ³ /h
Flow rate of regeneration air	540 m ³ /h
Flow rate of chilled water	1.0 m ³ /h
Flow rate of cooling water	6.5 m ³ /h
Rotation of the desiccant wheels	8 r/h

Figure 48 depicts the impact the regeneration temperature had on the dehumidification performance of the desiccant wheels. The dehumidification value of the first desiccant wheel was changing from a minimum of 2 g/kg to a maximum of 4.5 g/kg with increasing regeneration temperature, indicating that the first desiccant wheel dehumidification performance is mostly

dependent on the regeneration temperature. This is because higher temperature provides better desorption of the desiccant wheel, resulting in the wheels potential of adsorption in the moisture removal process of the incoming process air flow increases.

For the second desiccant wheel, the dehumidification performance was not as affected by the change in regeneration temperature as the performance for the first wheel. The moisture removal amount was close to 2.5 g/kg for all the different regeneration temperatures tested. This indicates that for the second stage dehumidification, the value of the regeneration temperature is not as crucial as for the first stage dehumidification. The most deciding factor for the second stage moisture removal is the relative humidity of the process air entering the desiccant wheel.

Compared with a desiccant system using one-stage dehumidification, where the regeneration temperature should be around 100°C [30], the regeneration temperature requirement for two stage dehumidification is lower according to the results from this experiment. During the ambient conditions from Figure 47 for a two stage desiccant dehumidification system, Figure 48 shows that it should be sufficient with a regeneration temperature in the range of 70-75°C regarding moisture removal performance. This is because, when splitting the dehumidification into a multistage process the required dehumidification of each wheel decreases compared with a system that uses only one-stage dehumidification. Adding the dehumidification done by the first and second desiccant wheels lead to the total dehumidification performed by the two stage system varying from 4.7 to 7.2 g/kg.

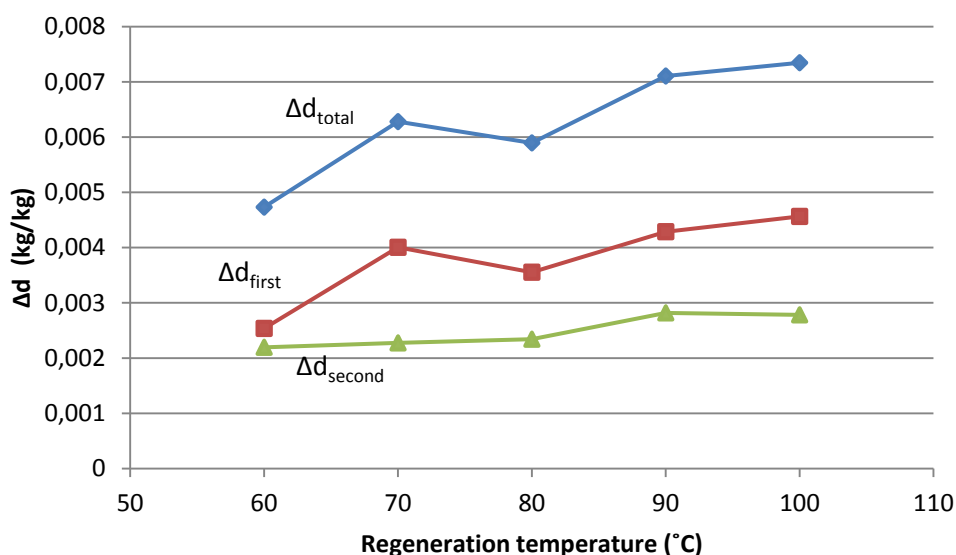


Figure 48: Effect of regeneration temperature on the moisture removal

Figure 49 represents the impact the regeneration temperature had on the COP_{th} and cooling capacity of the desiccant system. The cooling capacity did not vary that much with respect to the regeneration

temperature, where the variation between 60 and 70°C mostly was because of varying ambient conditions. The highest cooling capacity was obtained at a regeneration temperature around 70°C with a value of 6.12 kW indicating that the cooling capacity of the system is highest when low regeneration temperature is applied. The low variation in the cooling capacity shows that the heat exchangers installed in the system is capable of dealing with the sensible and latent heat exchange occurring when the process air is in contact with desiccant dehumidification units.

The COP_{th} was higher at low regeneration temperature and gradually decreased as the regeneration temperature increased. This is because increasing regeneration temperature means more heat added to the system, and since the cooling capacity of the system does not increase the COP_{th} decrease. Evaluating the results from Figure 48 and Figure 49 leads to the conclusion that the necessary regeneration temperature for the system, at these ambient conditions, is in the range of 70-75°C.

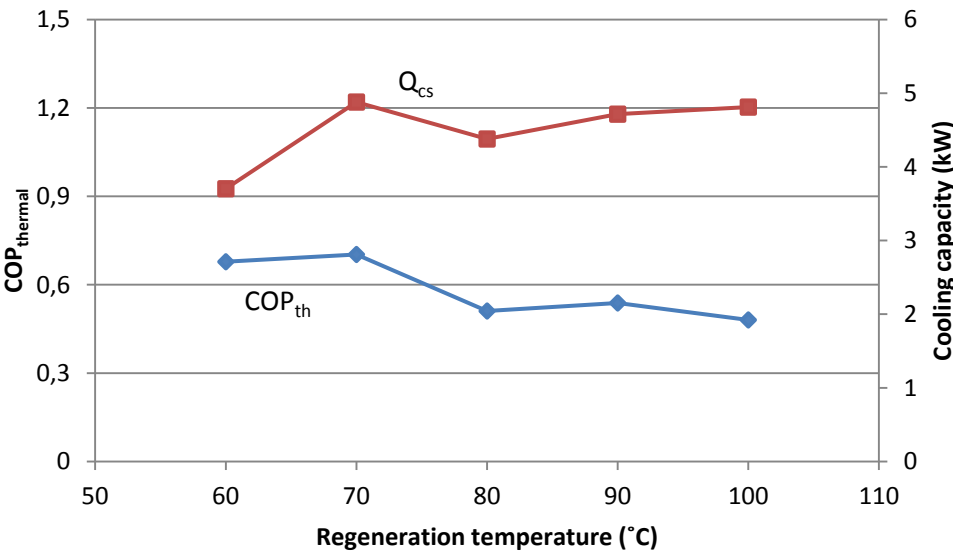


Figure 49: Effect of regeneration temperature on the cooling capacity and COP_{th}

4.2 Performance during Typical Working Conditions

This part of the testing program is done to investigate the total overall performance of the desiccant cooling system under typical working conditions in Shanghai. Three experiments during different working conditions are evaluated. The total overall performance basically means the obtainable cooling, dehumidification and water chilling by the system. The desiccant wheels ability to remove moisture form the process air and the evaporative cooler ability to chill water are therefore important aspects of the total performance. The dehumidification performance during the three

experiments is calculated using Equation 14 and Equation 15. The cooling capacity is calculated by Equation 4, COP_{th} by Equation 11 and COP_{el} by Equation 8.

4.2.1 ARI Summer Conditions

The first test result analyzed is from an experiment performed July 15th 2012. The ambient conditions during this experiment are shown in Figure 50. The weather conditions were cloudy, and the average ambient temperature was around 30°C with an average relative humidity of 56.6%. With these conditions the average absolute humidity was around 14.3 g/kg which means that the experiment was performed during conditions closest to ARI summer conditions. The average achieved regeneration temperature was around 80°C. The small and rapid variations in regeneration temperature occur because the auxiliary heater of 3kW was used during this experiment. This was done because of the available radiation intensity from the sun not being sufficient to provide the necessary regeneration temperature level. The set point temperature of the auxiliary heater is 65°C, meaning that the heater turns on when below and shuts down when above this temperature. This creates an oscillating regeneration temperature for values under 65°C.

Table 12 provides the values of the relevant system operating conditions used during the experiment. It is these conditions, together with the ambient conditions, that are the deciding factors of the overall performance of the system. As can be seen, there is a slight variation in flow rate of process and regeneration air. This is mainly done because the process air is covering more of the area of the desiccant wheels, as well as being in direct contact with the evaporative cooler. Generally, the process air should be chosen to operate with a greater flow rate than the regeneration air.

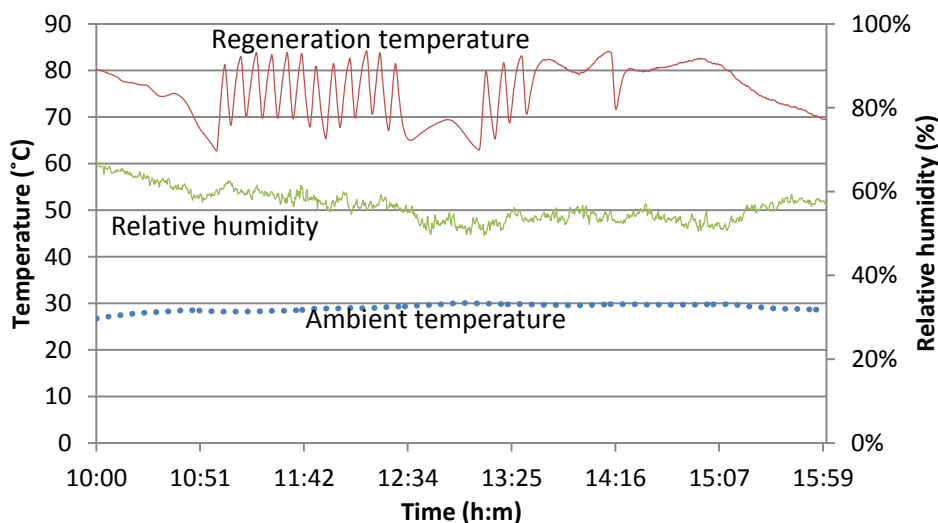


Figure 50: Ambient conditions, July 15th 2012

Table 12: System operation conditions, July 15th 2012

Parameter	Value
Flow rate of process air	1060 m ³ /h
Flow rate of regeneration air	840 m ³ /h
Flow rate of chilled water	1.0 m ³ /h
Flow rate of cooling water	6.5 m ³ /h
Rotation of the desiccant wheels	8 r/h

Figure 51 shows a psychrometric chart of the complete system process, including all the steps from start to finish for both the process air and regeneration air cycle. The values presented in the chart are gathered at the experiment time of 13:22. The temperature decrease from point 1 to 2 was relatively low compared to point 3 to 4 and point 5 to 6. These measurement points represent the air to water heat exchanger interactions, and the results show that the cooling effect of the two last heat exchangers was greater than for the first exchanger. Part of the reason behind this can be that the ambient temperature, which is the temperature of the air entering at point 1, was relatively low compared to the temperatures at point 3 and 5.

The psychrometric chart shows that the humidity ratio of the process air was reduced from 14 g/kg to around 6 g/kg. Point 6 is before the process air enters the regenerative evaporative cooling part of the system. At this point the process air can be used as ventilation air being supplied to the conditioned space. When the process air was used in the evaporative cooler, the humidity drastically increased from point 7 to 8 and was discharged to the environment at point 9.

The regeneration air cycle is from point 1 towards the direction of point 13. Point 11 is after the solar collectors and point 12 is after the auxiliary heater. As can be seen, the auxiliary heater contributed to a lot of the regeneration air temperature increase, because the ambient weather conditions were not optimal. At point 13 the regeneration air has desorbed the desiccant wheels and is discharged to the environment.

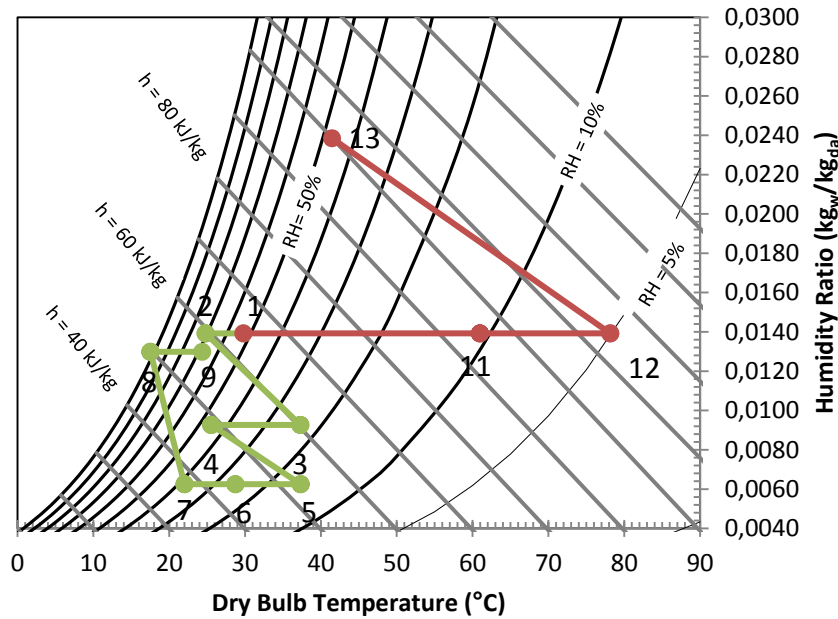


Figure 51: Psychrometric representation of the system processes during ARI summer conditions

Figure 52 shows the amount of dehumidification performed by the two desiccant wheels. The total dehumidification performance is essential when evaluating the system. This is because the absolute humidity ratio of the air entering the room, together with the temperature, is the deciding factor of whether or not the air is perceived as comfortable. The first desiccant wheel had an average moisture removal of 5.2 g/kg, while the average moisture removal of the second desiccant wheel was 2.9 g/kg. This means that the system achieved a total average moisture removal of 8.1 g/kg which is a respectable result. To get a better understanding of the meaning behind this result, it should be evaluated together with the ambient humidity ratio. In Shanghai, especially in summer, the humidity ratio is outside of the comfort zone and therefore needs to be modified before supplied to the conditioned space [35]. The average ambient humidity ratio for this experiment was as mentioned around 14 g/kg and the demand for qualified process air is maximum 12 g/kg. This means that the ambient air, with respect to humidity, under these conditions is close to qualified before entering the system. Because of this, an 8.1 g/kg moisture removal was more than sufficient to qualify the process air.

Figure 52 also shows the total efficiency of the dehumidification that was done by the desiccant wheels. The average efficiency was 56.5%, which is a good result. This dehumidification efficiency proves that with respect to dehumidification, the system performs very well under close to ARI summer conditions if the right operation conditions are chosen.

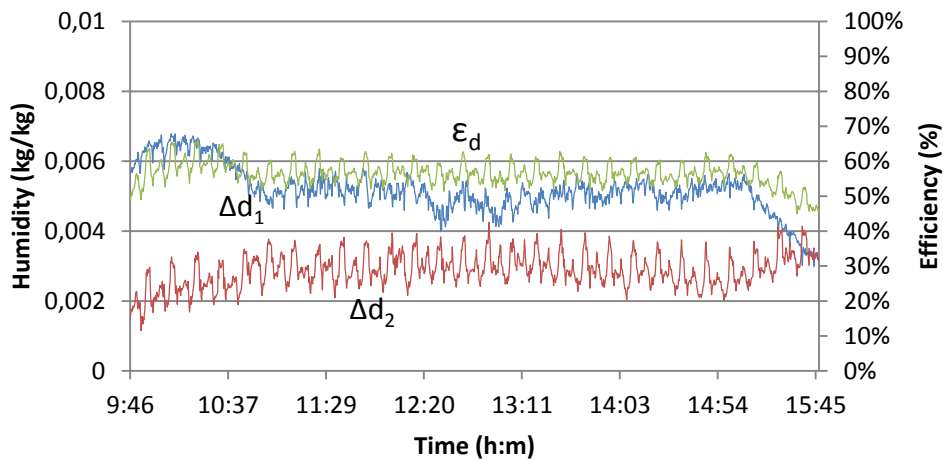


Figure 52: Dehumidification performance during ARI summer conditions

Figure 53 shows the temperature of the chilled water produced by the system. The average temperature of the chilled water production was about 16.5°C. This is very respectable and shows that the system under these conditions is capable of providing high quality chilling water. The capability of producing cold water is directly depending on the temperature of the process air entering the evaporative cooler. This temperature is also presented in Figure 53. Since the ambient temperature was relatively low, the system did not have a problem of keeping the temperature low during the dehumidification part of the system. This is shown by the average evaporative cooler air inlet temperature being just above 22°C.

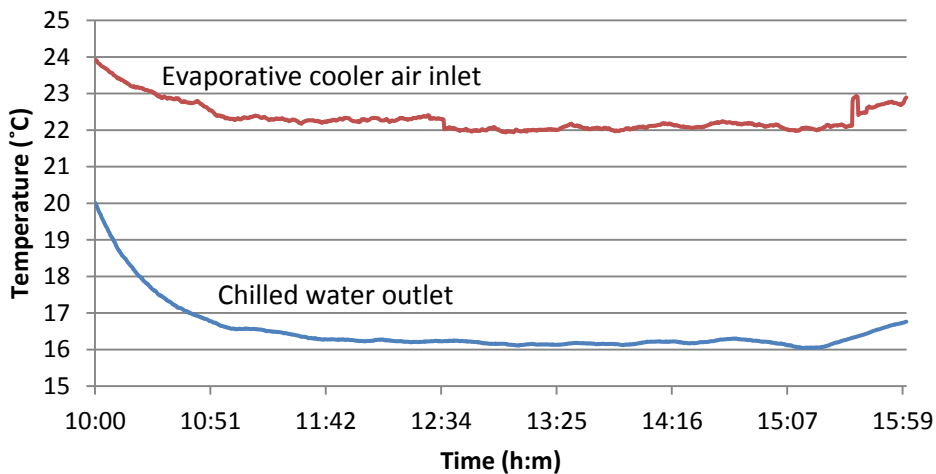


Figure 53: Chilling water temperature during ARI summer conditions

The system cooling capacity shows the ability to cool the process air flowing in the system. Figure 54 illustrates how this parameter varied during the day of the experiment. The average cooling capacity

was estimated to be around 7.4 kW. The cooling capacity could ideally be higher, but for these ambient conditions with an average ambient temperature below 30°C the result is sufficient.

Figure 54 also shows the COP_{th} and COP_{el} . Both are depending on the achieved cooling capacity and vary therefore in a similar way during the time of the experiment. The thermal capacity is also depending on the thermal energy added to the system from the solar collectors. The regeneration temperature during this experiment was relatively high which means that the heating system is capable of supplying good amount of heat. The average value of the heating capacity of the solar collectors during the experiment was 11.7 kW, leading to an average and maximum COP_{th} of 0.64 and 1.01 respectively. The average COP_{th} was relatively low but the maximum value, which is just over one, is very respectable. The COP_{el} had an average value of 4.82 and a maximum value of 5.74.

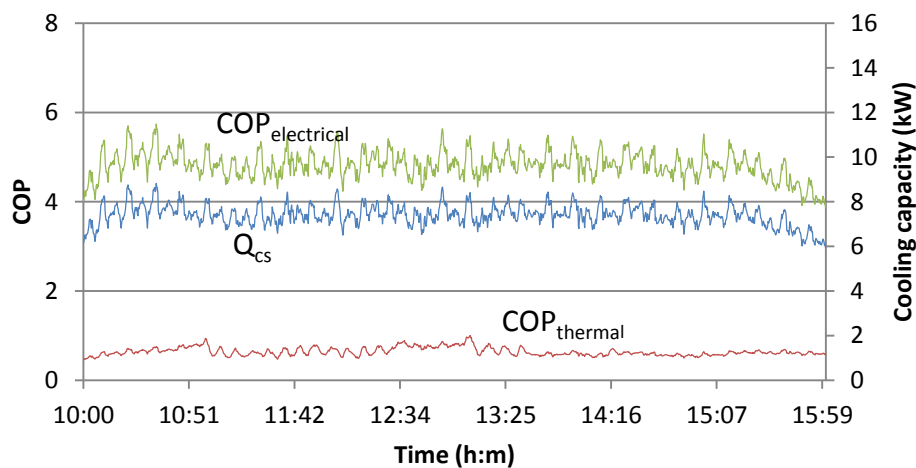


Figure 54: Cooling capacity and thermal and electrical COP during ARI summer conditions

The supply air quality boundaries are defined by the dry bulb temperature in the range from 20 to 27°C and humidity ratio in the range from 12 to 0 g/kg dry air [35]. Figure 55 shows how the two-stage desiccant system was able to take ambient air and process it to acceptable indoor condition. Some of the ambient temperature during the day was, as can be seen from this figure, already inside the boundaries of the qualified region. This shows that the cooling capacity of the system under these conditions was not so important as long as the system was capable of dealing with the temperature increase occurring in the dehumidification part of the system. As can be seen, the cooling of process air was more than enough and resulted in the inlet air temperature being almost too low. This is possible to handle by applying some proper control strategies of the supply air.

The ambient humidity ratio was too high and the dehumidification ability of the system was therefore more important than the cooling capacity. With the dehumidification efficiency of 56.5% the system was able to qualify the entire supply air load with a good margin.

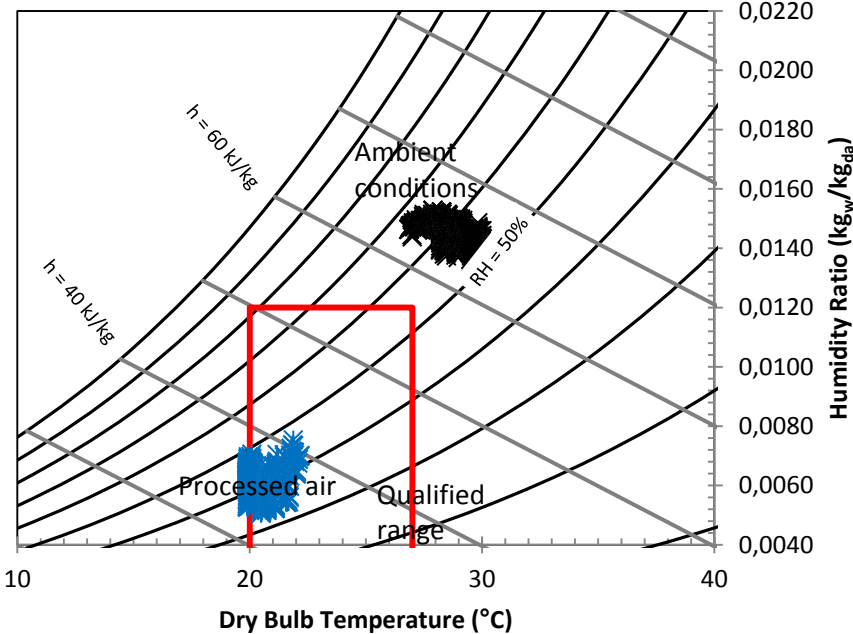


Figure 55: Supply air conditions during ARI summer conditions

4.2.2 ARI Humid Conditions

The second test results are from an experiment performed July 1st 2012. Figure 56 shows the ambient conditions during this experiment. The ambient temperature was stable over 30°C the whole day with an average value of 33.5°C, and the average relative humidity was 56%. The absolute humidity was relatively high with an average value around 18.1 g/kg. These ambient conditions can be classified to be close to ARI humid conditions. The achieved regeneration temperature during this experiment was very varying and is therefore divided in two different periods of time. The first period is from 10:00 to 12:45 where the average regeneration temperature was 73.2°C and the second is from 12:45 to 16:00 where the average regeneration temperature was 60.2°C. The variation is a result of shifting weather conditions and the fact that the auxiliary heater was not used. This variation has a noticeable influence on the performance indexes based on this experiment. Therefore, the indexes evaluated are taken from the first period of time where the regeneration temperature was more desirable. The system operation conditions that were used during this experiment are provided in Table 13.

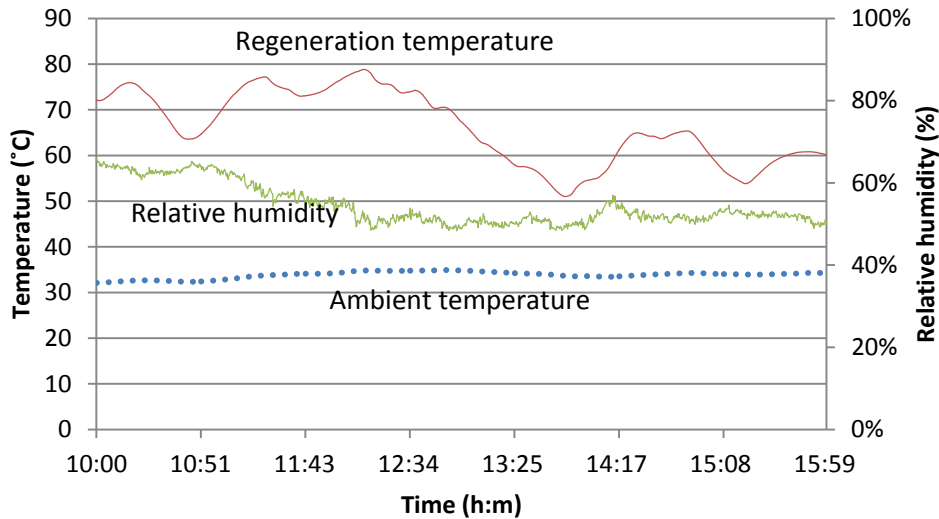


Figure 56: Ambient conditions, July 1st 2012

Table 13: System operation conditions, July 1st 2012

Parameter	Value
Flow rate of process air	900 m ³ /h
Flow rate of regeneration air	840 m ³ /h
Flow rate of chilled water	1.0 m ³ /h
Flow rate of cooling water	6.5 m ³ /h
Rotation of the desiccant wheels	8 r/h

Figure 57 shows the complete system process, confirming that every component and sensor was working properly. The values presented in the psychrometric chart are gathered at the experiment time of 12:54. For the process air cycle, starting at point 1 and ending at point 9, it can be seen that the first desiccant wheel performed most of the moisture removal of the process air. Further, it can be seen that all three air to water heat exchangers were capable of dealing with the sensible and latent heat load occurring during the dehumidification. The psychrometric chart also shows that the humidity ratio of the process air was reduced from 17 g/kg to around 6 g/kg. At point 9, being the discharge point of the process air, the relative humidity was approximately 100% and the absolute humidity ratio was almost back to the same level as the ambient air. This shows that even though the temperature at this point generally is low, the humidity ratio is too high for the air to be used as supply ventilation air. Regarding the regeneration air it can be seen, from point 11 to 12, that no auxiliary heater was used and all the regeneration heat was generated by the solar air collectors.

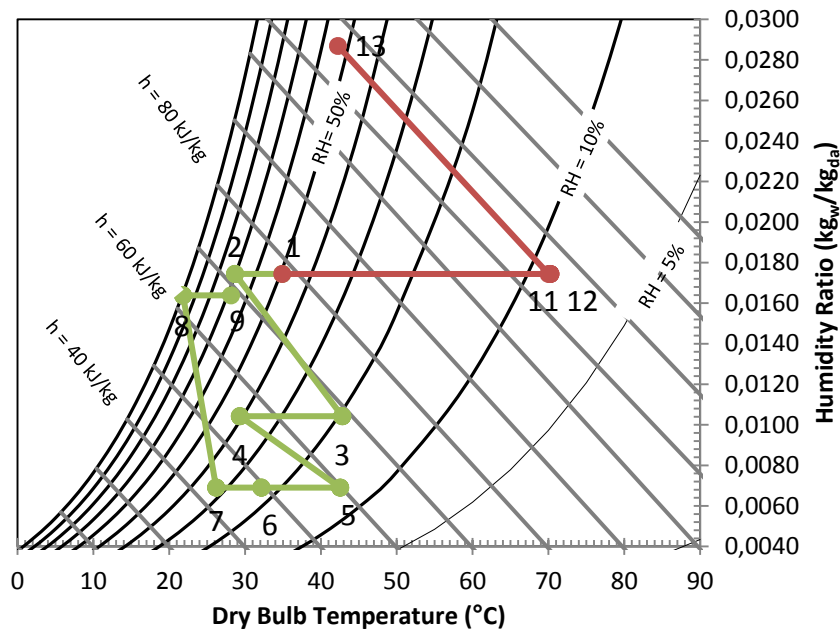


Figure 57: Psychrometric representation of the system processes during ARI humid conditions

The dehumidification performance of the system is presented in Figure 58. By comparing with the results that was obtained from the first experiment during ARI summer conditions, the difference is noticeable. The main reason is the differences in ambient conditions, but also the change in operation conditions is a factor influencing the results. The dehumidification performed by the first desiccant wheel is strongly related to the regeneration temperature as can be seen by comparing Figure 58 and Figure 56. The highest amount of moisture removed by this wheel was 9 g/kg, and this was achieved when the regeneration temperature was at its highest. The average dehumidification by the first desiccant wheel in the period from 10:00 to 12:45 was 7.1 g/kg. This result indicates good performance, and is higher compared with the result from the first experiment.

The dehumidification performance of the second desiccant wheel was also good. The average moisture removal in the same period of time was 3.5 g/kg. It is interesting to note the relation between the dehumidification of the first and second wheel. When the first wheel had low dehumidification performance the second wheel had increased moisture removal, and when first wheel had high dehumidification performance the moisture removal by the second wheel dropped. This shows that the performance of the second wheel is more dependent on the humidity ratio of the incoming process air flow than to the regeneration temperature. The second wheel evens out the varying performance of the first wheel and makes the total moisture removal achieved more stable. This becomes clear when studying the systems total dehumidification efficiency, which from 10:00 to 12:45 was close to stable with an average value of 57.9%.

To illustrate the dependence on the regeneration temperature, the average efficiency from 12:45 to 16:00 dropped down to 42.5% because of decreasing regeneration temperature. During this period the humidity ratio after the first wheel decreased, but the dehumidification performance of the second wheel was at the same level as before. This indicates that the performance of the second wheel also in some degree is depending on the regeneration temperature, and that when this temperature is too low the total moisture removal performance decreases.

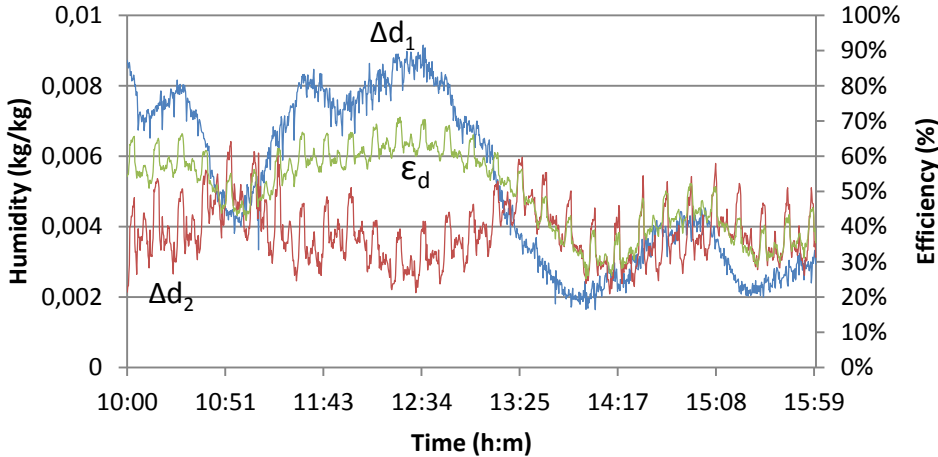


Figure 58: Dehumidification performance during ARI humid conditions

Figure 59 shows the temperature of the chilled water produced by the system. The average chilled water temperature was around 21°C, a respectable result considering the ambient condition. The cooling ability of the heat exchangers prior to the evaporative cooler is the reason that this chilled water temperature was achievable. At the beginning of the day, before the cooling tower was working properly, it is clear that the cooling effect of the heat exchangers was low. Around 10:30 the system started to operate properly and was therefore capable of cooling the process air from an ambient temperature close to 31°C down to a temperature below 27°C before entering the evaporative cooler. This is respectable considering the temperature increase that occurs during the dehumidification part of the system.

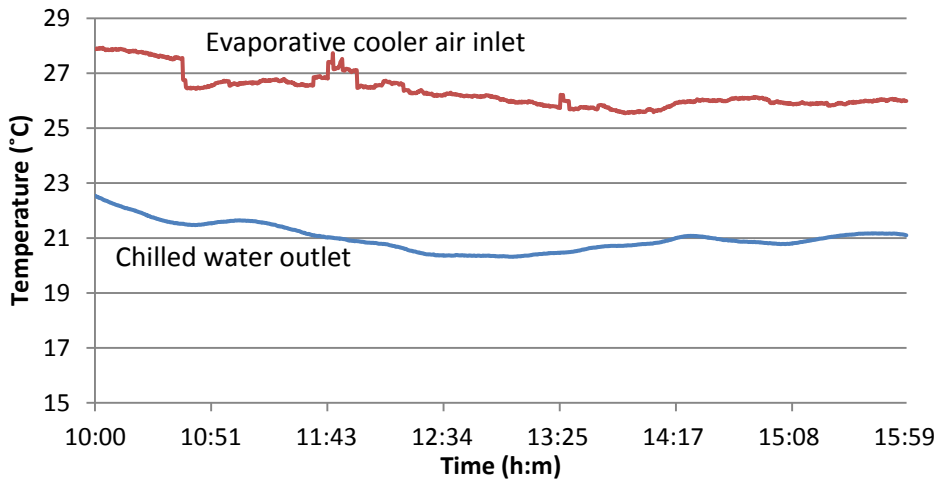


Figure 59: Chilling water temperature during ARI humid conditions

Figure 60 shows the cooling capacity, the COP_{th} and the COP_{el} of the system. In the optimal time period of the experiment the cooling capacity had an average value of 8.9 kW. Compared to the system cooling capacity from the experiment during ARI summer conditions, this result is noticeably better. This can be explained by the difference in ambient conditions. Since the ambient air temperature was higher for this experiment, the reduction in process air temperature is larger. This shows that the desiccant system functions very well under high temperature conditions. The achieved COP_{th} and COP_{el} also prove this. The average value of the COP_{th} during the optimal experiment period was 0.83 with a maximum value of 1.2, and the average value of the COP_{el} was 5.7 with a maximum value of 7.4.

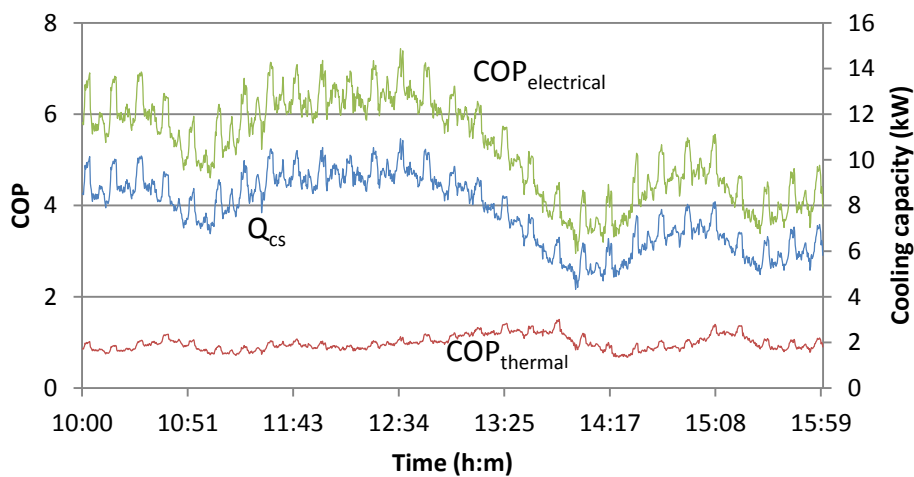


Figure 60: Cooling capacity and thermal and electrical COP during ARI humid conditions

The high dehumidification efficiency and cooling capacity of the system made it possible to produce qualified ventilation air even when the ambient temperature and humidity are high. This is illustrated in Figure 61, which shows the ventilation air production during the period of time when the regeneration temperature was acceptable. The process air started with an absolute humidity ratio in the range of 17 to 20 g/kg and ended up in the range of 12 g/kg down to approximately 6 g/kg, which is inside the qualified region defined according to the ASHRAE standards [35].

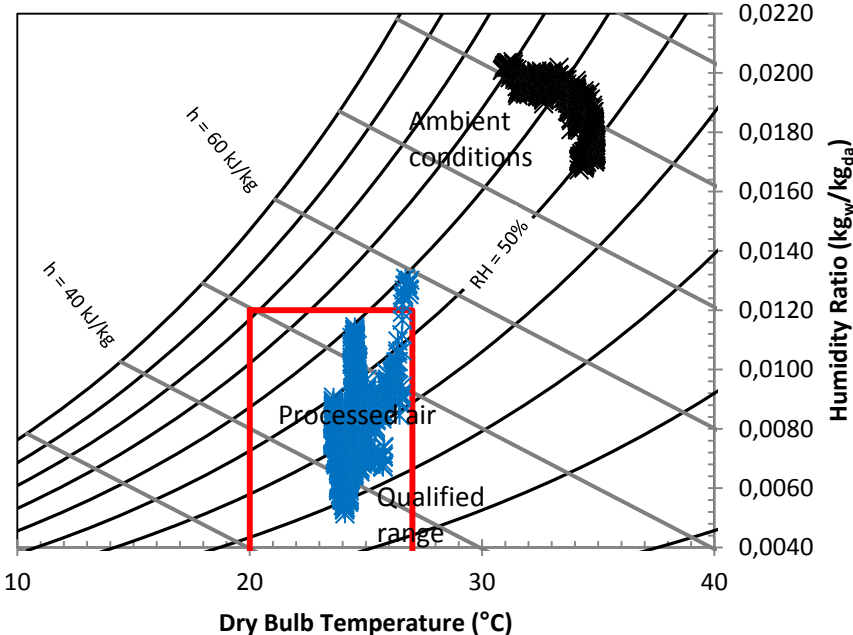


Figure 61: Supply air conditions during ARI humid conditions

4.2.3 Shanghai Summer Conditions

The ambient conditions during the last experiment are presented in Figure 62. The experiment was performed July 9th 2012 during Shanghai summer weather conditions with ambient temperature and humidity close to 32°C and 67% respectively. The average absolute humidity ratio was 19.9 g/kg, meaning that the air was very humid. The testing was done from 9:00 to 12:00 when the ambient conditions were desirable with respect to testing in Shanghai summer conditions. The weather was cloudy and therefore, to have an acceptable regeneration temperature during the experiment, the auxiliary heater of 3 kW was used. This can be seen on the oscillating curve of the regeneration temperature. The auxiliary heater ensured that the regeneration temperature was around 77°C during the experiment. The operation conditions were the same as for the experiment described in section 4.2.2, and are given in Table 13.

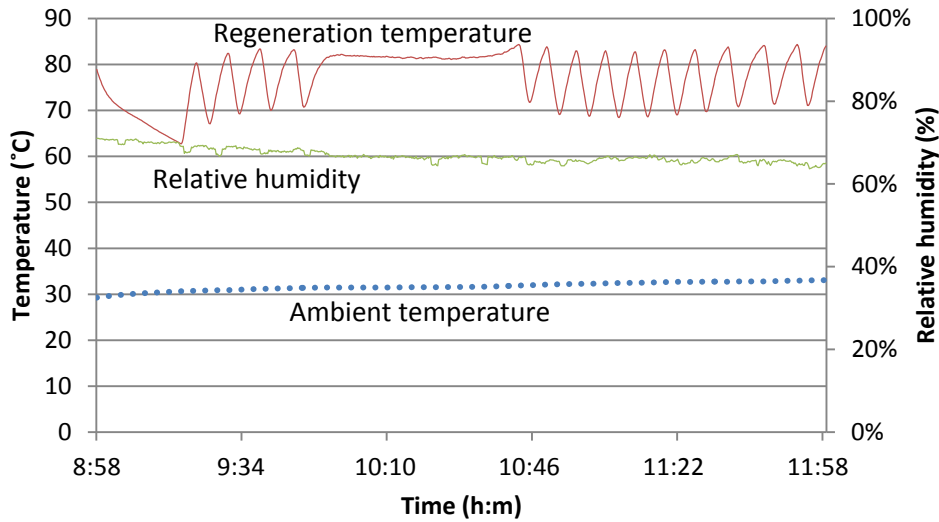


Figure 62: Ambient conditions, July 9th 2012

A psychrometric representation of the system processes during this experiment is provided in Figure 63. The values presented in the chart are gathered at the experiment time of 12:54. As for the other experiments, it can be noted that the system components and sensors were working properly throughout the experiment. As mentioned, the solar radiation available on this date is not enough to provide sufficient regeneration temperature and the auxiliary heater was run at 3 kW. This increased the temperature from 60°C to around 74°C and can be seen from point 11 to 12.

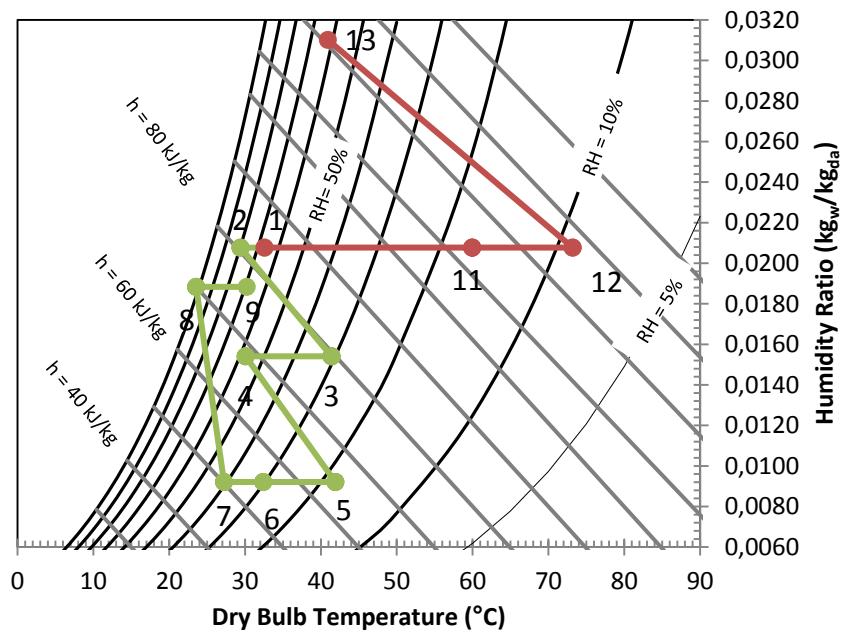


Figure 63: Psychrometric representation of the system processes during Shanghai summer conditions

Figure 64 shows the dehumidification performance of the system during Shanghai summer conditions. Compared with the results from the experiment during ARI humid conditions the dehumidification performance of this experiment is lower. The moisture removal performed by the two desiccant wheels is almost the same for each of the wheels, meaning that the dehumidification load was distributed close to equal. It can be seen that the system used some time before starting to perform sufficient dehumidification. After 9:30, the system somewhat stabilized and began to run with a stable performance during the rest of the experiment. The average moisture removal of the first desiccant wheel during this period was 4.3 g/kg, which is not as good as the performance during the ARI humid experiment. The reason behind this can be difference in the relative humidity of the regeneration air, which was higher during this experiment. The desiccant wheel desorption is better when the relative humidity of the regeneration air is because the air has a higher possibility of accepting moisture. The average humidity increase of the regeneration air during the ARI humid experiment was approximately 11.5 g/kg, while for this experiment it was around 10 g/kg.

The moisture removal of the second desiccant wheel was as mentioned almost the same as for the first wheel with an average value of 4.3 g/kg. Compared with the results from the ARI humid experiment this performance is slightly higher. This result is another example of that the second desiccant wheel performance is more dependent on the humidity ratio than the regeneration air temperature. The average total dehumidification efficiency of the system was 45.4%.

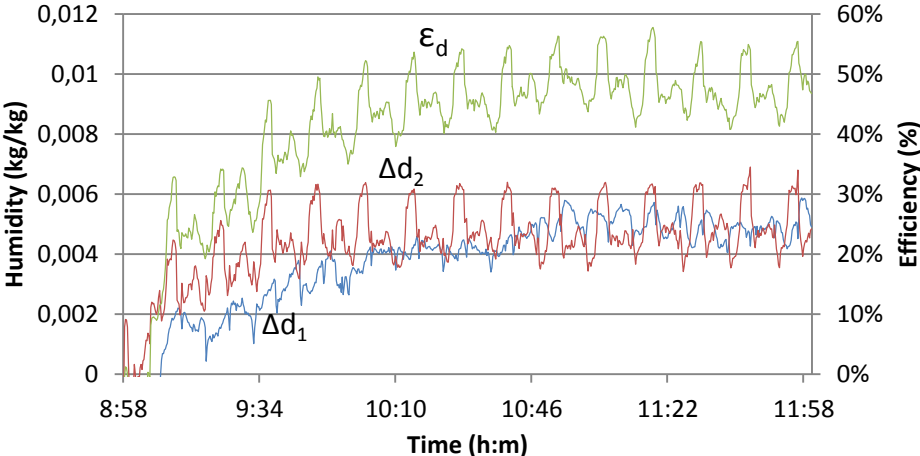


Figure 64: Dehumidification performance during Shanghai summer conditions

The chilled water production of the system during the experiment is showed in Figure 65. The water outlet temperature from the evaporative cooler was around 22°C. This is respectable considering the

ambient conditions which leads to an average temperature of the evaporative cooler inlet air around 27.5°C.

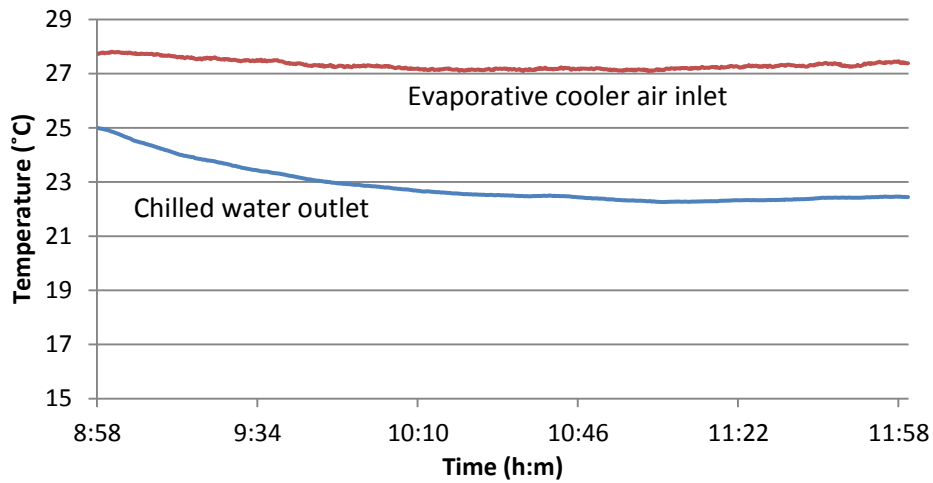


Figure 65: Chilling water temperature during Shanghai summer conditions

The cooling capacity, together with COP_{th} and COP_{el} , is represented in Figure 66. The cooling capacity also used time to stabilize, but reached an average value of 7 kW. Considered together with an average COP_{th} of 0.61 where the maximum value was 0.95 and an average COP_{el} of 4.7 where the maximum value was 6.2, these performance indexes indicate that the system performance is good under extreme ambient conditions.

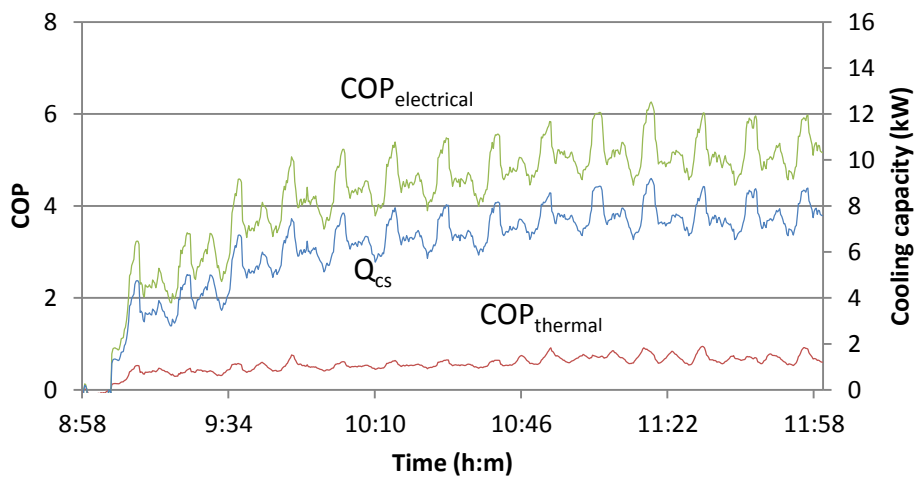


Figure 66: Cooling capacity and thermal and electrical COP during Shanghai summer conditions

Figure 67 shows the supply air produced by the system. The high ambient temperature and humidity ratio are clearly noticeable. Almost the entire supply air load was inside the qualified region, except for the ventilation air produced at the beginning of the experiment, before the system stabilized. The

results presented shows that the desiccant cooling system is capable of producing qualified air under weather conditions where the ambient temperature and humidity ratio are extreme.

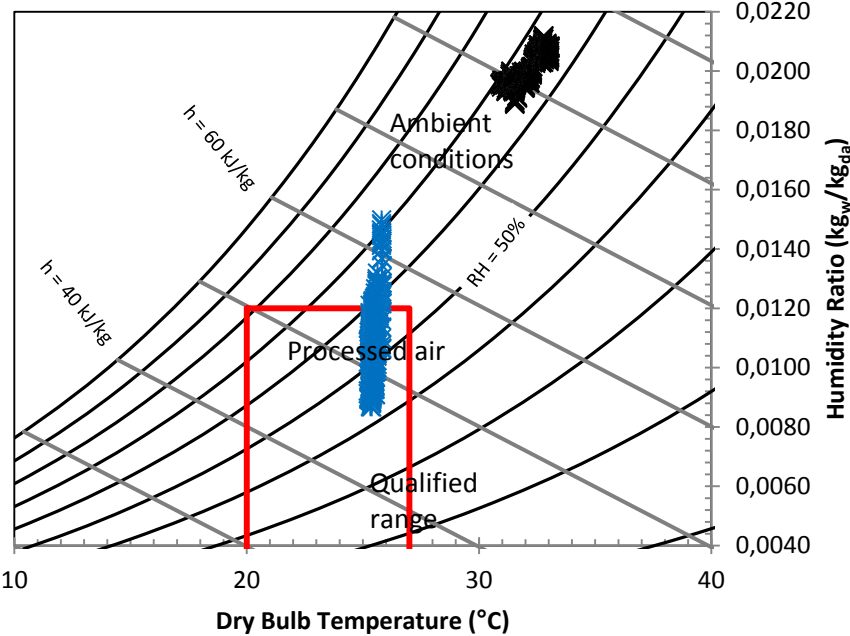


Figure 67: Supply air conditions during Shanghai summer conditions

4.2.4 Evaluation of the Performance during Different Conditions

The three experiments performed to test the overall performance of the desiccant system have proven that the performance is dependent on the ambient weather and the operation conditions. Table 14 presents all the obtained performance indexes, as well as the deciding ambient and operation conditions, during these three experiments. From this representation conclusions on when the system has its most optimal performance can be drawn.

Table 14: Performance indexes

Parameter	ARI summer	ARI humid	Shanghai summer	Unit
<i>Ambient temperature</i>	30	33.5	32	[°C]
<i>Ambient relative humidity</i>	56.6	56	67	[%]
<i>Ambient absolute humidity</i>	14.3	18.1	19.9	[g/kg]
<i>Regeneration temperature</i>	80	73.2	77	[°C]
<i>Process air flow rate</i>	1060	900	900	[m ³ /h]
<i>Regeneration air flow rate</i>	840	840	840	[m ³ /h]
<i>Cooling water flow rate</i>	1.0	1.0	1.0	[m ³ /h]
<i>Chilling water flow rate</i>	6.5	6.5	6.5	[m ³ /h]
Dehumidification efficiency	56.5	57.9	45.4	[%]
Chilled water temperature	16.5	21	22.5	[°C]
Cooling capacity	7.4	8.3	7	[kW]
COP_{th}, maximum	1.01	1.2	0.95	[-]
COP_{th}, average	0.64	0.83	0.61	[-]
COP_{el}, maximum	5.7	7.4	6.2	[-]
COP_{el}, average	4.8	5.7	4.7	[-]

Table 14 it can be seen that the overall lowest performance indexes are during Shanghai summer conditions. This is mainly because of the extreme weather conditions where the absolute humidity ratio is very high. The chosen operation conditions during the experiment can also be a factor that has impact on the results. The operation conditions for the experiment performed during ARI humid and Shanghai summer conditions are the same. The calculated indexes indicate that these operation conditions are best suited for a system running during close to ARI humid conditions.

Between ARI summer and ARI humid conditions, the results from the ARI humid experiment are the most optimal. The calculated performance indexes are close to equal, but almost all are slightly higher for the experiment performed during ARI humid conditions. The only result that is better for ARI summer is the chilled water outlet temperature, which mainly is because of the relatively low ambient temperature during this experiment.

The overall analysis from the results of the experiments indicate that the desiccant cooling system functions well under moderate, high and extreme humidity conditions and that the operation conditions needs to be selected properly. It can be said that the system excels the most optimal performance during ambient temperatures and humidity conditions in the range of ARI humid conditions.

4.3 Performance without the Pre-cooling Heat Exchanger

The pre-cooling heat exchanger is installed before the first desiccant wheel and is the first component that the process air interacts with when entering the system. The purpose of this heat exchanger is to decrease the enthalpy by sensible heat exchange and thus also decrease the temperature of the process air before entering the first desiccant wheel. To investigate the effect of this component, an experiment was performed with the valve controlling the amount of cooling water to the heat exchanger closed.

The experiment was performed June 12th 2012, and the performance data of the system were gathered between 10:15 and 17:00. The system operation parameters for this experiment are provided in Table 15. The weather conditions for this date were cloudy with an average ambient temperature of 27.8°C and an average relative humidity of 65%. The ambient operation conditions are presented in Figure 68. Because of the cloudy weather the auxiliary heater of 3 kW was turned on. The regeneration temperature achieved by the heating system was around 75-80°C.

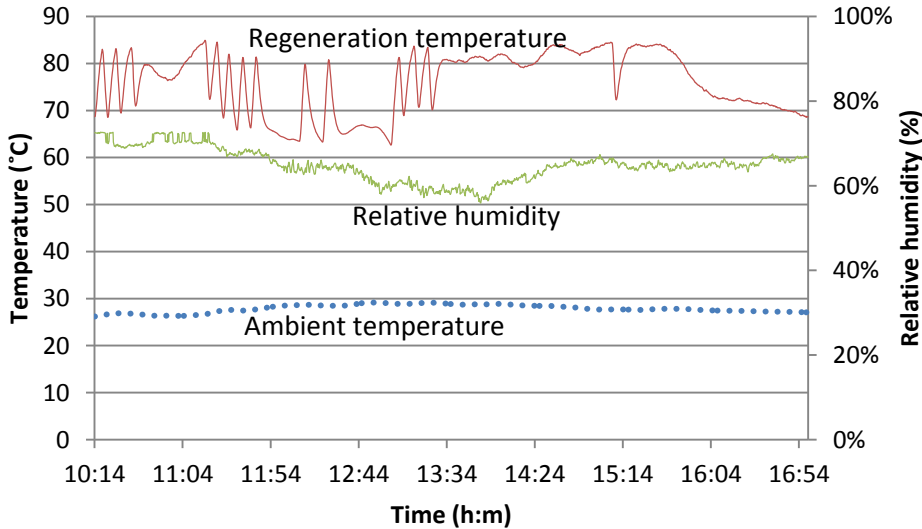


Figure 68: Ambient conditions, June 12th 2012

Table 15: Operation conditions, June 12th 2012

Parameter	Value
Flow rate of process air	611 m ³ /h
Flow rate of regeneration air	1312 m ³ /h
Flow rate of chilled water	1.0 m ³ /h
Flow rate of cooling water	6.5 m ³ /h
Rotation of the desiccant wheels	8 r/h

In the beginning of the day the system was run as usual with the valve of the first heat exchanger open. At 13:00 the valve was closed and the system was run without the pre-cooling heat exchanger until the end of the experiment. Figure 69 represents the enthalpy of the process air before and after the first heat exchanger. After 13:00 the enthalpy rapidly started approaching the ambient enthalpy and stabilized around 13:15 indicating that the pre-cooling heat exchanger had stopped functioning.

It is interesting to evaluate the dehumidification performance of the first desiccant wheel with and without the pre-cooling heat exchanger. The dehumidification of the first desiccant is presented in Figure 70. As the figure shows the difference in dehumidification performance was minimal, where most of the difference was a result of varying ambient humidity. The dehumidification efficiency of the first wheel with and without the first heat exchanger was approximately the same for the two operating conditions, both with a value close to 37%. This indicates that, for these ambient conditions, the pre-cooling heat exchanger was not necessary regarding achieving desired dehumidification performance of the first desiccant wheel. This can mainly be because the reduction in enthalpy that the heat exchanger is providing is not influencing the dehumidification capability of the desiccant wheel when the ambient temperature is in the range of 26-28°C.

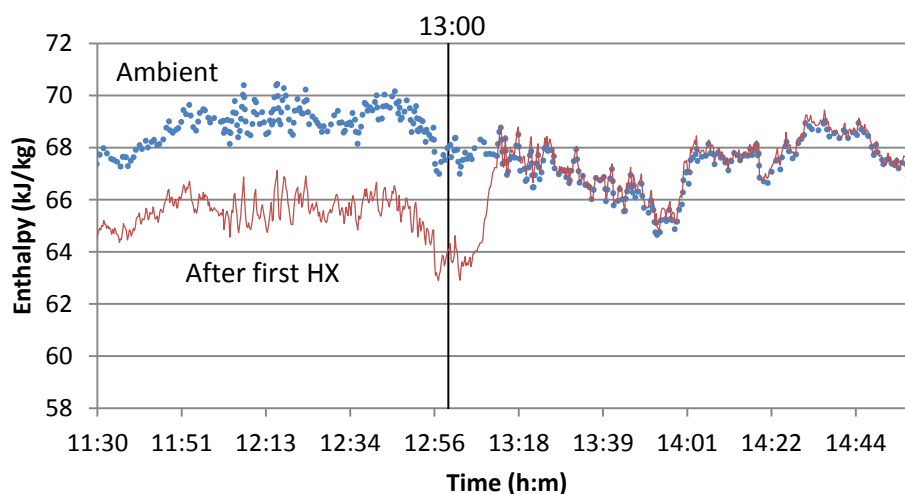


Figure 69: Enthalpy change during first heat exchanger

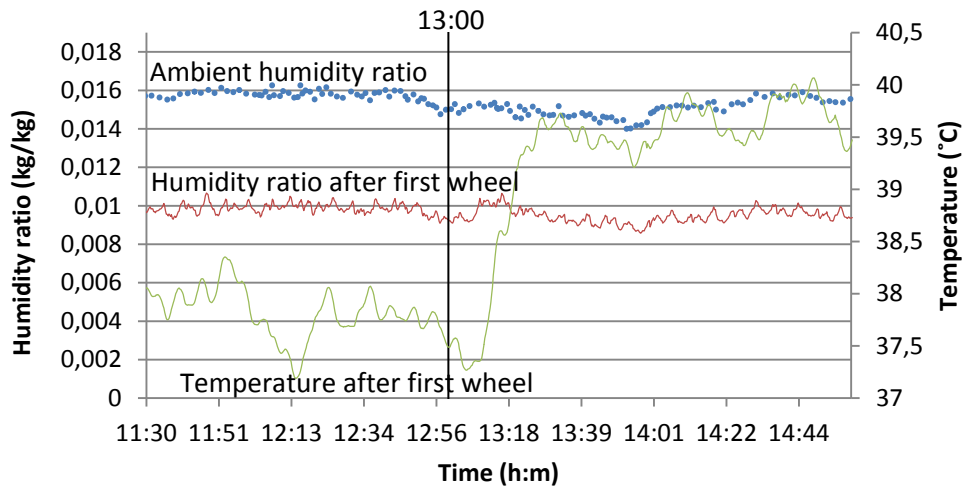


Figure 70: Humidity change during first desiccant wheel

The increase in outlet temperature of the first wheel, with and without the pre-cooling heat exchanger, is also indicated in Figure 70. To investigate if this temperature change have any impact on the rest of the systems dehumidification process the enthalpy values after the first wheel, after the second heat exchanger, after the second wheel and after the third heat exchanger are presented in Figure 71. When the valve was closed at 13:00 the enthalpy values experienced an increase over a short period of time before stabilizing around the same values as when the valve was open. The enthalpy value after the third heat exchanger was not affected by the change in operation condition, again indicating that the pre-cooling heat exchanger was unnecessary during these ambient conditions.

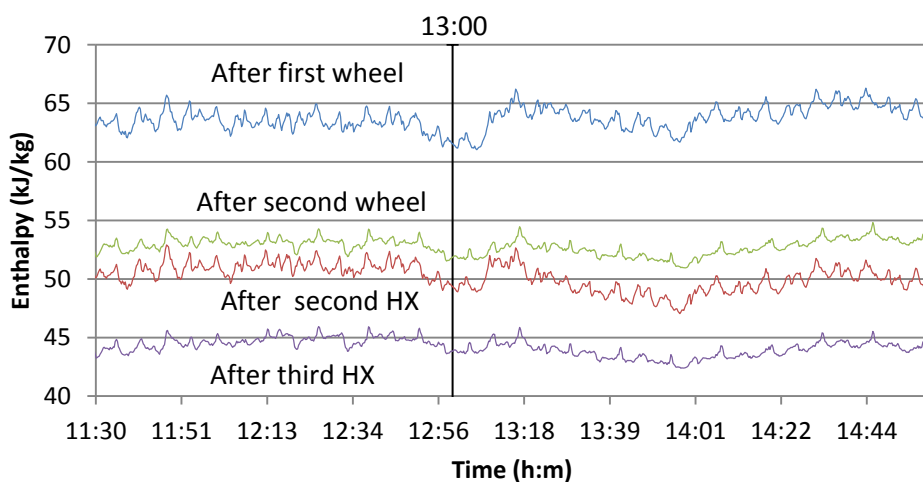


Figure 71: Enthalpy change during the dehumidification process

4.4 Performance with only the Second Desiccant Wheel Running

The dehumidification process is as mentioned a two-stage process where two desiccant wheels are connected in series. The second stage desiccant wheel is newly installed in the system, and it is therefore interesting to investigate the performance of this wheel separately. To properly evaluate the second wheel some experiments are carried out with only the second stage desiccant wheel running.

An experiment with this setup was performed July 2nd 2012. The ambient conditions are presented in Figure 72. The absolute humidity ratio was relatively high with an average value of 16.4 g/kg. The average ambient temperature was around 35°C and the achieved regeneration temperature was for the most part higher than 70°C.

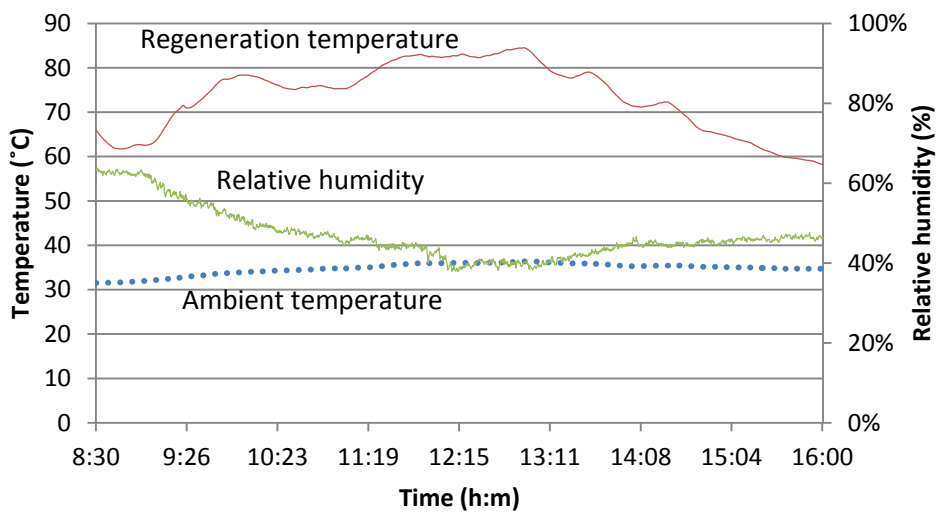


Figure 72: Ambient conditions: July 2nd 2012

Figure 73 depicts the system dehumidification performance during this experiment. From 8:30 to 9:30, the system was running as normal with both desiccant wheels operating. After this period of time the first desiccant wheel was stopped and the system was running with only the second wheel operating. The moisture removal of the second wheel increased rapidly and stabilized around 11.8 g/kg. The efficiency was also increasing and stabilized around 67.7%.

When the first wheel stops operating, it means that the second wheel is becoming the first stage dehumidification unit. As earlier mentioned, the first stage dehumidification process is more dependent on the regeneration temperature than the second stage dehumidification. Coincidentally, when the first wheel was stopped the regeneration temperature was increasing due to ambient weather conditions. This made the dehumidification performance of the second wheel very good compared with the situation when both wheels were operating.

Comparing the dehumidification efficiency with the efficiency from July 1st presented in Figure 58, shows that the efficiency for these two experiments are about the same. The dehumidification efficiency of this experiment is even a little higher which shows that the dehumidification performance of the second wheel is very good when run alone. This is also shown by the second wheel being capable of handling the entire humidity load of the process air during the experiment. When both wheels are running, the second wheel is acting as the second stage dehumidification where the performance is more dependent on the relative humidity of the entering air than the regeneration temperature. When the second wheel is acting as the first stage dehumidification unit, and the performance mainly is depending on the regeneration temperature, the performance is better than for the first wheel. This indicates that the installed second stage desiccant wheel should be switched and operated as the first stage dehumidification unit at least during periods of extreme humidity levels.

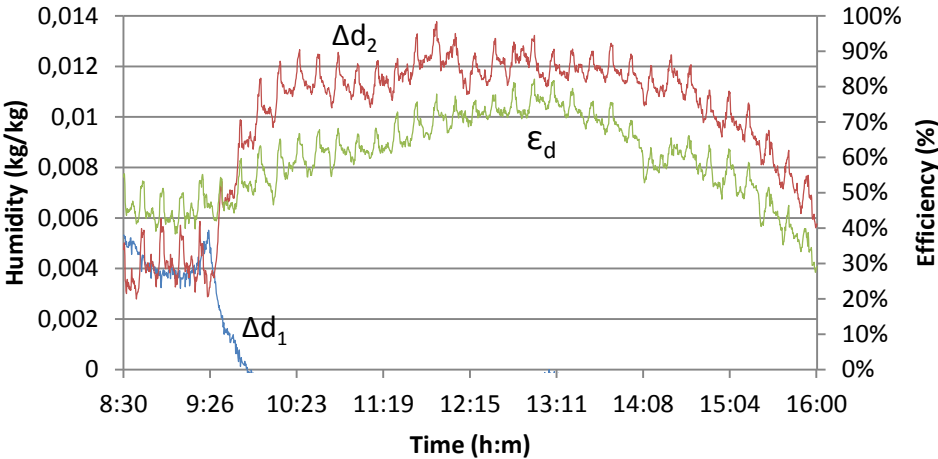


Figure 73: Dehumidification performance with one-stage dehumidification

Figure 74 represents the psychrometric chart of the system processes during the experiment. Point 2 to 5 is the dehumidification performed by the second desiccant wheel. This representation shows how well the second wheel is performing. It also shows a problem regarding the temperature at measuring point 6 that occurs as a result of using only one stage dehumidification. This temperature is relatively high and one of the reasons is that the temperature increase during one-stage dehumidification generally is higher than for multistage dehumidification. The high temperature level can create problems regarding lowering the process air at point 6 down to qualified ventilation air temperature.

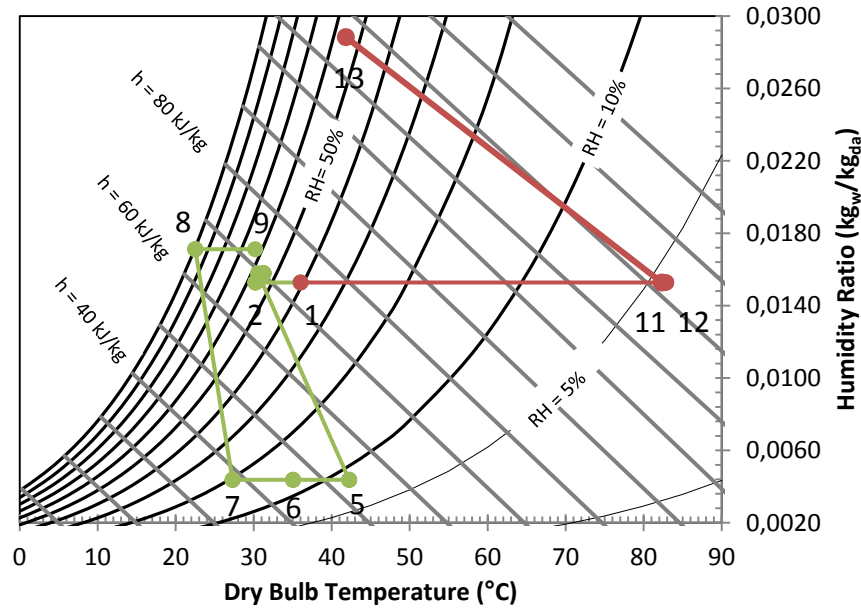


Figure 74: Psychrometric representation of the system processes with one-stage dehumidification

4.5 Performance of the Evacuated Tube Solar Air Collector

The performance of the evacuated tube solar air collectors is essential to the system performance when evaluating the energy efficiency of the system. The solar collectors are heavily dependent on the ambient weather conditions and solar radiation intensity. Therefore, it is interesting to investigate during which ambient conditions the collectors functions well. Equation 9, Equation 12 and Equation 13 are used in the evaluation.

To investigate the solar collector system it has been chosen to focus on two different experimental results. The first results are from an experiment where the weather was relatively sunny and the collectors experienced a lot of incident radiation. The other results are from an experiment where the weather was cloudy and a lower amount of radiation intensity was available.

4.5.1 during High Solar Radiation Intensity

The performance evaluation during high solar radiation intensity is done using values from the experiment performed July 1st 2012. Figure 75 shows the recorded solar collector conditions during this experiment. The weather on was partially cloudy which resulted in varying radiation intensity during the day. This has an effect on the achieved regeneration temperature which can be seen by studying the solar radiation and collector outlet temperature curve. The radiation intensity was highest, and relatively stable, from 11:30 to 13:00 with an average value of 883.3 W/m². This reflects

on the regeneration temperature, which also was highest during this period of time with an average value of 74.7°C. When the radiation intensity decreased, the collector outlet temperature also decreased. This can be seen by the lowest recorded intensity and regeneration temperature being around the same period with values of 129 W/m² and 51°C respectively.

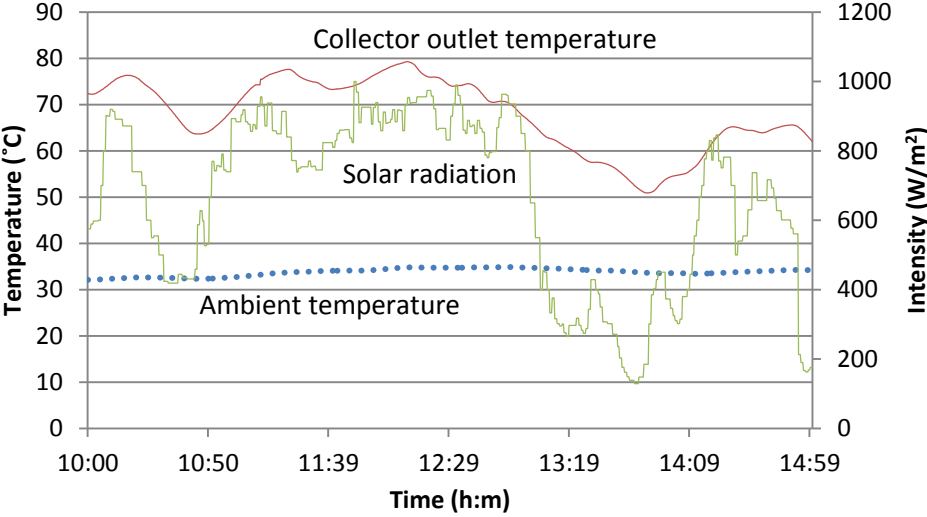


Figure 75: Solar collector conditions, high radiation intensity

The performance indexes obtained during this experiment are presented in Figure 76. The potential heat of the radiation hitting the evacuated tube solar air collectors was for the most part above 20 kW, and the heat added to the regeneration air flowing through the collectors was around 10 kW. The variation in these two values during the day also created varying collector efficiency. During the period of time when the solar radiation intensity was highest the average collector efficiency was 46.4%.

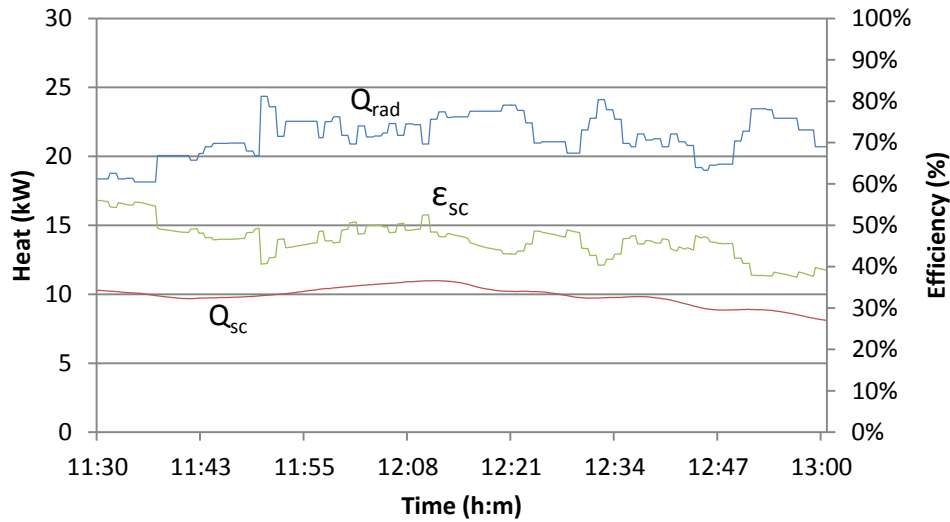


Figure 76: Solar collector performance indexes, high radiation intensity

4.5.2 during Moderate Solar Radiation Intensity

The data used to evaluate the collector performance during moderate radiation intensity is taken from an experiment performed July 14th. The solar collector conditions are shown in Figure 77. The ambient temperature during this experiment was about the same as for July 1st, but the solar radiation intensity was lower. From 11:30 to 13:00, the same time period as the first experiment, the average radiation intensity was 575.4 W/m². The effect of the lower solar radiation is clearly noticeable by studying the collector outlet temperature which was on average 67.3°C.

For the desiccant cooling system to operate optimal the regeneration temperature should at least be in the range of 70-75°C. This means that under these ambient conditions the auxiliary heating device should be activated to provide sufficient regeneration heat.

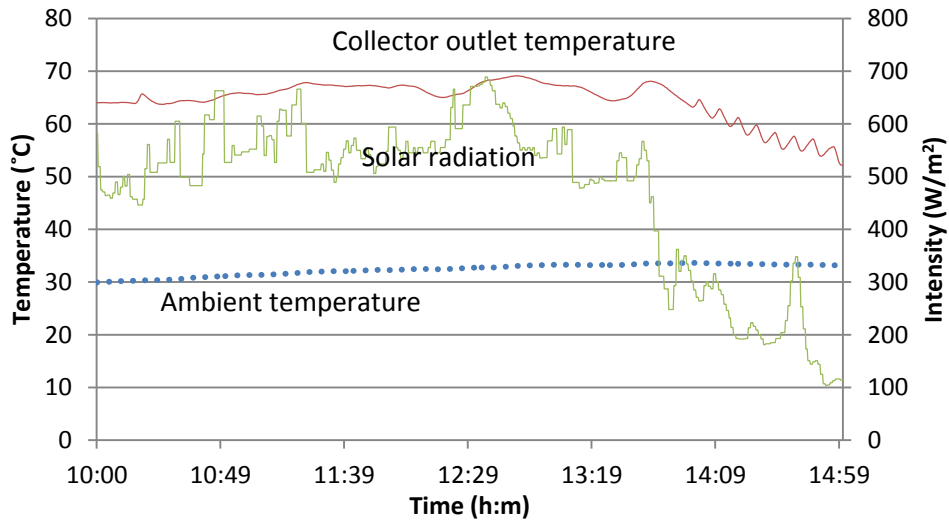


Figure 77: Solar collector conditions, moderate radiation intensity

Figure 78 shows the performance indexes obtained from this experiment. As a result of the lower radiation intensity, the potential radiation heat hitting the collectors was also lower. This gave a lower total amount of heat added to the regeneration air. However, the collector efficiency during this experiment was better with an average value of 61.6%. This efficiency is good and shows that the evacuated tube solar air collectors are capable of transforming more of the available solar radiation intensity when the intensity is moderate.

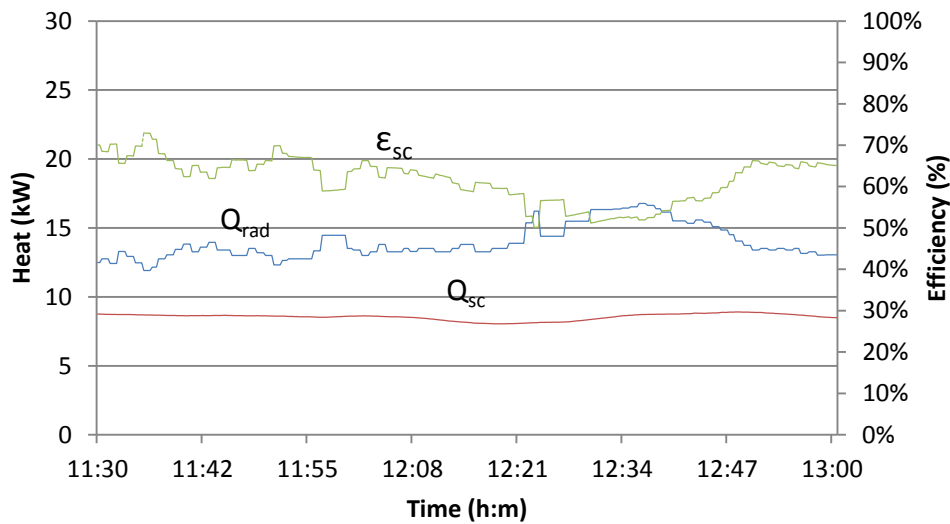


Figure 78: Solar collector performance indexes, moderate radiation intensity

4.6 Performance of the Regenerative Evaporative Cooler

The regenerative evaporative cooling process is consisting of the cross flow heat exchanger and the evaporative cooler. The process air first enters the cross-flow heat exchanger, then enters the evaporative cooler and lastly enters the cross flow heat exchanger again. This way the process air cooling achieved by the evaporative cooler is utilized to pre-cool the process air entering the evaporative cooler. Since the regenerative evaporative cooler performance is depending on two different units, it is interesting to investigate performance of both units. The efficiencies of the cross flow heat exchanger and the evaporative cooler are calculated by Equation 16, Equation 17 and Equation 18.

The evaluation of the regenerative evaporative cooler is done using values from two different experiments. The first experiment was performed when the ambient temperature was relatively low and the second experiment was performed when the ambient temperature was high. This is done to investigate if the cooler performance is affected by the ambient conditions.

4.6.1 during Moderate Ambient Temperature

The first performance evaluation is done using the measurement data from June 20th 2012 when the average ambient temperature was 24.6°C. Figure 79 shows the data obtained from 9:30 to 16:00 regarding the cross flow heat exchanger. The temperature of the air entering the heat exchanger from the dehumidification process, represented as T_6 , was around 25°C and was cooled down to an outlet temperature, represented as T_7 , of approximately 22°C. The achieved temperature of this air stream is very interesting because it is this air that enters the evaporative cooler. This should be as low as possible because low inlet temperature to the evaporative cooler means higher capacity for producing low temperature chilled water.

The last temperature presented in the figure, represented as T_8 , had an average value around 18.5°C and is the temperature of the air used to cool the entering process air. This temperature is interesting because it sets the limit of how low outlet temperature it is possible to achieve. All the temperatures relevant to the cross flow heat exchanger were relatively stable during the experiment and this lead to stable cross-flow efficiency with an average value of 49.5%.

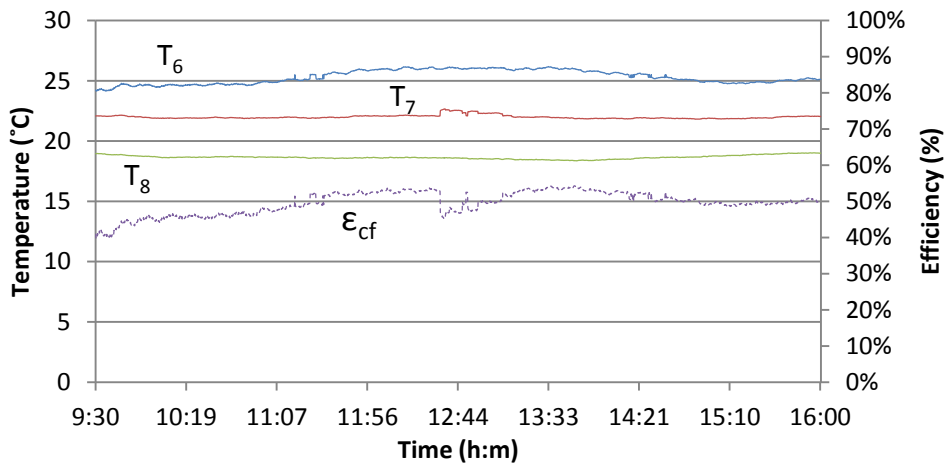


Figure 79: Cross-flow heat exchanger performance, moderate ambient temperature

Figure 80 shows the result of the evaporative cooler. The temperature marked as T_{wb} is the lowest possible achievable temperature of the evaporative cooler. This temperature is the wet bulb temperature of the inlet process air stream where the dry bulb temperature is marked as $T_{a,in}$. The figure shows that the evaporative cooler was capable of producing chilled water with a temperature approximately 17.5°C. The efficiency of the evaporative cooler is calculated based on the temperature decrease of the air interacting with the water. The air cooling efficiency was varying with the varying wet bulb temperature and had an average value of around 76% which is a good result. The chilling water efficiency is not represented in the figure but had an average value of around 57%.

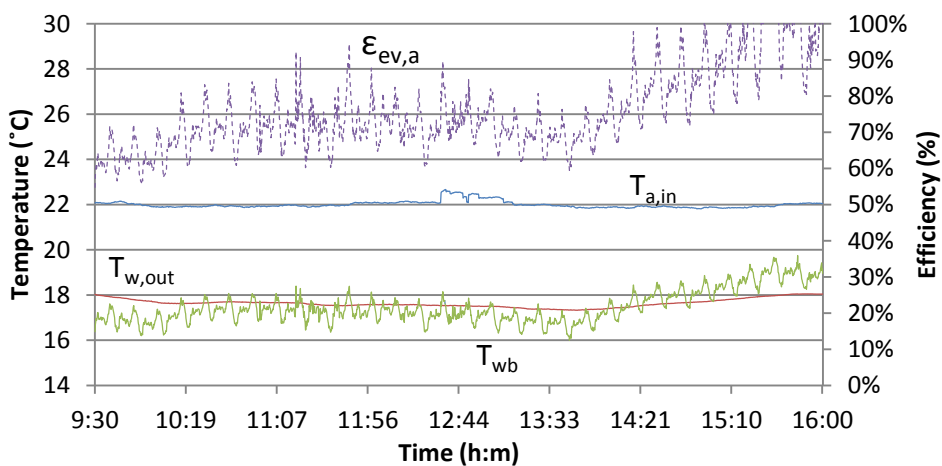


Figure 80: Evaporative cooler performance, moderate ambient temperature

4.6.2 during High Ambient Temperature

The second performance evaluation is done using the values from July 1st where the ambient temperature was around 33.6°C. Figure 81 shows the results from the cross-flow heat exchanger. Since the ambient temperature was high, the temperatures involved with the exchanger were also high compared with the results from the first experiment. The temperature of the air entering was around 32°C, the temperature of the air leaving was around 26°C and the temperature of the air cold source was around 22°C. The efficiency of the cross-flow heat exchanger was low at the beginning of the experiment but increased rapidly and stabilized at approximately 55%. This is a higher efficiency compared to the efficiency from the first experiment, and shows that the cross-flow heat exchanger is performing well under high ambient temperatures.

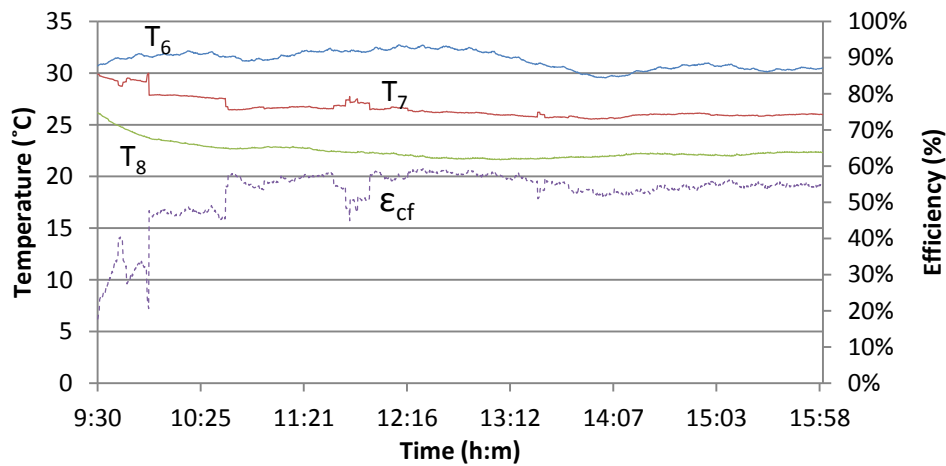


Figure 81: Cross-flow heat exchanger performance, high ambient temperature

The results of the evaporative cooler are presented in Figure 82. Because of the high ambient temperature, the temperature of the produced chilled water was higher with an average value of 21°C. The efficiency of the evaporative cooler was a little unstable because of a varying wet bulb temperature of the inlet air flow. The average air cooling efficiency was around 48% and the chilling water efficiency was around 21%. Compared with the evaporative cooler efficiencies achieved during the first experiment, the efficiencies from this experiment is lower. This indicates that the evaporative cooler has good performance when the ambient temperature is moderate, and can be explained by the dependence the evaporative cooler efficiencies has to the air interacting with the water. When the ambient temperature is relatively low, the temperature of the water entering the evaporative cooler is also low meaning that the chilling effect of the air becomes higher.

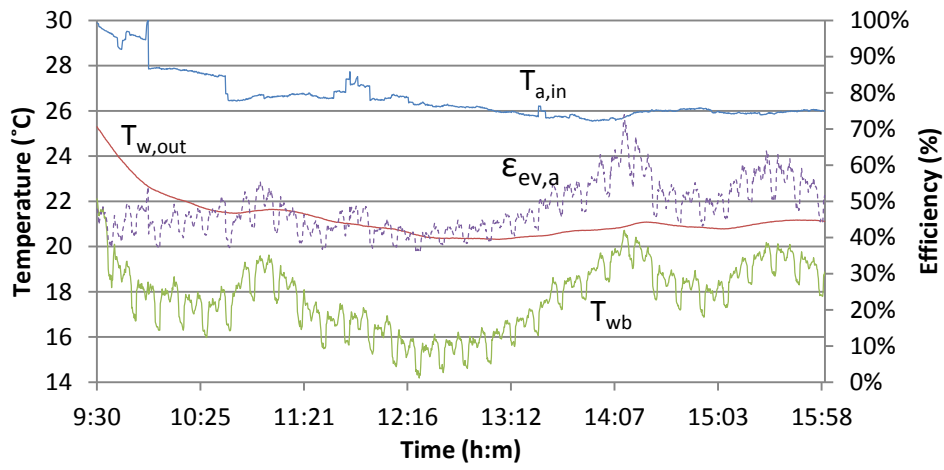


Figure 82: Evaporative cooler performance, high ambient temperature

5 Conclusion

In this thesis, a novel open cycle two-stage desiccant dehumidification system with regenerative evaporative water chilling has been experimentally studied. The system is installed at Shanghai Jiao Tong University and is a part of the Green Energy Laboratory initiative. Desiccant cooling systems are a great HVAC alternative to high energy consuming conventional air-conditioning units. One of the reasons is that desiccant systems can be powered by low grade energy sources while using only small amounts of electrical power. The investigated system uses solar thermal power generated by evacuated tube solar air collectors as the main source of energy.

The goal of this thesis was to evaluate the overall system performance with the main focus on dehumidification and cooling capability. A lot of experiments were performed during June and July 2012 with varying ambient and operational conditions.

Total dehumidification performance was showed to increase with increasing regeneration temperature. The necessary temperature of the regeneration air with respect to achieving desired moisture removal was evaluated to be in the range of 70-75°C. It was shown that the first stage desiccant wheel performance was very dependent on the regeneration temperature, and that the second stage dehumidification was more dependent on the relative humidity of the entering process air. This resulted in the first stage dehumidification varying together with the regeneration temperature and the second stage desiccant wheel compensating for the varying first stage performance.

Results from the experiments regarding the overall performance indicated that the desiccant cooling system functioned well under both high and extreme humidity conditions if the operation conditions were selected properly. However, the system excelled the most optimal performance during high absolute humidity conditions, and had an average dehumidification efficiency of 58%. The COP_{th} and COP_{el} were around 0.8 and 5.7 respectively, with a peak COP_{th} of 1.2. The system cooling capacity was around 9 kW and the achieved outlet temperature of the produced chilling water was below 21°C. Considering an ambient temperature of 34°C and relative humidity of 56%, the performance was respectable. The performance of the system made it possible to produce qualified processed ventilation air with a temperature in the range of 20-26°C and an absolute humidity ratio below 12 g/kg.

The effect of the pre-cooling heat exchanger was showed not to be crucial regarding the dehumidification performance of the system. Further, it was showed that the newly installed second stage desiccant wheel had a very good performance when acting as the first stage dehumidification

unit. When run alone, the newer desiccant wheel was capable of providing sufficient moisture removal in the range of 10-13 g/kg, and had a high dehumidification efficiency of 67%. This indicated that during extreme humidity conditions the second stage desiccant wheel should be switched and operated as the first stage dehumidification unit.

Solar air collector efficiency was around 47-60% during days with high to normal radiation intensity. When solar radiation was available, the solar collectors were capable of heating the regeneration air to temperatures above 70°C, but during cloudy weather the regeneration temperature decreased. This showed that when periods of low solar radiation occur, an auxiliary heating device must be used to help increase the regeneration temperature to a required level.

The regenerative evaporative cooler used to produce chilled water was performing well during all experiments and was able to produce low temperature chilled water. During periods of high ambient temperature the cooler produced chilled water below 21°C, and during periods of moderate ambient temperature chilled water below 16°C was achieved. The best performance regarding the efficiency of the cooler was achieved during experiments of moderate ambient temperature with a water chilling efficiency around 57% and an air chilling efficiency around 76%. The efficiency of the cross-flow heat exchanger was in the range of 50-55% during the experiments.

6 Further work

- Further work based on the results presented in this thesis should be to develop a simulation model where simulated theoretical values and performance indexes can be compared to real experimental measurements and calculations. This will not only help in the performance analysis, but also make it easier to identify optimal operation conditions for further testing.
- Economic evaluations should be carried out based on the results. This will help in evaluating the tradeoff between the initial cost of purchasing and installing units like pre-cooling heat exchangers and the benefits achieved regarding the system performance. Also, a life cycle assessment should be performed to investigate the impact the desiccant system has on the environment.
- Several new experiments should be performed with varying operation conditions during different ambient conditions. The measurements should then be used to establish optimal process and regeneration air flow rates during different weather conditions. Also the flow rates of the cooling and chilling water should be varied to evaluate how this affects the total system performance.
- Further, the possibility of applying processed ventilation air to the conditioned space should be implemented in the system. This can be done by making it possible to divide the process air into two separate air streams before entering the regenerative evaporative cooler. One air stream is then directed towards the cooler and the other is directed towards the conditioned space. An air to water heat exchanger should also be installed at a point before the processed air enters the conditioned space, so that the produced chilled water can be utilized to cool the supply air. When supplying ventilation air becomes possible, measurements of the air entering the building should be carried out.
- A setup that allows for the desiccant system to be used as a heating cycle during the winter should be investigated. The evacuated tube solar air collectors have high efficiency and could be able to provide heated fresh air to the conditioned space during cold periods. The possibility of using the desiccant wheels to humidify the process air if the ambient air is too dry should also be investigated.

References

- [1] D. La, Y. Dai*, H. Li, Y. Li, J. K. Kiplagat and R. Wang, "Experimental investigation and theoretical analysis of solar heating and humidification system with desiccant rotor," SJTU, Shanghai, 2010.
- [2] H.-M. Henning, "Solar assisted air conditioning of buildings – an overview," Fraunhofer Institute for Solar Energy Systems ISE, Freiburg, 2006.
- [3] A. A. Pesaran, T. R. Penney and A. W. Czanderna, "Desiccant Cooling: State-of-the-Art Assessment," National Renewable Energy Laboratory, Colorado, 1992.
- [4] J. Dai, D. La, Y. Li, R. Wang and T. Ge, "Technical development of rotary desiccant dehumidification and air conditioning: A review," SJTU, Shanghai, 2009.
- [5] T. Ge, Y. Li, R. Wang* and Y. Dai, "Experimental study on a two-stage rotary desiccant cooling system," SJTU, Shanghai, 2008.
- [6] H. Li, Y. Dai*, Y. Li, D. La and R. Wang, "Experimental investigation on a one-rotor two-stage desiccant cooling/heating system driven by solar air collectors," SJTU, Shanghai, 2011.
- [7] A. Khalid, "Experimental Investigation and Mathematical Modeling of a Low Energy Consuming Hybrid Desiccant Cooling System for the Hot and Humid Areas of Pakistan," NED University of Engineering & Technology, Karachi, 2007.
- [8] P. Esser, "Principles in Adsorption to Polystyrene," Thermo Fisher Scientific Inc, 2010.
- [9] P. Hofmann, "Lecture Notes on Surface Science," 2012. [Online]. Available: <http://philiphofmann.net/surflec3/surflec013.html>. [Accessed 8 May 2012].
- [10] V. C. Mei, F. C. Chen, Z. Lavan, R. K. C. Jr and G. Meckler, "An Assessment of Desiccant Cooling and Dehumidification Technology," MARTIN MARIETTA ENERGY SYSTEMS, INC., Tennessee, 1992.
- [11] K. Daou, R. Wang* and Z. Xia, "Desiccant cooling air conditioning: a review," SJTU, Shanghai, 2004.
- [12] C. Ruivo, J. Costa and A. R. Figueiredo, "Heat and Mass Transfer in Desiccant Wheels," University of Algarve, Algarve, 2008.
- [13] H. Amaia, S. Tanabeb, T. Akimotoc and T. Genmac, "Thermal sensation and comfort with different task conditioning systems," Waseda University, Tokyo, 2006.
- [14] S. Pettersen, "Design and analysis of integrated energy systems including heat pumps for Nordic family houses," NTNU, Trondheim, 2011.
- [15] B. S. Romdhane, "The air solar collectors: Comparative study, introduction of baffles to favor the heat transfer," Institut Supérieur des Sciences Appliquées et de Technologie, Gabes, 2006.
- [16] H. Li, Y. Dai*, Y. Li, D. La and R. Wang, "Case study of a two-stage rotary desiccant cooling/heating system driven by evacuated glass tube solar air collectors," SJTU, Shanghai,

2011.

- [17] SolarPlusGreen LLC, "SolarPlusGreen," 2012. [Online]. Available: <http://www.solarplusgreen.com/tube-vs-plate.htm>. [Accessed 15 May 2012].
- [18] R. Liang, L. Ma, J. Zhang and D. Zhao, "Theoretical and experimental investigation of the filled-type evacuated tube solar collector with U tube," Dalian University of Technology, Dalian, 2011.
- [19] L. Ma*, Z. Lu, J. Zhang and R. Liang, "Thermal performance analysis of the glass evacuated tube solar collector with U-tube," Dalian University of Technology, Dalian, 2010.
- [20] A. Yadav and V. Bajpai, "An Experimental Study on Evacuated Tube Solar Collector for Heating of Air in India," World Academy of Science, Engineering and Technology, Kurukshetra, 2011.
- [21] L. Xu, Z. Wang, G. Yuan, X. Li and Y. Ruan, "A new dynamic test method for thermal performance of all-glass evacuated solar air collectors," Key Laboratory of Solar Thermal Energy and Photovoltaic System of Chinese Academy of Sciences, Beijing, 2012.
- [22] H.-M. Henning, "The potential of solar energy use in desiccant cooling cycles," Fraunhofer ISE, Freiburg, 2000.
- [23] SINTEF, "MULIGHETSSTUDIE SOLENERGI I NORGE," SINTEF, Trondheim, 2011.
- [24] M. J. Moran and H. N. Shapiro, "Fundamentals of Engineering Thermodynamics," in *Fundamentals of Engineering Thermodynamics*, West sussex, England, John Wiley and Sons, 2006, pp. 609-610.
- [25] Omega, "Omega.com," 2012. [Online]. Available: <http://www.omega.com/ppt/pptsc.asp?ref=PR-10&Nav=temc03>. [Accessed 27 April 2012].
- [26] Shinyei, "Room Temperature and Humidity Transmitter," Shinyei, Tokyo, 2012.
- [27] Beijing HSC Measurement Technology CO, "Trade.cn," 2012. [Online]. Available: <http://www.trade.cn/product/59260.html>. [Accessed 27 April 2012].
- [28] M. J. Moran and H. N. Shapiro, "Fundamentals of Engineering Thermodynamics - Fifth Edition," in *Fundamentals of Engineering Thermodynamics - Fifth Edition*, West sussex, England, John Wiley and Sons, 2006, p. 123.
- [29] ALNOR, "CompuFlow Thermo-anemometer Model 8585/8586," TSI Incorporated, Shoreview, 2002.
- [30] D. La, Y. Dai*, Y. Li, T. Ge and R. Wang, "Study on a novel thermally driven air conditioning system with desiccant dehumidification and regenerative evaporative cooling," SJTU, Shanghai, 2010.
- [31] M. A. Mandegari and H. Pahlavanzadeh, "Introduction of a new definition for effectiveness of desiccant wheels," Tarbiat Modares University, Tehran, 2009.
- [32] C. Marques, C. Fontes*, M. Embiruçu and R. Kalid, "Efficiency control in a commercial counter flow wet cooling tower," Universidade Federal da Bahia, Salvador, 2009.

- [33] C. Sheng* and A. A. Nnanna, "Empirical correlation of cooling efficiency and transport phenomena of direct evaporative cooler," Purdue University Calumet, Hammond, 2012.
- [34] D. La, Y. Dai*, Y. Li, T. Ge and R. Wang, "Use of regenerative evaporative cooling to improve the performance of a novel one-rotor two-stage solar desiccant dehumidification unit," SJTU, Shanghai, 2011.
- [35] ASHRAE, "ASHRAE Standard Project Committee 55," American Society of Heating, Refrigerating and Air-Conditioning Engineers, Atlanta, 2004.
- [36] Keithley, "Model 2700 Multimeter," Keithley Instruments, Inc., Cleveland, 2002.
- [37] D. La, Y. Dai*, Y. Li, T. Ge and R. Wang, "Study on a novel thermally driven air conditioning system with desiccant dehumidification and regenerative evaporative cooling," SJTU, Shanghai, 2010.
- [38] D. La, Y. Dai*, Y. Li, T. Ge and R. Wang, "Use of regenerative evaporative cooling to improve the performance of a novel one-rotor two-stage solar desiccant dehumidification unit," SJTU, Shanghai, 2011.
- [39] AIR-ERV, "Alibaba," 2012. [Online]. Available: http://www.alibaba.com/product-gs/322621706/cross_flow_heat_exchanger.html. [Accessed 23 May 2012].
- [40] C. D. Baird, R. A. Bucklin, C. A. Watson and F. A. Chapman, "Evaporative Cooling System for Aquacultural Production," University of Florida, Gainesville, 1993.
- [41] Z. Li and K. Sumathy, "Technology development in the solar absorption air-conditioning systems," University of Hong Kong, Hong Kong, 2000.

List of Figures

Figure 1: Overview of solar assisted systems installed in Europe [2]	2
Figure 2: Basic open-cycle desiccant cooling system using 100% fresh air.....	3
Figure 3: Psychrometric comparison between one-stage and multistage systems [4].....	4
Figure 4: Cross section area of (a) TTSDC and (b) OTSDC [4]	4
Figure 5: Schematic of a two-rotor two-stage desiccant cooling system [5]	5
Figure 6: Schematic of a one-rotor two-stage desiccant cooling system [6]	5
Figure 7: Hydroxyl groups on the surface of silica gel [7]	7
Figure 8: Synchronously alternating polarities establishing bonds between molecules [8].....	7
Figure 9: Adsorption isotherms of Type 1E, Type 1M, linear, Type 3M and Type 3E [4]	10
Figure 10: Principles of a desiccant cooling system [11].....	11
Figure 11: Psychrometric graph on desiccant cooling [11]	11
Figure 12: Desiccant wheel [12]	12
Figure 13: Schematic on the function of desiccant wheels [4]	12
Figure 14: Setup of an evacuated tube solar collector [20]	16
Figure 15: Schematic of a basic evacuated tube solar collector array [21].....	16
Figure 16: Schematic of an evacuated solar air collector tube [16].....	17
Figure 17: Two different desiccant cooling system using solar air collectors as heat source [22]	17
Figure 18: The GEL-building located in Shanghai Jiao Tong University	19
Figure 19: The roof of the GEL-building and the desiccant cooling system	20
Figure 20: Schematic of the conditioned space	20
Figure 21: Electrical control locker	21
Figure 22: The two desiccant wheels	22
Figure 23: The cooling water piping system.....	23
Figure 24: The cross-flow heat exchanger	24
Figure 25: Principle of a cross-flow heat exchanger	24
Figure 26: The cross-flow direct evaporative cooler.....	25
Figure 27: Principle of the evaporative cooling unit	25
Figure 28: Pipes transferring heated air to the system.....	26
Figure 29: Entering point of the regeneration air	27
Figure 30: Evacuated tube solar air collector array	27
Figure 31: The auxiliary heater of the system, 3 kW, 6 kW and 9 kW	28
Figure 32: The cooling tower connected to the system.....	29
Figure 33: Electrical powered motor	30

Figure 34: Regeneration air fan.....	30
Figure 35: Schematic of the desiccant cooling system.....	31
Figure 36: The chilling water piping system.....	33
Figure 37: Psychrometric chart of a basic two-stage desiccant cooling system	33
Figure 38: The broken chilling water pump	35
Figure 39: The new chilling water pump	35
Figure 40: The PT1000 sensors.....	37
Figure 41: PT100 sensor covered by a silicon substance	37
Figure 42: The THT-N263A sensor	38
Figure 43: THT-N263A sensor measuring	38
Figure 44: The solar radiometer	39
Figure 45: The CF8585-model TSI anemometer.....	40
Figure 46: Schematic on the real two-stage desiccant cooling system.....	44
Figure 47: Ambient conditions, June 21 st 2012	48
Figure 48: Effect of regeneration temperature on the moisture removal.....	49
Figure 49: Effect of regeneration temperature on the cooling capacity and COP _{th}	50
Figure 50: Ambient conditions, July 15 th 2012	51
Figure 51: Psychrometric representation of the system processes during ARI summer conditions	53
Figure 52: Dehumidification performance during ARI summer conditions	54
Figure 53: Chilling water temperature during ARI summer conditions	54
Figure 54: Cooling capacity and thermal and electrical COP during ARI summer conditions.....	55
Figure 55: Supply air conditions during ARI summer conditions	56
Figure 56: Ambient conditions, July 1 st 2012	57
Figure 57: Psychrometric representation of the system processes during ARI humid conditions	58
Figure 58: Dehumidification performance during ARI humid conditions	59
Figure 59: Chilling water temperature during ARI humid conditions	60
Figure 60: Cooling capacity and thermal and electrical COP during ARI humid conditions.....	60
Figure 61: Supply air conditions during ARI humid conditions	61
Figure 62: Ambient conditions, July 9 th 2012	62
Figure 63: Psychrometric representation of the system processes during Shanghai summer cond	62
Figure 64: Dehumidification performance during Shanghai summer conditions	63
Figure 65: Chilling water temperature during Shanghai summer conditions	64
Figure 66: Cooling capacity and thermal and electrical COP during Shanghai summer conditions	64
Figure 67: Supply air conditions during Shanghai summer conditions	65

Figure 68: Ambient conditions, June 12 th 2012.....	67
Figure 69: Enthalpy change during first heat exchanger.....	68
Figure 70: Humidity change during first desiccant wheel.....	69
Figure 71: Enthalpy change during the dehumidification process.....	69
Figure 72: Ambient conditions: July 2 nd 2012.....	70
Figure 73: Dehumidification performance with one-stage dehumidification.....	71
Figure 74: Psychrometric representation of the system processes with one-stage dehumidi.....	72
Figure 75: Solar collector conditions, high radiation intensity.....	73
Figure 76: Solar collector performance indexes, high radiation intensity.....	74
Figure 77: Solar collector conditions, moderate radiation intensity.....	75
Figure 78: Solar collector performance indexes, moderate radiation intensity.....	75
Figure 79: Cross-flow heat exchanger performance, moderate ambient temperature.....	77
Figure 80: Evaporative cooler performance, moderate ambient temperature.....	77
Figure 81: Cross-flow heat exchanger performance, high ambient temperature.....	78
Figure 82: Evaporative cooler performance, high ambient temperature.....	79
Figure 83: The user interface of the recording software Keithley 2700.....	93
Figure 84: Processed air at (a) point 6 and (b) point 10.....	96

List of Tables

Table 1: Specifications of the cooling tower	29
Table 2: Assisting components of the desiccant system	30
Table 3: Explanation of the stages occurring in the desiccant cooling system	34
Table 4: The testing equipment	36
Table 5: Parameters used in Equation 6 and Equation 7	41
Table 6: Measurements done of the process air.....	45
Table 7: Measurements done of the regeneration air	45
Table 8: Measurements done in the chilled water cycle	46
Table 9: Measurements done in the cooling water cycle	46
Table 10: ARI and typical Shanghai summer conditions [34]	47
Table 11: System operation conditions, June 21 st 2012.....	48
Table 12: System operation conditions, July 15 th 2012.....	52
Table 13: System operation conditions, July 1 st 2012	57
Table 14: Performance indexes.....	66
Table 15: Operation conditions, June 12 th 2012	68
Table 16: THT-N263A sensor characteristics [26]	91
Table 17: TBQ-2 radiometer characteristics [27]	91
Table 18: CF8585 anemometer characteristics [29]	92

List of Equations

Equation 1: Adsorption of water molecules.....	8
Equation 2: Satisfied total sorption.....	8
Equation 3: Mass flow rate.....	39
Equation 4: Cooling capacity	40
Equation 5: Total electrical demand	41
Equation 6: Electrical work of the pump.....	41
Equation 7: Electrical work of the fan	41
Equation 8: Electrical coefficient of performance.....	41
Equation 9: Heating capacity of solar collector.....	42
Equation 10: Heating capacity of auxiliary heater	42
Equation 11: Thermal coefficient of performance	42
Equation 12: Total incident radiation heat	42
Equation 13: Efficiency of the solar collectors	42
Equation 14: Total moisture removal.....	43
Equation 15: Dehumidification efficiency of desiccant wheel	43
Equation 16: Efficiency of the cross-flow heat exchanger	43
Equation 17: Chilling water efficiency of the evaporative cooler	43
Equation 18: Air cooling efficiency of the evaporative cooler	43
Equation 19: Temperature output from PT1000 sensor.....	93
Equation 20: Temperature output from PT100 sensor.....	93
Equation 21: Temperature output from THT-N263A sensor	93
Equation 22: Relative humidity output from THT-N263A sensor	93
Equation 23: Maximum theoretical heat transfer rate	95
Equation 24: Theoretical supply air temperature	95

Appendix A: Detailed Characteristics of Test Components

Table 16 to Table 18 represents detailed characteristics of some of the test components used in the experiments.

Table 16: THT-N263A sensor characteristics [26]

Model	THT-N263A
Mounting system	Duct mounting
Humidity sensor	Shinyei Hument HPR-MQ-M3
Input voltage	12 to 24V DC
Measurement temperature range	-0 to +50°C
Measurement humidity range	20 to 90% RH (non-condensing) Optionally available from 10 or 20 to 100% RH
Humidity output	4 to 20mA Linear output for 0 to 100% RH full scale
Humidity detecting accuracy	+/- 3% RH (at 25°C, 60% RH)
Temperature output	4 to 20mA Linear output for 0 to 50 full scale
Temperature detecting accuracy	+/- 0.5°C
Storage temperature	-20 to +70°C
Case material	ABS

Table 17: TBQ-2 radiometer characteristics [27]

Model	TBQ-2 radiometer
Spectral range	300 to 3000nm
Signal range	0 to 2000W/m ²
Output signal	0 to 20mV
Sensitivity	7 to 14μV/Wm ²
Response time	≤ 35 seconds (99%)
The resistance	~350ohm
Stability of a year	+/- 2%
Cosine response	≤ 10% (10°, solar elevation angle)
Azimuth response error	≤ 7% (10°, solar elevation angle)
Temperature error	4% (-40°C to +40°C)
Operating temperature	-50°C to 50°C
Operating humidity	0 to 100% RH

Table 18: CF8585 anemometer characteristics [29]

Model	CF8585
Velocity range	0 to 9999ft/min (0 to 50m/s)
Velocity accuracy	+/- 3% of reading or +/- 3ft/min (whichever is greatest)
Velocity resolution	1 ft/min under 500 ft/min (0.05m/s under 10m/s), 5ft/min at 500ft/min and over (0.1m/s at and over 10m/s)
Volumetric flow rate range	Actual range is a function of maximum velocity and duct size
Duct dimensions	1 to 250 inches in increments of 0.1 inches (1 to 635cm in increments of 0.1cm)
Time constant intervals	1 to 10, 20, 25 or 30 seconds
Logging intervals	2 to 10, 15, 20, 25 or 30 seconds
Probe diameter	9.54mm
Power source	Four C size batteries

Appendix B: The Data Recording Software

The computer which is connected to the temperature and humidity sensors uses software to record and compare all the measured values. This software is called Keithley 2700 and offers a complete solution for multi-point measurement and control. The software records resistance signals from the sensors which, by using Equation 19 to Equation 22, can be converted to show the temperature and humidity test results [36].

$$T_{PT1000} = 0.254907R - 254.907$$

Equation 19: Temperature output from PT1000 sensor

$$T_{PT100} = 2.5R - 250$$

Equation 20: Temperature output from PT100 sensor

$$T_{THT-N263A} = 12.5R - 12.5$$

Equation 21: Temperature output from THT-N263A sensor

$$RH_{THT-N263A} = 0.25R - 0.25$$

Equation 22: Relative humidity output from THT-N263A sensor

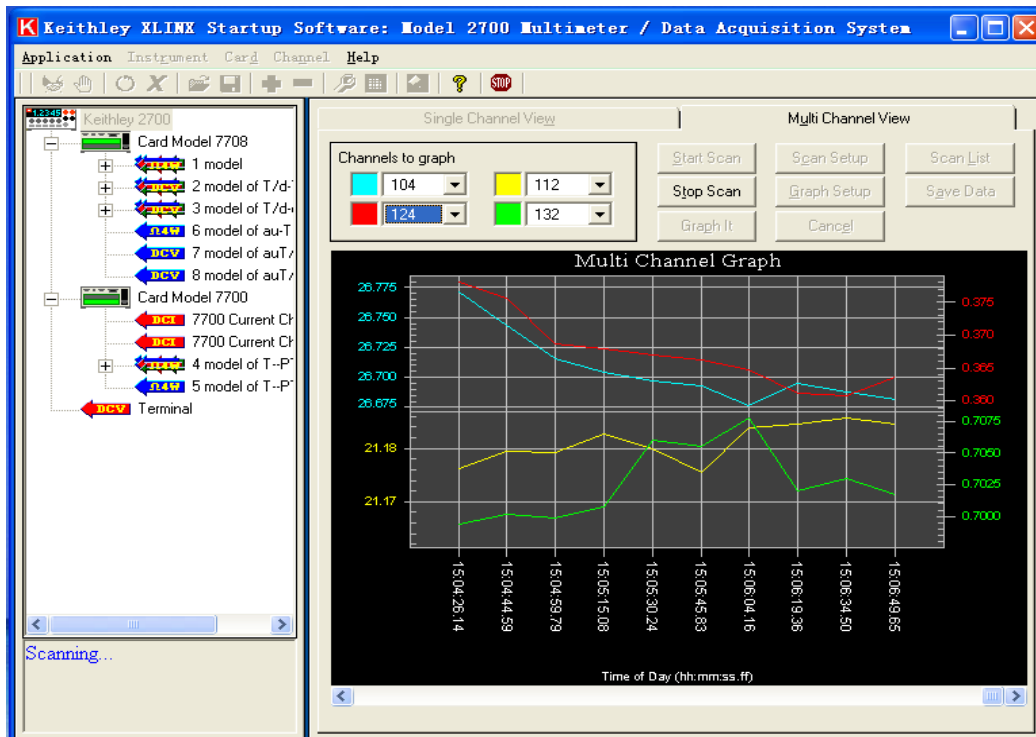


Figure 83: The user interface of the recording software Keithley 2700.

The user interface of Keithley 2700 is showed in Figure 83. The multi channel graph is capable of showing four different measurement points with respect to time. The points can be changed by using the drop boxes under “Channels to graph” to select different channels. The channels selected in Figure 83 are 104, 112, 124, and 132. Channel 104 and 124 are connected to a temperature and humidity sensor placed after the first desiccant wheel, and channel 112 and 132 are connected to a temperature and humidity sensor placed after the regenerative evaporative cooler. The axis on the left shows the temperature for 104 and 112 respectively, and the axis on the right shows relative humidity for 112 and 132 respectively. The values of the axis change according to which channels are chosen in the drop boxes. The ability to choose four different channels at once makes it easy to compare results from different measuring points in the system and allows for fast recognition of unstable and non-reliable results. If a new test point needs to be added to the system, there must be created a new model with the appropriate settings. The model can then be accessed at the left of the user interface.

Appendix C: Theoretical Estimation of Supply Air Temperature

Figure 35, presented in section 2.3, shows the desiccant cooling system with the ability to divide the process air at point 6 and use a part of this air as supply air for the air condition unit. As already mentioned this was not possible to achieve when the system experiments were carried out. The experiments were performed on the system setup that is presented in Figure 46, where no process air is used as supply air.

A part of the testing purpose was to evaluate the systems capability to create supply air within the qualified region with respect to temperature and humidity. Therefore, a theoretical supply air temperature at point 10 is calculated using Equation 23 and Equation 24.

$$Q_{\max} = \dot{m}_{\text{pro}} C_{p,a} (T_6 - T_{21})$$

Equation 23: Maximum theoretical heat transfer rate

Using the result from Equation 23 in Equation 24, and solving with respect to $T_{10,\text{theo}}$ gives the theoretical supply air temperature.

To be able to calculate $T_{10,\text{theo}}$ some assumptions are made:

- An heat exchanger efficiency (ϵ_{theo}) equal 70%
- Fluid properties are constant

$$\epsilon_{\text{theo}} = \frac{\dot{m}_{\text{pro}} C_{p,a} (T_6 - T_{10,\text{theo}})}{Q_{\max}} \rightarrow T_{10,\text{theo}} = T_6 - \frac{\epsilon_{\text{theo}} Q_{\max}}{\dot{m}_{\text{pro}} C_{p,a}}$$

Equation 24: Theoretical supply air temperature

Figure 84 shows the process air temperature and humidity at point 6 and point 10 during July 1st. It is point 6 which is used to calculate the theoretical temperature at point 10. The absolute humidity is the same at point 6 and point 10.

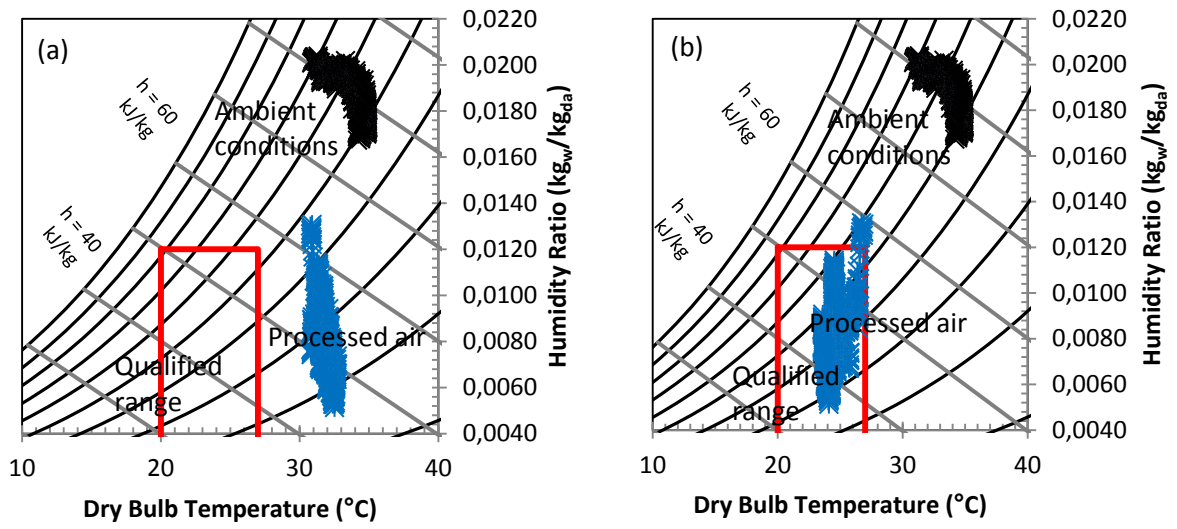


Figure 84: Processed air at (a) point 6 and (b) point 10

Appendix D: Draft of Scientific Paper

Investigation on an open cycle water chiller based on desiccant dehumidification

Sindre Pettersen, Yong Li, Haibin He, Ruzhu Wang, Trygve M. Eikevik, Arne M. Bredesen

Norwegian University of Science and Technology

Shanghai Jiao Tong University

Abstract

A novel desiccant cooling system has been installed and experimentally investigated at Shanghai Jiao Tong University (SJTU). The system uses two-stage desiccant dehumidification as well as regenerative evaporative cooling for production of chilled water. The purpose of the investigation is based on the environmental aspect of HVAC system solutions. The system uses solar thermal power as the main heat source and has therefore great potential in being an environmentally friendly alternative to conventional air conditioning systems with high energy consumption, and reducing the use of non-renewable energy sources. First, the necessary regeneration temperature level is established to be in the range of 70-75°C. Then, results from an experiment performed during high ambient temperature and humidity conditions are evaluated. The system achieves an average thermal and electrical COP of 0.8 and 5.7 respectively, where the thermal COP has a peak value of 1.2. The total dehumidification performance is varying with the regeneration temperature, but has an average value of 58% when the temperature is sufficient. The solar collectors providing heat to the regeneration air has an average efficiency of 47%. The evaporative cooler producing chilled water is capable of providing water at a temperature below 21°C during periods of high ambient temperature and below 16°C during periods of moderate ambient. The dehumidification and cooling performance of the desiccant system makes it possible to provide qualified supply air with average temperature 24°C and absolute humidity below 12 g/kg.

1 Introduction

Increase of the energy consumption around the world and desire to prevent further increased global warming has set a major focus on developing energy efficient and environmentally friendly system solutions. In the summer season especially, air conditioning systems represents a growing market in commercial and residential buildings. Two of the main reasons behind this are that the demands for acceptable living standards are increasing as well as the comfort demands of the occupants. The air-conditioning unit covers both temperature and humidity control, which leads to conventional vapor compression cooling systems consuming large amounts of electrical energy as well as exhausting a lot of usable waste heat [1]. Traditional vapor compression air-conditioning systems usually cools the air down to below dew point temperature to be able to deal with both sensible and latent heat loads. This results in a problem concerning large energy consumption when the system is used to satisfy the temperature and humidity requirements of a conventional building.

Utilization of innovative and clean energy sources has lead technology research in new directions. One of the most important clean energy sources is solar power. Solar-assisted air-conditioning systems are therefore an interesting field of research, and this is still in the early stage of development. One attractive alternative to traditional vapor compression air-conditioning are

desiccant cooling systems where solid desiccant wheels are used to dehumidify the air. Usually evaporative cooling ensures that the air temperature is decreased to acceptable indoor standards. The desiccant cooling system is driven by thermal power which can be provided by solar air collectors.

At Shanghai Jiao Tong University studies has been carried out on desiccant systems that achieves close to isothermal dehumidification. This is done by dividing the desiccant dehumidification in multiple stages resulting in high moisture removal and low regeneration temperature requirements. Two different system configurations has been tested; two-rotor two-stage desiccant cooling [2] and one-rotor two-stage desiccant cooling [3]. Both systems have been proven to have good performance where the TTSDC and OTSDC both have a thermal COP close to one.

In 2010, a new desiccant cooling system was installed at SJTU. This system uses two desiccant wheels for dehumidification as well as a regenerative evaporative cooler for chilled water production. In this paper, it is this system that will be investigated and evaluated by performing real life experiments and testing. The desiccant system is showed in Figure 1. The purpose of the investigation is based on the environmental aspect of HVAC system solutions. The desiccant cooling system uses solar thermal power as the main heat source and has therefore great potential in being an environmentally friendly alternative to conventional air conditioning systems with high energy consumption and in reducing the use of non-renewable energy sources.

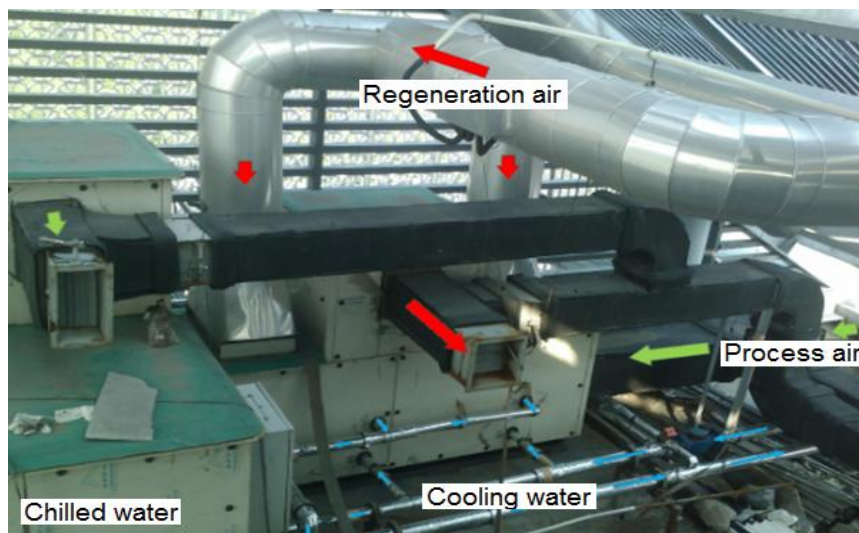


Figure 1: The desiccant cooling system investigated

2 System Description and Working Principles

The novel open cycle two-stage desiccant system driven by solar thermal air collectors is used to produce chilled water and dehumidified air. To have the ability to perform both of these tasks, the system is divided in four processes where different fluids are active:

- Process air
- Regeneration air
- Chilling water cycle
- Cooling water cycle

Figure 2 represents a schematic of the system setup with the different working fluids. The process air part is starting at the entering point of the first heat exchanger and the regeneration air part is starting at the entering point of the solar collectors. The cooling water cycle used to cool the process air is represented by the lines connected to the cooling tower and the chilling water cycle is represented by the separate cycle at the evaporative cooler. Figure 3 shows some of the main system components installed in the system.

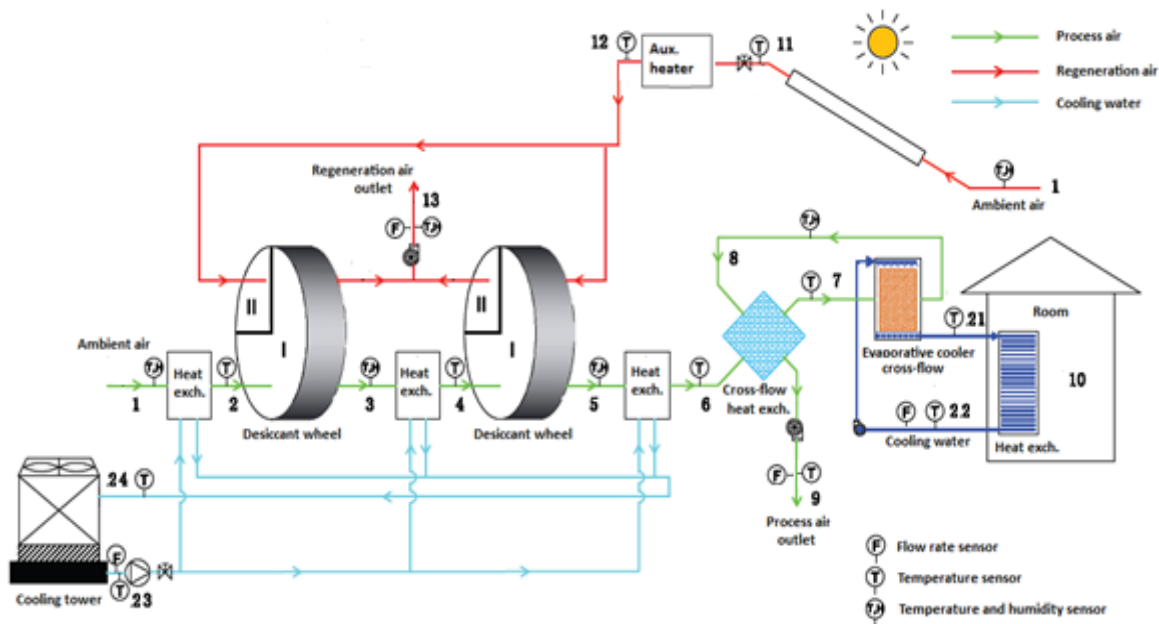


Figure 2: Schematic of the desiccant cooling system

The system process starts with ambient air entering the process part and regeneration part of the system (state 1). The process part starts with the air being dehumidified by the two desiccant wheels (stage 2-3 and 4-5). The desiccant used in the wheels has a lithium chloride and silica gel based composition that adsorbs water molecules to its surface. The desiccant wheels are divided in two different regions by clip boards. One region is for the process air and one region is for the regeneration air, the ratio is approximately 3:1. Three air to water heat exchangers are included before (stage 1-2), between (stage 3-4) and after (stage 5-6) the dehumidification. The exchangers use cooling water generated in a cooling tower to remove some of the sensible and latent heat obtained when the process air interacts with the desiccant wheels. The heat from the desiccant wheels are coming from the regeneration part of the system. The regeneration air is heated by 24 m^2 of evacuated tube solar air collectors (stage 1-11) before entering an auxiliary heater that increases the temperature if necessary (stage 11-12). After this the regeneration air is divided in two separate streams entering each of the desiccant wheels. The hot regeneration air removes the moisture from the desiccant material by desorption (stage 12-13) and is then exhausted to the surroundings.



Figure 3: Important system components

After dehumidification of the process air, the air enters the chilling water production part of the system. This part starts with the process air being cooled by a cross-flow heat exchanger (stage 6-7). The process air exits the heat exchanger and enters an evaporative cooler. The evaporative cooler works by the cross flow principle and the air is in direct contact with water. When in contact with water, the process air creates chilled water (stage 7-8) that runs in a separate cycle and can be used to lower the temperature of ventilation air entering the building. The temperature of the process air interacting in the evaporative cooler is decreased because of the occurring evaporation. The cold process air leaving the evaporative cooler is used as the cold source in the cross-flow heat exchanger (stage 8-9). After this the humid process air is exhausted to the surroundings. Figure 4 represents the psychrometric chart of the system processes.

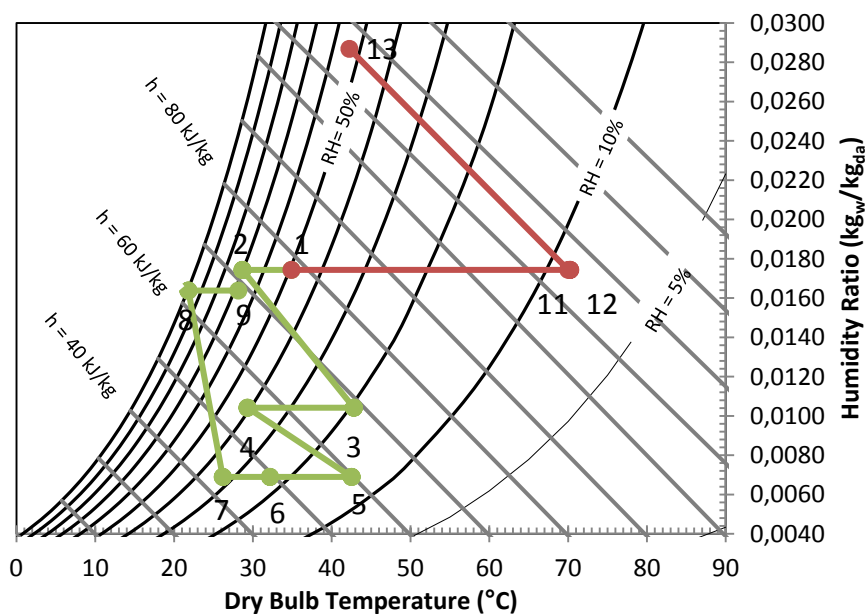


Figure 4: Psychrometric representation of the system processes during high humidity conditions

3 Instrument and Control

When performing the experiments there are needs of some different equipment for testing and gathering data from the system. The testing equipment used depends on which data are interesting to evaluate at the different stages of the system. Temperature, relative humidity, solar radiation intensity and fluid flow rate are all data which must be recorded. The relevant equipment used for the experiments are listed in Table 1. Regarding adjusting the air flow rate in the process and regeneration part of the system, a frequency converter is adopted.

Table 1: The testing equipment

Instrument	Model	Range	Accuracy
Temperature sensor	PT100/PT1000	-200 - 500°C	+/- 0.2°C
Temperature and humidity sensor	THT-N263A	20 – 90%	+/- 3%
Solar radiation intensity	TBQ-2	0 - 2000W/m ²	+/- 2%
Flow rate	CF8585	0 - 50 m/s	+/- 3 %

4 Performance Indexes

The two-stage desiccant cooling system uses heat and work to drive the cycle, and there are several indexes which can be used to indicate the system performance. The first parameter which is interesting to evaluate is the cooling capacity of the system given in Equation 1. The cooling capacity indicates the total achieved cooling of the process cycle.

$$Q_{cs} = m_{pro}(h_1 - h_6)$$

Equation 1: Cooling capacity

The electrical COP is calculated using Equation 2, which is the cooling capacity obtained by the system divided by the systems total electrical input. The total electrical input is based on electrical energy from water pumps, air fans and desiccant wheel rotation motors used in the system.

$$COP_{el} = \frac{Q_{cs}}{W_{el}} = \frac{m_{pro}(h_1 - h_6)}{W_{pump} + W_{fan} + W_{motor}}$$

Equation 2: Electrical coefficient of performance

Here the work of the pump and the work of the fan are calculated using Equation 3 and Equation 4 respectively [4]. The parameter values used in the calculations are stated in Table 2.

$$W_{pump} = \frac{gm_w H}{\eta_{pump}\eta_k}$$

Equation 3: Electrical work of the pump

$$W_{fan} = \frac{m_a \Delta P z}{\rho_a \eta_{fan} \eta_{me}}$$

Equation 4: Electrical work of the fan

Table 2: Parameters used in Equation 3 and Equation 4

Parameter	Value	Unit
H	20	m
η_{pump}	60	%
η_k	85	%
ΔP_{pro}	1000	Pa
ΔP_{reg}	800	Pa
η_{fan}	85	%
η_{me}	100	%
z	1.3	-

Another coefficient of performance which is calculated is the thermal COP, which is based on the thermal energy input of the system. The thermal energy inputs are calculated using Equation 5 and Equation 6, and the thermal COP is calculated using Equation 7.

$$Q_{sc} = C_{p,a} m_{reg} (T_{11} - T_1)$$

Equation 5: Heating capacity of solar collector

$$Q_{aux} = C_{p,a} m_{reg} (T_{12} - T_{11})$$

Equation 6: Heating capacity of auxiliary heater

$$COP_{th} = \frac{Q_{cs}}{Q_{sc} + Q_{aux}} = \frac{m_{pro} (h_1 - h_6)}{C_{p,a} m_{reg} (T_{12} - T_1)}$$

Equation 7: Thermal coefficient of performance

The efficiency of the solar air collector indicates how much of the incident solar radiation the collector is capable of transforming into thermal energy. This efficiency is calculated using Equation 8.

$$\varepsilon_{sc} = \frac{Q_{sc}}{Q_{rad}} = \frac{C_{p,a} m_{reg} (T_{11} - T_1)}{I_{rad} A_{sc}}$$

Equation 8: Efficiency of the solar collector

The total moisture removal by the desiccant wheels and the wheels dehumidification efficiency is given by Equation 9 and Equation 10 respectively. By setting $d_{out,ideal}$ equal zero the efficiency when compared to a desiccant wheel with absolute moisture removal is calculated.

$$\Delta d = d_{in} - d_{out}$$

Equation 9: Total moisture removal

$$\varepsilon_d = \frac{d_{in} - d_{out}}{d_{in} - d_{out,ideal}}$$

Equation 10: Dehumidification efficiency of desiccant wheel

In order to describe the performance of the cross-flow heat exchanger the efficiency is calculated using Equation 11, where T_8 is the lowest achievable temperature of the cross-flow heat exchanger.

$$\varepsilon_{cf} = \frac{T_6 - T_7}{T_6 - T_8}$$

Equation 11: Efficiency of the cross-flow heat exchanger

The efficiency of the evaporative cooler producing chilled water is evaluated using Equation 12. The value of $T_{w,in}$ is important because this shows the achievable temperature of the chilling water. The evaporative cooler also produces cold air, and this efficiency is calculated using Equation 13.

$$\varepsilon_{ev,w} = \frac{T_{w,in} - T_{w,out}}{T_{w,in} - T_{in,wb}}$$

Equation 12: Chilling water efficiency of the evaporative cooler

$$\varepsilon_{ev,a} = \frac{T_7 - T_8}{T_7 - T_{7,wb}}$$

Equation 13: Cooling air efficiency of the evaporative cooler

5 The Test Program

The open cycle desiccant cooling system has been operated during the summer of 2012. The goal of the test program is to test the different components involved in the desiccant cooling system and evaluate the overall performance of the system. Numerous experimental test runs has been performed and a lot of performance data has been registered. All the different measurement points are numbered in Figure 2. The type of measurement and data recorded during the test program is listed from Table 3 to Table 6.

Table 3: Measurements done of the process air

Point	Type of measurement	Description
1	Temperature and humidity	Ambient air inlet
2	Temperature	After the pre-cooling heat exchanger
3	Temperature and humidity	After the first desiccant wheel
4	Temperature	After the interstage heat exchanger
5	Temperature and humidity	After the second desiccant wheel
6	Temperature	After the third cooling heat exchanger
7	Temperature	After the cross-flow heat exchanger
8	Temperature and humidity	After the evaporative cooler
9	Temperature and flow rate	At the outlet, after the regeneration part of the cross-flow heat exchanger

Table 4: Measurements done of the regeneration air

Point	Type of measurement	Description
1	Temperature and humidity	Ambient air inlet
11	Temperature and flow rate	After the solar collector
12	Temperature	After the auxiliary heater
13	Temperature, humidity and flow rate	At the outlet, after the desiccant wheels

Table 5: Measurements done in the chilled water cycle

Point	Type of measurement	Description
21	Temperature	Chilled water supply temperature
22	Temperature and flow rate	Chilled water return temperature

Table 6: Measurements done in the cooling water cycle

Point	Type of measurement	Description
23	Temperature and flow rate	Cooling water supply temperature
24	Temperature	Cooling water return temperature

In addition to the measurements mentioned, the incident solar radiation on the solar collectors is also measured.

Since the desiccant cooling system uses thermal energy from evacuated tube solar air collectors as the main source of energy, the system is functioning best at days where the incident sun radiation intensity is high. Therefore, it has been focused on performing experiments during days with high radiation intensity. The weather conditions during the test period is varying and is therefore classified under the standard conditions called Air-conditioning and Refrigeration Institute conditions and typical Shanghai summer conditions given in Table 7 [5].

Table 7: ARI and typical Shanghai summer conditions [5]

Condition	Ambient air conditions	
	Dry bulb temperature (°C)	Relative humidity (%)
ARI summer	35	40
ARI humid	30	60
Shanghai summer	34	65

6 Results and Discussion

6.1 Performance during Typical Working Conditions

One of the most important factors deciding the system performance is the regeneration temperature. Therefore, an experiment was carried out with varying regeneration temperatures in the range of 60-100°C to establish the necessary temperature level for this two-stage system. The results showed that regeneration temperatures above 70°C are sufficient with respect to dehumidification performance.

A lot of experiments were performed during June and July 2012 with varying ambient and operational conditions. Results from experiments close to ARI summer, ARI humid and Shanghai summer is all evaluated. The following graphs presented are from an experiment performed July 1st where the ambient temperature and absolute humidity ratio were high and the conditions were close to ARI humid conditions. The system operation conditions during the experiment are presented in Table 8. The ambient conditions are presented in Figure 5 together with the achieved regeneration temperature. As can be seen, the solar radiation intensity was varying during the test period which gave a varying regeneration temperature. From 10:00 to 12:45, the average regeneration temperature was 73.2°C and this period is used to calculate the performance indexes.

The complete psychrometric system process is showed in Figure 4. For the process air cycle, which starts at state 1 and ends in state 9, it can be seen that the first desiccant wheel performed most of the moisture removal from the process air. Further, it can be seen that all three air to water heat exchangers were capable of dealing with the sensible and latent heat load occurring during the dehumidification part of the system. The psychrometric chart also shows that the humidity ratio of the process air was reduced from 17 g/kg to around 6 g/kg. At state 9, being the discharge point of the process air, the relative humidity was almost 100% and the absolute humidity ratio was almost back to the same level as the ambient air.

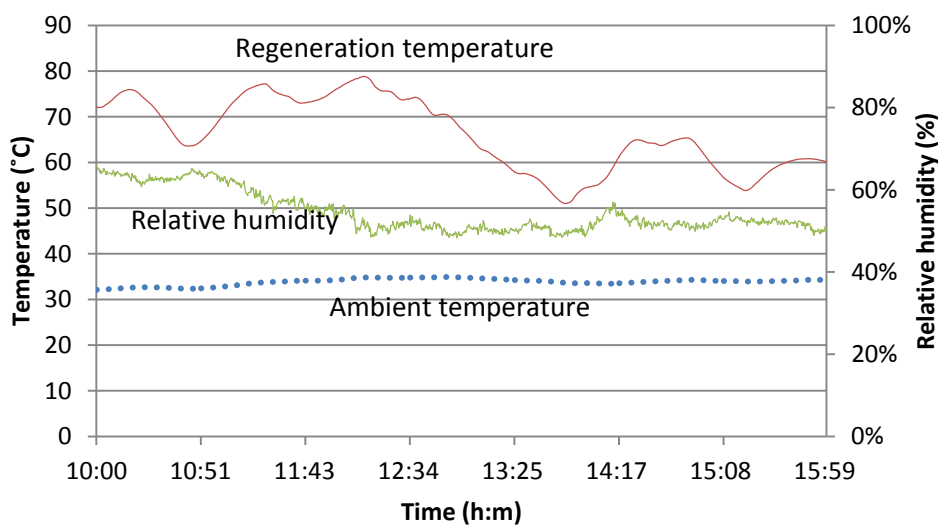


Figure 5: Ambient conditions during the experiment

Table 8: System operation conditions during the experiment

Parameter	Value
Flow rate of process air	900 m ³ /h
Flow rate of regeneration air	840 m ³ /h
Flow rate of chilled water	1.0 m ³ /h
Flow rate of cooling water	6.5 m ³ /h
Rotation of the desiccant wheels	8 r/h

The dehumidification performance of the system is calculated using Equation 9 and Equation 10, and is presented in Figure 6 where the dependence of the regeneration temperature is clearly shown. The first stage desiccant wheel is more dependent on the regeneration temperature than the second desiccant wheel and when the regeneration temperature drops, the first wheel performance drops drastically. When the dehumidification performance of the first wheel decreases, the second wheel performance increases. This gives more stable total dehumidification efficiency. When the regeneration temperature becomes too low, the total efficiency decreases. This can be seen in the period starting from 12:45 where the average efficiency was 42.5%. The average dehumidification efficiency during appropriate regeneration temperature was 57.9%.

Figure 7 shows the cooling capacity, the thermal COP and the electrical COP achieved by the system. These indexes are calculated by Equation 1, Equation 7 and Equation 2 respectively. As can be seen, also these indexes vary with the regeneration temperature. The average value of the thermal COP during the optimal experiment period was 0.83 with a maximum value of 1.2 and the average value of the electrical COP was 5.7 with a maximum value of 7.4. This shows that the system functions very well during high ambient temperature and humidity conditions.

The performance indexes obtained during the experiment regarding the evacuated tube solar air collector are calculated using Equation 5 and Equation 8, and are presented in Figure 8. The potential heat of the radiation hitting the evacuated tube solar air collectors was, for the most time, above 20 kW and the heat added to the regeneration air flowing through the collectors was around 10 kW. The variation in these two values during the day also creates varying collector efficiency. During the period of time when the solar radiation intensity was highest the average collector efficiency was 46.4%.

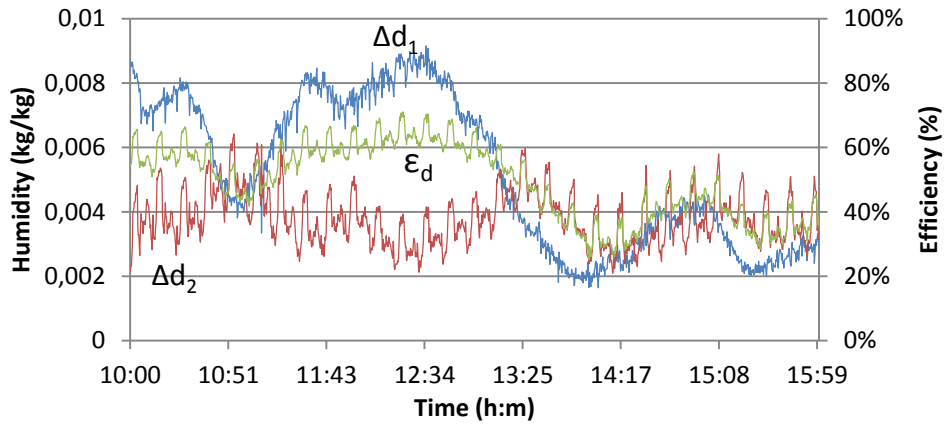


Figure 6: Dehumidification performance

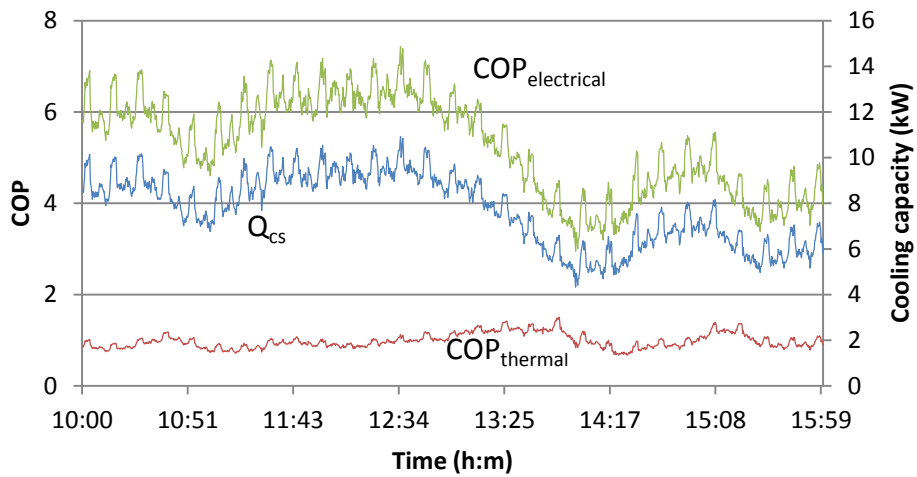


Figure 7: Cooling capacity and thermal and electrical COP

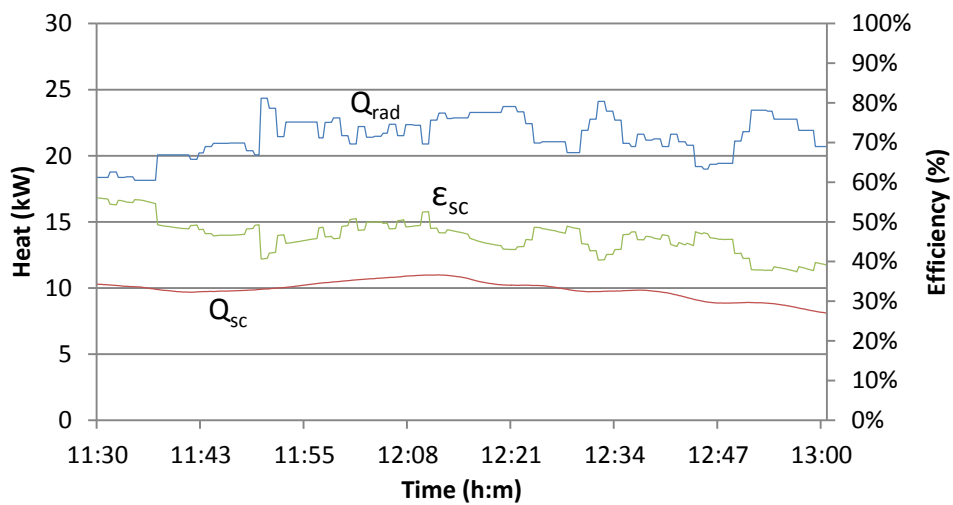


Figure 8: Solar collector performance

The high dehumidification efficiency and cooling capacity of the system makes it possible to produce qualified ventilation air even when the ambient temperature and humidity are high. This is illustrated in Figure 9, which shows the ventilation air production during the period of time when the regeneration temperature was acceptable. The process air started with an absolute humidity ratio in the range of 17 to 20 g/kg and ended up in the range of 12 g/kg down to approximately 6 g/kg, which is inside the qualified region defined according to the ASHRAE standards [6].

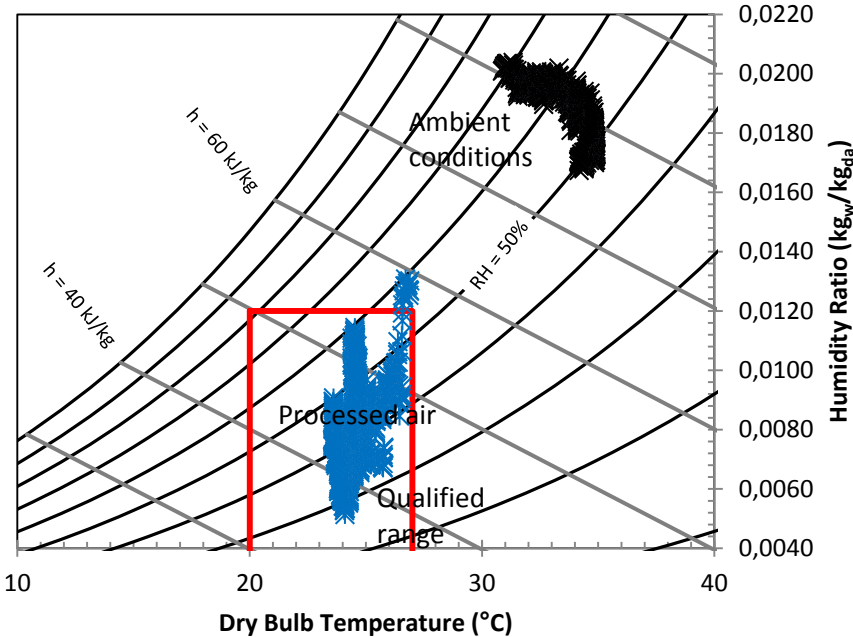


Figure 9: Supply air conditions

As mentioned, also experiments with ambient conditions close to ARI summer and Shanghai summer conditions were carried out and evaluated. Table 9 presents all the performance indexes, as well as the deciding ambient and operation conditions, obtained during close to ARI summer, ARI humid and Shanghai summer conditions. The results of the experiments indicate that the desiccant cooling system functions well under moderate, high and extreme humidity conditions and that the operation conditions needs to be selected properly. It can be said that the system excels the most optimal performance during ambient temperatures and humidity conditions in the range of ARI humid conditions.

Table 9: Performance indexes

Parameter	ARI summer	ARI humid	Shanghai summer	Unit
<i>Ambient temperature</i>	30	33.5	32	[°C]
<i>Ambient relative humidity</i>	56.6	56	67	[%]
<i>Ambient absolute humidity</i>	14.3	18.1	19.9	[g/kg]
<i>Regeneration temperature</i>	80	73.2	77	[°C]
<i>Process air flow rate</i>	1060	900	900	[m ³ /h]
<i>Regeneration air flow rate</i>	840	840	840	[m ³ /h]
<i>Cooling water flow rate</i>	1.0	1.0	1.0	[m ³ /h]
<i>Chilling water flow rate</i>	6.5	6.5	6.5	[m ³ /h]
Dehumidification efficiency	56.5	57.9	45.4	[%]
Cooling capacity	7.4	8.3	7	[kW]
COP_{th}, maximum	1.01	1.2	0.95	[-]
COP_{th}, average	0.64	0.83	0.61	[-]
COP_{el}, maximum	5.7	7.4	6.2	[-]
COP_{el}, average	4.8	5.7	4.7	[-]

6.2 Chilled water production

The regenerative evaporative cooling process is consisting of a cross-flow heat exchanger and the evaporative cooler. The process air first enters the cross flow heat exchanger, then enters the evaporative cooler and lastly enters the cross flow heat exchanger again. This way the process air cooling achieved by the evaporative cooler is utilized to pre-cool the process air entering the evaporative cooler. Since the regenerative evaporative cooler performance is depending on two different units, it is interesting to investigate performance of both units. Equation 11, Equation 12 and Equation 13 are used in the evaluation.

Figure 10, Figure 11 and Figure 12 shows the temperature of the chilled water produced by the system during ARI summer, ARI humid and Shanghai summer. The relevant ambient conditions can be found in Table 9. From the experiment performed during ARI summer conditions, the average temperature of the chilled water production was about 16.5°C. This is very respectable and shows that the system under these conditions is capable of providing high quality chilling water. The capability of producing cold water is directly depending on the temperature of the process air entering the evaporative cooler, which also is presented in the mentioned figures. The average chilled water temperature was around 21°C for the experiment performed during ARI humid conditions. The ambient temperature for this experiment was higher than for the first experiment and this results in a higher chilled water temperature because the evaporative cooler air inlet temperature is higher. For the experiment performed during Shanghai summer conditions, the chilled water temperature was around 22°C. This is respectable considering the high ambient temperature leading to an average temperature of the evaporative cooler inlet air around 27.5°C.

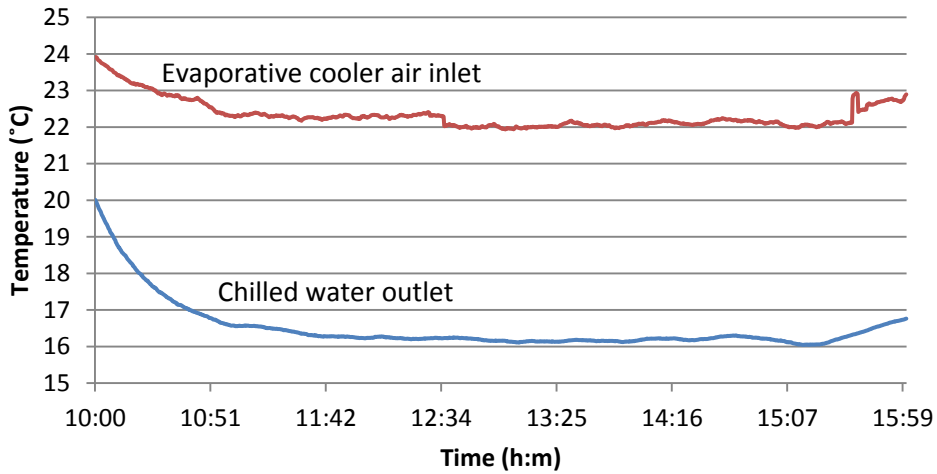


Figure 10: Chilling water temperature during ARI summer conditions

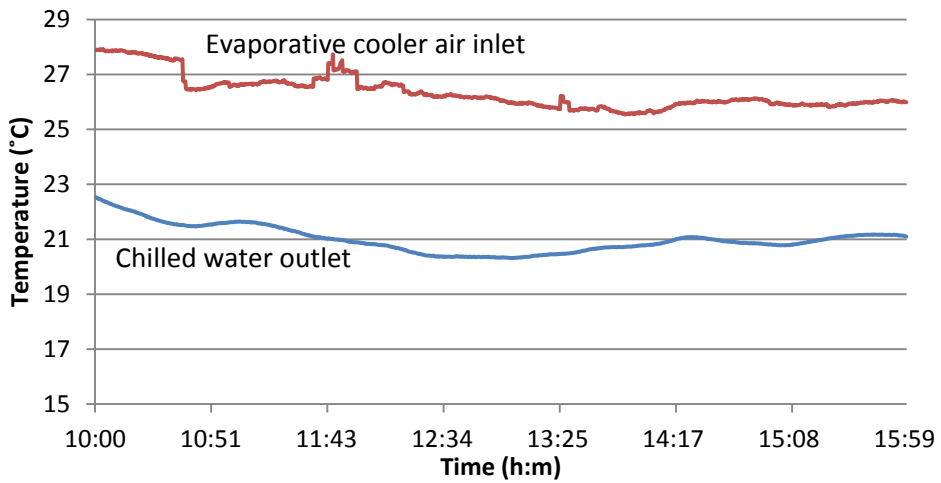


Figure 11: Chilling water temperature during ARI humid conditions

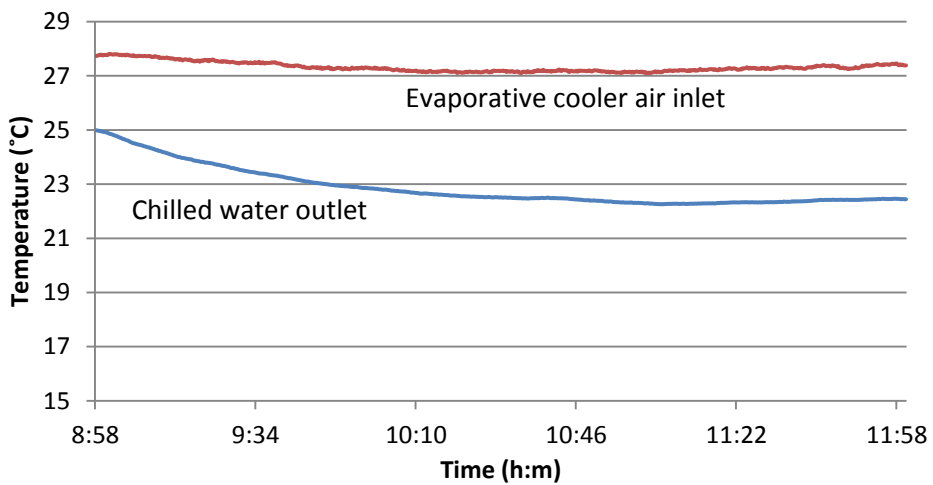


Figure 12: Chilling water temperature during Shanghai summer conditions

The regenerative evaporative cooling process excelled good performance during all experiments and was able to produce low temperature chilled water. Chilled water in the range of 16-22°C was achieved, and these low temperature levels can be used in lowering the temperature of the ventilation air. The best performance regarding the efficiency of the cooler was achieved during experiments of moderate ambient temperature with a water chilling efficiency around 57% and an air chilling efficiency around 76%. The efficiency of the cross-flow heat exchanger was in the range of 50-55% during the experiments.

7 Conclusion

In this paper, a novel open cycle two-stage desiccant dehumidification system with regenerative evaporative water chilling has been experimentally studied. The system uses solar thermal power generated by evacuated tube solar air collectors as the main source of energy.

Total dehumidification performance was showed to increase with increasing regeneration temperature. The necessary temperature of the regeneration air to achieve desired moisture removal was evaluated to be in the range of 70-75°C.

The system excelled good performance during high absolute humidity conditions, and had an average dehumidification efficiency of 58%. The thermal and electrical COP was around 0.8 and 5.7 respectively, with a peaking thermal COP of 1.2. The best achieved system cooling capacity was around 9 kW. Considering an ambient temperature of 34°C and relative humidity of 56%, the performance was very respectable.

Solar air collector efficiency was around 47% during the period of high radiation intensity. When solar radiation was available, the solar collectors were capable of heating the regeneration air to temperatures above 70 °C, but during cloudy weather the regeneration temperature decreased. This showed that when periods of low solar radiation occur, an auxiliary heating device must be used to help increase the regeneration temperature to a required level.

The regenerative evaporative cooler used to produce chilled water was performing well during all experiments and was able to produce low temperature chilled water. During periods of high ambient temperature the cooler produced chilled water below 21°C, and during periods of moderate ambient temperature chilled water below 16°C was achieved. The best performance regarding the efficiency of the cooler was achieved during experiments with moderate ambient temperature with a water chilling efficiency around 57% and an air chilling efficiency around 76%.

References

- [1] D. La, Y. Dai*, H. Li, Y. Li, J. K. Kiplagat and R. Wang, "Experimental investigation and theoretical analysis of solar heating and humidification system with desiccant rotor," SJTU, Shanghai, 2010.
- [2] T. Ge, Y. Li, R. Wang* and Y. Dai, "Experimental study on a two-stage rotary desiccant cooling system," SJTU, Shanghai, 2008.
- [3] H. Li, Y. Dai*, Y. Li, D. La and R. Wang, "Experimental investigation on a one-rotor two-stage desiccant cooling/heating system driven by solar air collectors," SJTU, Shanghai, 2011.
- [4] D. La, Y. Dai*, Y. Li, T. Ge and R. Wang, "Study on a novel thermally driven air conditioning system with desiccant dehumidification and regenerative evaporative cooling," SJTU, Shanghai, 2010.
- [5] D. La, Y. Dai*, Y. Li, T. Ge and R. Wang, "Use of regenerative evaporative cooling to improve the performance of a novel one-rotor two-stage solar desiccant dehumidification unit," SJTU, Shanghai, 2011.
- [6] ASHRAE, "ASHRAE Standard Project Committee 55," American Society of Heating, Refrigerating and Air-Conditioning Engineers, Atlanta, 2004.